Pliocene Volcanic Rocks of the Coso Range, Inyo County, California

U.S. GEOLOGICAL SURVEY PROFESSIONAL PAPER 1383

Pliocene Volcanic Rocks of the Coso Range, Inyo County, California

By STEVEN W. NOVAK *and* CHARLES R. BACON

U.S. GEOLOGICAL SURVEY PROFESSIONAL PAPER 1383

UNITED STATES GOVERNMENT PRINTING OFFICE, WASHINGTON: 1986

DEPARTMENT OF THE INTERIOR

DONALD PAUL HODEL, *Secretary*

U.S. GEOLOGICAL SURVEY

Dallas L. Peck, *Director*

Library of Congress Cataloging-in-Publication Data

Novak, Steven W.
Pliocene volcanic rocks of the Coso Range, Inyo County, California.

U.S. Geological Survey Professional Paper 1383
Bibliography: p. 40–42
Supt. of Docs. No.: I 19.16:1383
1. Geology, Stratigraphic—Pliocene. 2. Volcanic ash, tuff, etc.—California—Coso Range. 3. Geology—California—Coso Range. I. Bacon, Charles R. II. Title. III. Series: Geological Survey Professional Paper 1383.
QE695.N67 1986 552'.2'0979487 86-600084

**For sale by the Books and Open-File Reports Section,
U.S. Geological Survey, Federal Center, Box 25425, Denver, CO 80225**

CONTENTS

ILLUSTRATIONS

TABLES

PLIOCENE VOLCANIC ROCKS OF THE COSO RANGE, INYO COUNTY, CALIFORNIA

By STEVEN W. NOVAK[1] *and* CHARLES R. BACON

ABSTRACT

The Coso Range is east of the Sierra Nevada and immediately south of Owens Valley, California. Major volcanic episodes occurred in the Coso Range at about 6 m.y., 4-2.5 m.y., and later than 1 m.y. The Pliocene episode (4-2.5 m.y. ago) was by far the most voluminous, and during it more than 30 km^3 of basalt to high-silica rhyolite magma was erupted. Basalt originated from monogenetic vents in the eastern part of the range, andesite and dacite generally from polygenetic centers within the basalt field, and rhyodacite and high-silica rhyolite from a large silicic center in the northwest.

Petrographic features, such as quartz xenocrysts in basalt, sieved plagioclase phenocrysts, broad compositional ranges of phenocrysts within single samples, and occurrence of commingled bombs and lava flows, indicate that many of the intermediate-composition rocks formed by mixing of basaltic magma with silicic material. Sieved plagioclase, common in the intermediate silica rocks, reflects sudden thermal and compositional changes of magma brought about by mixing; in general, finely sieved crystals have been partially resorbed and coarsely sieved crystals have experienced rapid growth. Major- and trace-element contents of the intermediate-composition rocks also are compatible with an origin involving mixing; mass-balance calculations show that fractionation of olivine + plagioclase + clinopyroxene, combined with assimilation of silicic magma, accurately models the composition of andesite and dacite. This mixed magma was generated in small volume, thermally and compositionally zoned magmatic systems underlying polygenetic volcanoes.

A larger volume, highly silicic center near Haiwee Ridge evolved 3.1-2.5 m.y. ago. This system erupted high-silica rhyolite air-fall and ash-flow tuff and in its later stages rhyodacite lava flows. The Haiwee Ridge system probably consisted of well-mixed, convecting rhyodacite capped by high-silica rhyolite during its early stages.

The evolution of the Coso volcanic field, from early basalt to polygenetic intermediate-composition volcanoes to a comparatively large-volume silicic center, is thought to reflect systematic changes in the least principal stress (S_3) and the related tectonic extension rate. Beginning about 4 m.y. ago, basalt was erupted onto a surface of little relief, ponding in a shallow north-trending basin. Average residence time of magma in the crust evidently was short and the eruption/intrusion ratio was high. At this time the magnitude of S_3 was greatest and the extension rate probably the least.

Intermediate-composition magma was produced mainly between 3.5 and 3.3 m.y., at a time when S_3 may have decreased and the extention rate increased. Residence time is inferred to have been low to medium, and the eruption/intrusion ratio also medium. By the time relatively voluminous rhyodacitic and rhyolitic magma was erupted from the Haiwee Ridge center, a series of north-south-trending grabens had developed, indicating that the extension rate probably was high and S_3 had decreased to a minimum value. Absence of basalt or intermediate-composition lava in these late stages suggests long residence time and a low eruption/intrusion ratio. Thus, Pliocene volcanism progressed through a sequence of compositions and eruptive patterns that reflect the transition from tectonic stability to extension.

[1]Present address: Charles Evans and Associates, 301 Chesapeake Dr., Redwood City, CA 94063.

INTRODUCTION

The Coso volcanic field (Duffield and others, 1980; Duffield and Bacon, 1981), located east of the Sierra Nevada between Owens Valley and the Garlock fault, is one of many Neogene volcanic centers in the Basin and Range province. Three periods of volcanic activity occurred within the Coso Range during the last 6 million years. The oldest episode of mainly basaltic volcanism with subordinate intermediate-composition lava, and minor high-silica rhyolite occurred on the north flank of the range in the late Miocene, about 6 m.y. ago (Bacon and others, 1982). Pleistocene high-silica rhyolite and associated basaltic rocks occur in the southwest part of the range (Bacon, 1982; Bacon and others, 1981, 1984; Bacon and Metz, 1984). The Pliocene volcanic episode, the subject of this paper, was by far the most voluminous of the three and its products were the most varied. This episode was centered in the east and central parts of the range and took place between about 4.0 and 2.5 m.y. ago (fig. 1). Pliocene volcanic rocks include basalt in the north-central and eastern areas, andesite and dacite at localized polygenetic centers generally within the area of basalt, and rhyodacite and high-silica rhyolite in a silicic eruptive center that makes up the northwestern part of the Coso Range. Granitic rocks of the Sierra Nevada batholith and associated metamorphic rocks form the basement of the volcanic field.

Normal faults cut all of the Pliocene rocks of the Coso Range. Right-lateral strike-slip faulting within the field is suggested by topography, the left-stepping sense of a series of echelon grabens that cut Pliocene rocks, and current seismicity (Walter and Weaver, 1980). The overall pattern of faulting indicates extension in a west-northwest–east-southeast direction. Flow directions and thickness variations of Pliocene lava flows indicate that little fault offset occurred in the area before about 3 m.y. ago. Increased displacement of older lavas relative to younger flows demonstrates that extension has continued throughout the history of the Coso volcanic field. Thus, the Pliocene volcanic rocks were erupted while the area was in transition from comparative stability to rapid extension.

This paper describes the petrography and chemical composition of the Pliocene volcanic rocks, discusses

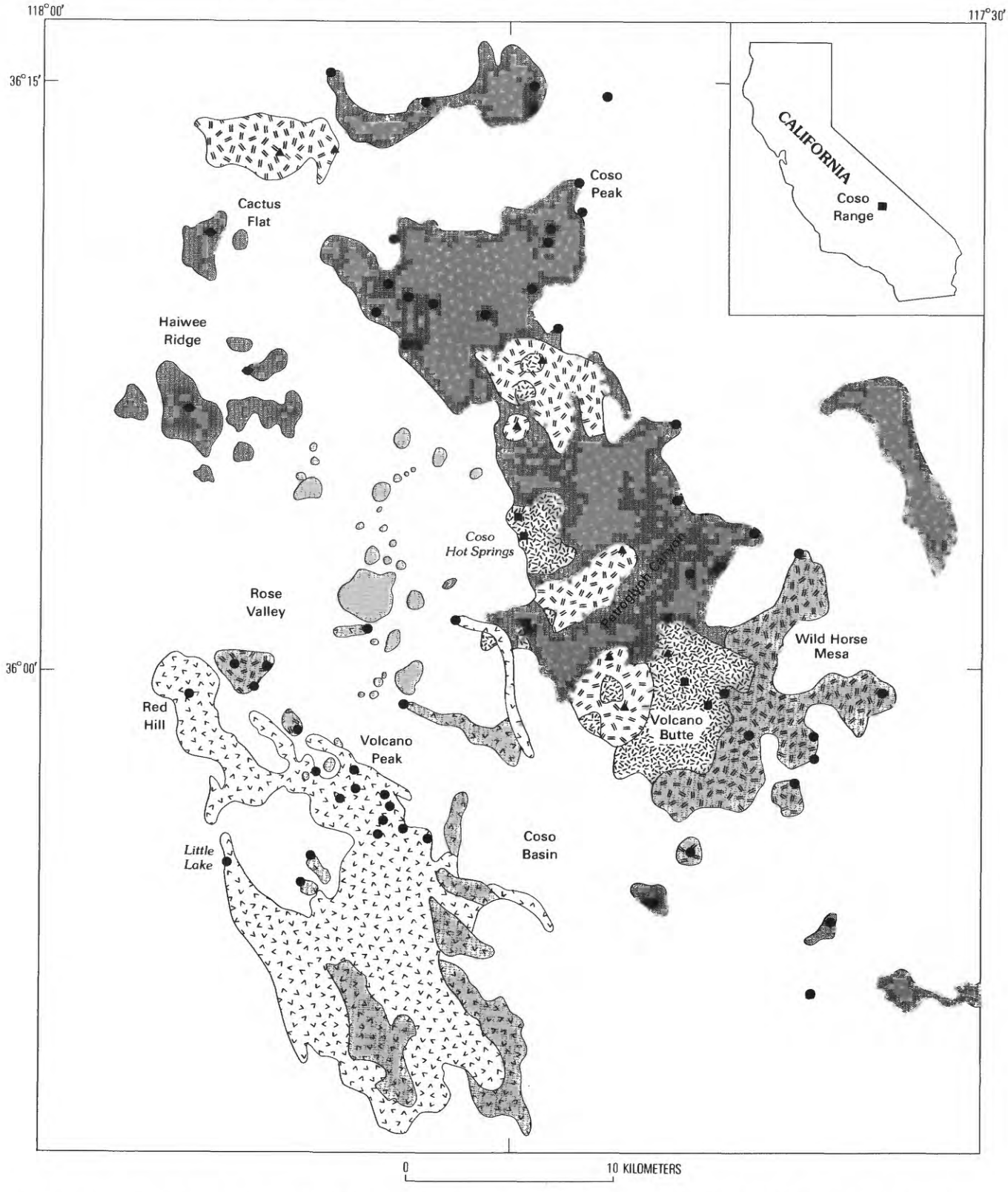

FIGURE 1.—Simplified geologic map of the Coso volcanic field (modified from Duffield and Bacon, 1981). Faults omitted for clarity.

their petrogenesis, and attempts to relate the compositional evolution of the volcanic field to tectonic processes. Electron-microprobe mineral analyses are interpreted to show that many of the intermediate rocks contain mixed populations of phenocrysts derived from basaltic and silicic magmas. These analyses are also used in conjunction with major-element whole-rock chemical analyses to model the petrogenesis of the lavas. Models based on major-element data are tested for compatibility with trace-element abundances determined by instrumental neutron activation analysis (INAA). Finally, we relate the composition and volume of volcanic rocks to the rate of tectonic extension through the inferred relative magnitudes of regional principal compressive stresses.

Rock names used in this paper are based on SiO_2 weight percent expressed on an anhydrous basis with the analysis recalculated to total 100 percent. Because many samples have suffered posteruption oxidation, analyses were recalculated with a uniform atomic $Fe^{2+}/Fe^{2+}+Fe^{3+}$ ratio. A value of 0.86 was chosen for this ratio on the basis of a plot of Fe^{2+} versus $Fe^{2+}+Fe^{3+}$, but we recognize that this probably misrepresents the true oxidation state of some samples. In this classification, basalt has <53 percent SiO_2, andesite 53-63 percent, dacite 63-68 percent, rhyodacite 68-71 percent, and rhyolite >71 percent. Breaks between basalt and andesite and between andesite and dacite are arbitrary because there is both mineralogical and chemical continuity among these rock types. Rhyodacite forms a readily separable group confined to the Haiwee Ridge eruptive center. The break between rhyodacite and rhyolite is placed so as to minimize the terminology necessary to describe the silicic rocks of the Haiwee Ridge eruptive center. This classification is convenient in that names assigned on the basis of phenocryst mineralogy and field criteria correspond well to names based on anhydrous SiO_2 content. It differs slightly from the scheme used by Duffield and others (1980), but results in little change in relative volumes of rock types.

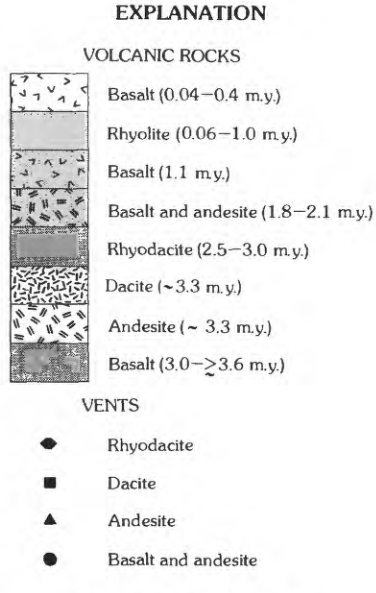

FIGURE 1.—Continued

PETROGRAPHY

We believe that much of the compositional variation among Pliocene volcanic rocks of the Coso field resulted from mixing of basaltic and silicic magmas, or from contamination of basaltic melts by crustal material. This section describes textural and mineralogical features of the volcanic rocks and presents petrographic evidence in support of the mixing and contamination hypotheses. A summary of K-Ar ages and estimated modes for all samples examined is given in table 1, along with their respective map units from Duffield and Bacon (1981). Petrographic descriptions and mineral compositions determined by microprobe are presented together for a given rock type so the two can be easily related. Minerals in thin sections of seven representative rocks were analyzed by electron microprobe using techniques described by Bacon and Duffield (1981) (see fig. 2 and table 10 for sample localities). Photomicrographs of representative rocks are shown in figure 3. Diagrams summarizing the compositional variation of minerals are shown in figures 4 to 9 and representative analyses are given in tables 2 to 6. Listed mineral analyses are averages of at least five spot analyses, and core and rim compositions were determined for most crystals.

BASALT

Rocks classified as basalt (<53 weight percent SiO_2) are holocrystalline diktytaxitic lavas containing phenocrysts of olivine and plagioclase, and in some cases clinopyroxene, in a groundmass of finer plagioclase, olivine, clinopyroxene, and Fe-Ti oxides. Phenocrysts tend to form glomeroporphyritic clots. Two groups can be distinguished within the basalts. Samples with <51 percent SiO_2 have euhedral phenocrysts and only rarely contain quartz and sieved plagioclase xenocrysts; these appear to be the least contaminated basalts. In basalts with >51 percent SiO_2, sieved plagioclase is common,

TABLE 1.—*Phenocryst contents, K-Ar ages, and map units of analyzed Coso Range volcanic rocks*

[Samples arranged in order of increasing SiO_2^* (SiO_2^* = SiO_2 recalculated with analysis normalized to total 100 percent volatile free and with atomic $Fe^{2+}/Fe^{2+}Fe^{3+}$ = 0.86; see text); mineral abundances by visual estimation; K-Ar dates from Duffield and others (1980); map units from Duffield and Bacon (1981)]

Symbols:
A - abundant (>5 percent)
C - common (1-5 percent)
R - rare (<1 percent)

a - included in olivine
b - resorbed
c - included in sieved plagioclase
d - included in clinopyroxene
e - included in plagioclase
f - rims or replaces hornblende
g - included in hornblende
h - included in biotite
i - overgrowth on orthopyroxene
j - included in orthopyroxene

Sample	64	65	66	68	45	56	70	71	72	63	73	74	75	76	77	78	79	80	81	82	83	84	85
SiO_2*	49.5	50.0	50.1	50.4	50.8	51.0	51.0	51.5	51.7	51.8	52.1	52.5	52.6	52.7	53.5	53.5	53.6	54.5	54.5	54.5	55.1	55.2	55.3
K-Ar age (m.y.)	-	-	-	-	3.64	3.64	-	-	-	3.56	-	-	-	-	-	-	-	-	-	-	-	-	-
Map unit	Tbs	Tbp	Tbp	Tbc	Tbc	Ta	QTbr	Tm	Tbp	Tbu	Tbp	Tbpp	Tbp	Tbp	-	Tm	Tbr	Tbr	Tbr	Ta	Ta	Tbp	Tbp
Olivine	C	A	C	R	C	C	C,b	C	C,b	C	A,e	R,d	C	C,e	C,d,e	C	C,b	C,b	C,e	R	-	C,b	-
Plagioclase sieved	R	-	-	-	-	-	C	R	C	R	R	R	C	R	A	R	A	A	-	R	-	A	R
Plagioclase clear-	A	A	A	-	-	-	C	C	C	C	A	R	R	A	C	A	C,d	C	A	R	-	R	-
Clinopyroxene	-	-	-	R	C	-	R,b	R,b	C,b	-	-	C,b	-	-	R,b	R	C,c	A,b	C	-	-	-	C,b
Orthopyroxene	-	-	-	-	-	-	-	-	-	-	-	-	-	-	-	-	-	-	-	-	-	-	-
Hornblende	-	-	-	-	-	-	-	-	-	-	-	-	-	-	-	-	c	c	-	-	-	-	R,b
Biotite	-	-	-	-	-	-	-	-	-	-	-	-	-	-	-	-	-	-	-	-	-	-	-
Quartz	b	-	-	-	-	-	-	-	-	-	-	-	b	-	-	-	b	b	-	-	b	b	b
Potassium feldspar	-	-	-	-	-	-	-	-	-	-	-	-	-	-	-	-	-	-	-	-	-	-	-
Oxides	-	a	a	-	a	-	-	-	-	c	c	-	-	-	-	R	R,c,d	R,d	a,d,e	-	-	a,d	-
Zircon	-	-	-	-	-	-	-	-	-	-	-	-	-	-	-	-	-	-	e	-	-	-	-
Apatite	-	-	-	-	-	-	-	-	-	-	-	-	-	-	-	-	c	c	e	-	-	-	-

Sample	40	86	87	88	89	62	90	91	92	93	94	95	96	97	98	99	100	101	102	103	104	105	106	44
SiO_2*	56.5	56.7	56.7	56.9	57.2	57.5	57.8	58.8	59.7	61.3	61.4	62.1	63.4	63.7	64.0	66.0	67.5	68.3	68.7	68.9	68.9	69.4	70.4	76.2
K-Ar age (m.y.)	3.54	-	-	-	-	-	-	-	-	-	-	3.66	-	-	-	-	-	-	-	-	2.54	-	-	3.14
Map unit	Ta	Tap	Tan	Td	Ta	Tm	Tac	Tac	Td	Td	Tap	Td	Td	Tdo	Tdy	Ta	Trd	Tcp	Trd	Trd	Trd	Trd	Trd	Tc
Olivine	R,b	-	R	C	R	C,e	R	-	R,b	-	R,b	-	-	R,b,d	-	R,b	-	-	-	-	-	-	-	-
Plagioclase sieved	C	A	C	A	C	R	C	A	R	A	C	R	C	C	A	C	A	A	C	C	A	A	R	-
Plagioclase clear-	A	C	R	R	-	A	R	C	R,b	C	C	-	R	-	-	A	C	R	A	R	C	R	A	C
Clinopyroxene	C,b	R	R,b	C	-	C,e	R	-	R	-	R	R	R	R	R	-	-	-	-	-	-	-	-	-
Orthopyroxene	R,b	-	-	R	-	-	R	-	C	R	R	R	R	R	R	-	R,c	-	-	R	R,b	R.b	-	-
Hornblende	-	-	-	R,b	-	-	-	-	R,b	C,b	C,b	R,b	C,b	R,b,d	R,b	R,b,c,e	C,c,i	R	C,c	C,e	C,c,i	C,c	C	-
Biotite	-	-	-	-	-	-	-	-	-	-	-	R,b	-	R.b	R,b	C,c,e	C,c	C,c	C,c,g	C	C	C,c	C,c,g	R
Quartz	-	b	b	-	b	-	-	b	-	-	b	-	b	b	b	b	-	-	C,b	-	-	-	b	R
Potassium feldspar	-	-	-	-	-	-	-	-	-	-	-	-	-	-	-	-	-	-	R,b	-	-	-	-	C
Oxides	-	-	-	-	-	a	j	d	R,a,d	R,f	a,f	f	f	f	f	e,f	R,c,h	R,h	R,c	R,g,j	R,c,g	h	R,h	R
Zircon	-	-	c	-	-	-	-	-	-	-	-	-	e	-	-	g	e,g	h	R	R	c,h	h	R	-
Apatite	-	-	c	-	-	-	-	-	-	-	-	-	-	-	-	e,h	e,h	-	e	-	h	h	e	-

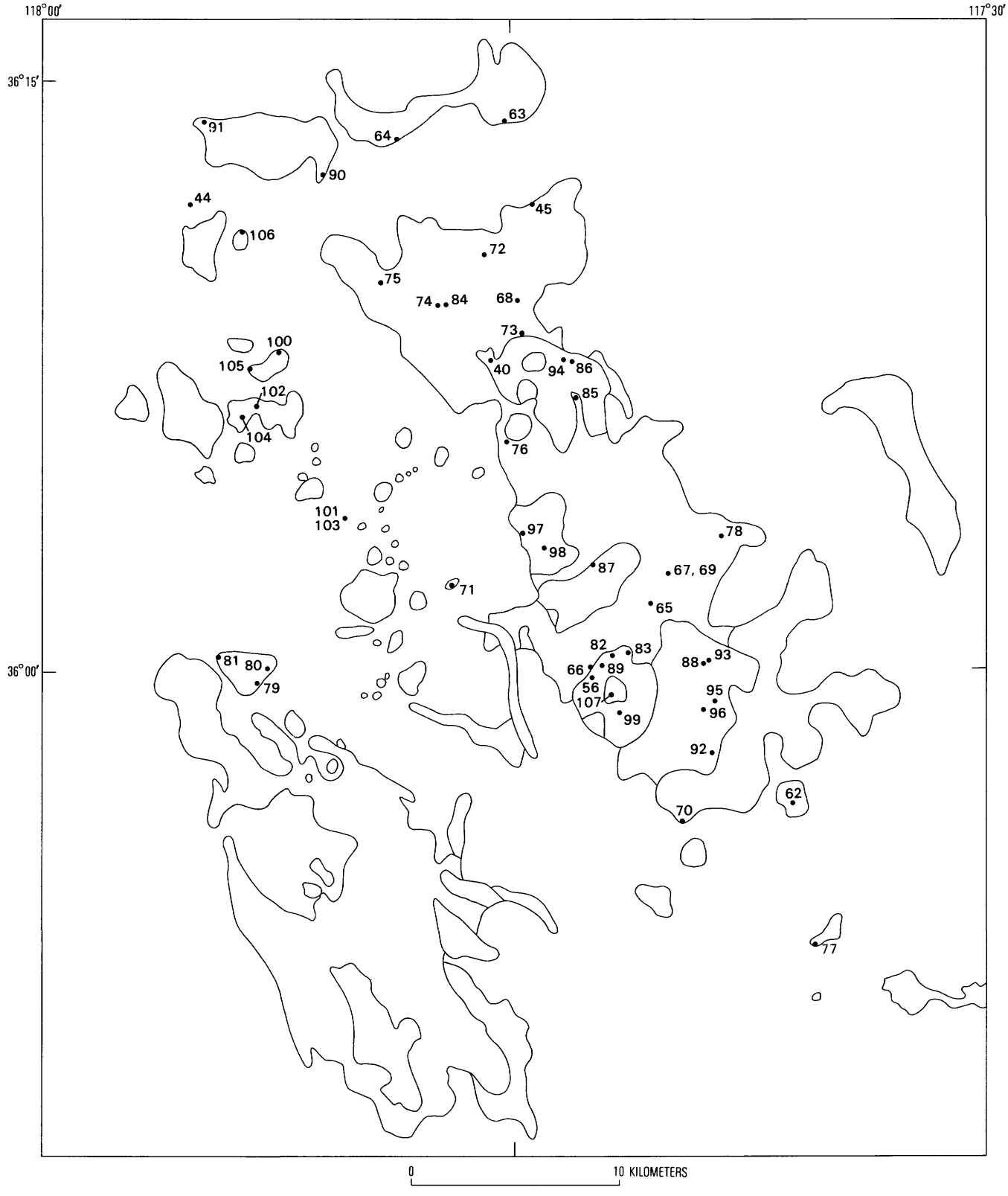

FIGURE 2.—Sample localities for rocks described in this paper. Outlines of rock units from figure 1.

TABLE 2.—*Microprobe analyses and structural formulas of olivine phenocrysts from Coso Range Pliocene volcanic rocks*

[SiO_2* = whole-rock SiO_2 recalculated with analysis normalized to total 100 percent volatile free and with atomic $Fe^{+2}/Fe^{+2}+Fe^{+3}$ = 0.86; oxides in weight percent; formulas based on 4 oxygens; total Fe reported as FeO]

Sample	65		45		84		92		107		99
SiO_2*	50.0		50.8		55.2		59.7		-		66.0
	Core	Rim	Core	Rim	Core	Rim	Core	Rim	Core	Rim	
SiO_2	39.8	39.6	40.2	39.1	40.3	39.1	40.1	38.8	40.1	39.3	40.5
FeO	15.9	17.7	14.6	21.3	14.2	20.3	11.9	21.4	14.7	20.4	7.48
MgO	43.7	42.2	44.6	38.3	45.3	39.8	47.7	39.8	44.8	39.1	50.5
CaO	.31	.37	.28	.46	.29	.33	.34	.28	.27	.31	.26
MnO	.25	.28	.24	.41	.20	.32	.16	.29	.23	.37	.22
NiO	.16	.16	.14	.07	.21	.15	.27	.28	.11	.13	.37
Total	100.12	100.31	100.00	99.61	100.50	100.00	100.47	100.85	100.21	99.64	99.33
Si	1.004	1.004	1.006	1.015	1.003	1.007	.991	.997	1.004	1.016	.993
Fe	.334	.376	.306	.463	.295	.438	.245	.460	.308	.441	.153
Mg	1.641	1.595	1.667	1.483	1.682	1.529	1.756	1.527	1.670	1.509	1.843
Ca	.008	.010	.008	.013	.008	.009	.009	.008	.007	.009	.007
Mn	.005	.006	.005	.009	.004	.007	.003	.006	.005	.008	.005
Ni	.003	.003	.003	.001	.004	.003	.005	.006	.002	.003	.007
Fo-(percent)	82.3	80.2	83.8	75.3	84.3	77.0	86.9	76.1	83.8	76.6	91.5

TABLE 3.—*Microprobe analyses and structural formulas of chrome spinel from Coso Range Pliocene volcanic rocks*

[SiO_2* = whole-rock SiO_2 recalculated with analysis normalized to total 100 percent volatile free and with atomic $Fe^{+2}/Fe^{+2}+Fe^{+3}$ = 0.86; oxides in weight percent; formulas based on 32 oxygens; total Fe reported as FeO; calculated FeO and Fe_2O_3 derived from charge balance. a, euhedral inclusion in olivine; b, intergrown with plagioclase in inclusion in olivine]

Sample	65		45	84	
SiO_2*	50.0		50.8	55.2	
	a	b	a	a	a
Al_2O_3	48.2	30.0	26.4	35.4	38.6
FeO	14.6	28.3	27.1	27.5	23.2
MgO	18.3	12.6	13.3	12.9	15.0
MnO	.03	.18	.17	.13	.07
TiO_2	.45	2.02	1.22	1.03	.75
Cr_2O_3	14.2	24.2	30.5	21.0	19.5
Total	95.73	97.34	98.64	98.08	97.01
Calculated					
FeO	10.8	18.5	16.6	18.2	15.0
Fe_2O_3	4.27	10.9	11.7	10.3	9.07
Total	96.21	98.39	99.86	98.99	98.03
Al	12.64	8.61	7.56	9.87	10.57
Fe^{+3}	.72	2.00	2.14	1.83	1.59
Fe^{+2}	2.00	3.76	3.37	3.61	2.92
Mg	6.07	4.57	4.82	4.55	5.20
Mn	.01	.04	.04	.03	.01
Ti	.08	.37	.22	.18	.13
Cr	2.50	4.66	5.86	3.93	3.58

orthopyroxene rimmed by clinopyroxene may be present, and quartz xenocrysts with granular clinopyroxene armor are frequently encountered. Quartz xenocrysts are present, however, even in the most mafic basalts.

OLIVINE

Olivine occurs as euhedral 1-5 mm phenocrysts that make up 5-10 percent of the basalts. Most crystals have a thin orange brown rim of iddingsite, and many contain small chrome spinel inclusions. Olivine phenocrysts are commonly intergrown with plagioclase in glomeroporphyritic clots. Compositions of olivine phenocrysts from two basalts are given in table 2 and plotted in figure 4. Cores of crystals with spinel inclusions are forsterite-rich (Fo_{86-87}) and show little variation in forsterite content, whereas cores without spinels show greater variation in forsterite content (for example, sample 45: Fo_{74-82}). The Fo content of olivine in the basalt is not as high as in some other Pliocene Coso Range volcanic rocks. Nearly all crystals are zoned to more Fe-rich rims which have the same or lower Ni content and higher Mn content than cores.

CHROME SPINEL

Many olivine phenocrysts in the basalts contain small (<0.1 mm) inclusions of chrome spinel (fig. 3*A*).

TABLE 4.—*Microprobe analyses and structural formulas of pyroxene from Coso Range Pliocene volcanic rocks*
[SiO_2^* = whole-rock SiO_2 recalculated with analysis normalized to total 100 percent volatile free and with atomic $Fe^{+2}/Fe^{+2} + Fe^{+3} = 0.86$; oxides in weight percent; formulas based on 6 oxygens; total Fe reported as FeO]

	Clinopyroxene							Orthopyroxene		
Sample	45		84		92		99	84	92	
SiO_2*	50.8		55.2		59.7		66.0	55.2	59.7	
	Rim	Core	Rim	Core	Rim	Core	Core	Core	Rim	Core
SiO_2	50.7	51.4	49.5	50.8	53.1	53.1	50.5	52.3	54.5	54.6
Al_2O_3	5.06	4.46	6.11	3.89	2.61	1.91	2.57	.26	2.03	2.58
FeO	4.83	4.73	5.23	6.87	4.91	7.01	4.91	25.0	10.2	7.96
MgO	15.3	15.7	15.3	15.7	16.8	16.7	16.8	18.9	30.7	32.6
CaO	22.7	22.8	20.4	20.9	20.5	19.4	20.5	2.47	1.61	1.43
Na_2O	.32	.28	.56	.37	.43	.36	.47	.07	.05	.06
MnO	.11	.12	.12	.17	.13	.22	.13	.71	.20	.15
TiO_2	.84	.79	.86	.95	.40	.33	.84	.19	.19	.16
Cr_2O_3	.45	.27	.91	.27	.37	.08	.30	.02	.14	.58
Total	100.27	100.58	98.92	99.86	99.28	99.17	97.04	99.86	99.65	100.11
Si	1.851	1.871	1.828	1.869	1.949	1.964	1.894	1.988	1.920	1.896
Al^{IV}	.149	.129	.172	.131	.051	.036	.106	.012	.080	.104
ΣTet	2.000	2.000	2.000	2.000	2.000	2.000	2.000	2.000	2.000	2.000
Al^{VI}	.069	.063	.094	.037	.062	.047	.008	.000	.005	.002
Fe	.148	.145	.161	.212	.151	.217	.154	.796	.302	.232
Mg	.831	.851	.843	.862	.916	.922	.942	1.070	1.614	1.685
Mn	.003	.004	.004	.005	.004	.007	.004	.023	.006	.004
Ti	.023	.022	.024	.026	.011	.009	.024	.005	.005	.004
Cr	.013	.008	.027	.008	.011	.002	.009	.001	.004	.016
Ca	.890	.889	.806	.823	.807	.767	.825	.101	.061	.053
Na	.023	.020	.040	.026	.031	.026	.034	.005	.003	.004
ΣOCT	2.000	2.000	2.000	2.000	1.993	1.997	2.000	2.001	2.000	2.000

Although most of the spinel inclusions have similar Fe/Fe+Mg and Cr/Cr+Al ratios, a range of compositions occurs in basalt sample 65 (fig. 5 and table 3). Chrome spinel is present in two forms in this sample: as euhedral octahedra, and as spinel-silicate symplectic intergrowths. The two appear identical in transmitted light, and there is no systematic relationship between spinel morphology and composition. The silicate phase in the symplectic intergrowths is rich in Ca and Al and is probably anorthite-rich plagioclase.

PLAGIOCLASE

Plagioclase in 3-7 mm phenocrysts forms 1-10 percent of the basalt and commonly is intergrown with olivine in glomeroporphyritic clots (fig. 3*A*). The groundmass of the basalt is dominated by minute plagioclase laths with intergranular olivine, pyroxene, and Fe-Ti oxides.

Basalts with 51-53 percent SiO_2 contain, in addition to a small proportion of clear euhedral grains, large sieved plagioclase phenocrysts. The sieve texture consists of fine-grained irregular inclusions in the cores or outer zones of crystals. Most sieved phenocrysts have clear plagioclase overgrowths of varying thickness which commonly give the crystal a euhedral outline. These phenocrysts appear blocky in contrast to the lathlike habit of nonsieved crystals (fig. 3*B*), although this may be an artifact of the orientation of crystals relative to the thin section, since the number examined is small. Inclusions are interconnected and are filled with the same phases which make up the groundmass of the rock; they are inferred to represent trapped silicate

melt that later crystallized. Sieved plagioclase crystals in andesites and dacites described later contain brown glass inclusions which were obviously trapped melt.

Melt inclusions in phenocrysts can form either by partial dissolution of a phenocryst during reaction with surrounding liquid or by entrapment during rapid growth of the host crystal. Partial dissolution requires rapid diffusion of plagioclase components outward, and magmatic liquid components into small channelways within the sieved crystal. Sieve texture has been duplicated experimentally in this manner (partial dissolution) by introducing plagioclase crystals that are more sodic than equilibrium phenocryst compositions into basaltic melts (Lofgren and Norris, 1981). Similar tex-

TABLE 5.—*Microprobe analyses and structural formulas of amphibole from Coso Range Pliocene volcanic rocks*

[SiO_2^* = whole rock SiO_2 recalculated with analysis normalized to total 100 percent volatile free and with atomic $Fe^{+2}/Fe^{+2}+Fe^{+3}$ = 0.86; oxides in weight percent; formulas based on 24 anions; total Fe reported as FeO]

Sample	99				100			
SiO_2*	66.0				67.5			
	Core	Rim	Core	Rim	Core	Rim	Core	Rim
SiO_2	40.8	42.1	41.1	41.6	41.1	42.8	40.4	40.4
Al_2O_3	11.5	9.74	11.3	11.0	14.8	11.6	15.3	15.2
FeO	15.8	18.4	15.1	16.1	9.78	15.2	11.8	12.8
MgO	11.3	10.0	12.2	11.4	15.0	12.5	13.6	12.6
CaO	10.8	10.9	9.74	9.89	10.6	10.2	10.7	10.3
Na_2O	2.00	1.66	2.54	2.38	2.39	1.70	2.33	2.29
K_2O	.94	1.24	.81	.92	.62	.75	.76	.75
TiO_2	2.46	1.43	3.06	2.70	2.88	1.71	3.17	3.04
MnO	.51	.52	.31	.31	.14	.36	.16	.17
F	.14	.16	.19	.17	.15	.17	.14	.17
Cl	.02	.05	.02	.02	.01	.03	.01	.01
Less O = F, Cl	.07	.08	.09	.08	.06	.08	.06	.07
Total	96.20	96.12	96.28	96.41	97.41	96.94	98.31	97.66
Si	6.236	6.513	6.236	6.328	5.995	6.406	5.906	5.961
Al^{IV}	1.746	1.487	1.764	1.672	2.005	1.594	2.094	2.039
ΣTet	8.000	8.000	8.000	8.000	8.000	8.000	8.000	8.000
Al^{VI}	.308	.289	.257	.300	.539	.452	.542	.604
Ti	.283	.166	.349	.309	.316	.192	.348	.337
Mg	2.575	2.306	2.760	2.585	3.262	2.789	2.964	2.771
Fe	1.834	2.239	1.634	1.806	.883	1.567	1.146	1.288
ΣM1-M3	5.000	5.000	5.000	5.000	5.000	5.000	5.000	5.000
Fe	.186	.141	.282	.242	.310	.335	.297	.291
Mn	.066	.068	.040	.040	.017	.046	.020	.021
Ca	1.748	1.791	1.583	1.612	1.657	1.619	1.675	1.628
Na	-	-	.095	.106	.016	-	.008	.060
ΣM4	2.000	2.000	2.000	2.000	2.000	2.000	2.000	2.000
Ca	.021	.016	-	-	-	.017	-	-
Na	.593	.498	.652	.596	.660	.493	.652	.595
K	.183	.245	.156	.179	.115	.143	.142	.141
ΣA	.797	.759	.808	.775	.775	.653	.794	.736
F	.068	.078	.091	.082	.069	.080	.065	.079
Cl	.005	.013	.005	.005	.002	.007	.002	.003

tural effects have been observed in plagioclase that has been partly melted during laboratory experiments (Tsuchiyama and Takahashi, 1984). Sigurdsson (1971) suggested that sodic plagioclase in a hybrid rock from Iceland formed a sieve zone by partial fusion following mixing of silicic and mafic magmas. Sieved plagioclase in many ocean floor basalts (Dungan and Rhodes, 1978) and in andesitic rocks of the Medicine Lake volcano (Gerlach and Grove, 1982) is believed to have formed by partial dissolution.

Skeletal growth of plagioclase crystals has been produced experimentally by undercooling the melt from

TABLE 6.—*Microprobe analyses and structural formulas of biotite*

[SiO_2^* = whole-rock SiO_2 recalculated with analysis normalized to total 100 percent volatile free and with atomic $Fe^{+2}/Fe^{+2} + Fe^{+3} = 0.86$; total Fe reported as FeO]

Sample	99				100			
SiO_2*	66.0				67.5			
	core	rim	core	rim	core	rim	core	rim
SiO_2	36.9	36.5	36.0	35.8	37.4	37.2	37.8	37.9
Al_2O_3	14.2	13.7	14.0	14.2	14.5	14.4	14.1	14.2
FeO	21.2	19.5	21.1	20.0	46.9	16.6	20.5	18.8
MgO	10.7	11.3	10.6	10.8	13.2	13.4	11.3	12.4
CaO	.03	.11	.06	.09	.06	.05	.04	.03
Na_2O	.53	.63	.52	.55	.88	.92	.37	.70
K_2O	9.10	9.00	9.10	8.90	8.40	8.43	9.03	9.08
TiO_2	4.10	4.20	4.20	4.20	4.65	4.60	4.14	3.99
MnO	.32	.26	.31	.29	.16	.21	.28	.22
F	.22	.35	.25	.38	.29	.37	.25	.30
Cl	.04	.04	.04	.05	.04	.04	.04	.03
Less O = F,Cl	.10	.16	.12	.17	.13	.17	.12	.14
Total	97.14	95.27	95.95	94.92	96.22	95.89	97.62	97.38
Si	2.849	2.865	2.820	2.823	2.848	2.841	2.884	2.883
Al^{IV}	1.151	1.135	1.180	1.177	1.152	1.159	1.116	1.117
ΣTet	4.000	4.000	4.000	4.000	4.000	4.000	4.000	4.000
Al^{VI}	.141	.132	.112	.143	.149	.137	.151	.156
Ti	.238	.248	.247	.249	.266	.264	.238	.228
Mg	1.231	1.322	1.238	1.270	1.498	1.525	1.285	1.406
Fe	1.369	1.280	1.382	1.319	1.076	1.060	1.308	1.196
Mn	.021	.017	.021	.019	.010	.014	.018	.014
ΣOct	3.000	3.000	3.000	3.000	3.000	3.000	3.000	3.000
Ca	.002	.009	.005	.008	.005	.004	.003	.002
Na	.079	.096	.079	.084	.130	.136	.055	.103
K	.896	.901	.909	.895	.816	.821	.879	.881
Σ	.977	1.006	.993	.987	.951	.961	.937	.986
F	.054	.087	.062	.095	.070	.089	.060	.072
Cl	.005	.005	.005	.007	.005	.005	.005	.004

which they were crystallizing (Lofgren, 1974), forming coarse sieve texture. Undercooling might be caused by mixing of cooler differentiated magma with basaltic magma. Several natural examples of sieve texture have been attributed to rapid crystal growth following a mixing or contamination event that undercooled the host magma (Hibbard, 1981; Kuo and Kirkpatrick, 1982). Disequilibrium textures of sieved phenocrysts are therefore thought to have formed during mixing of magmas of different composition, either by dissolution or by rapid growth. The interconnected, irregular shape of melt inclusions, the common coincidence of polysynthetic twin planes with inclusion boundaries, and the rounded or amoeboid cores of crystals suggest that sieved pla-

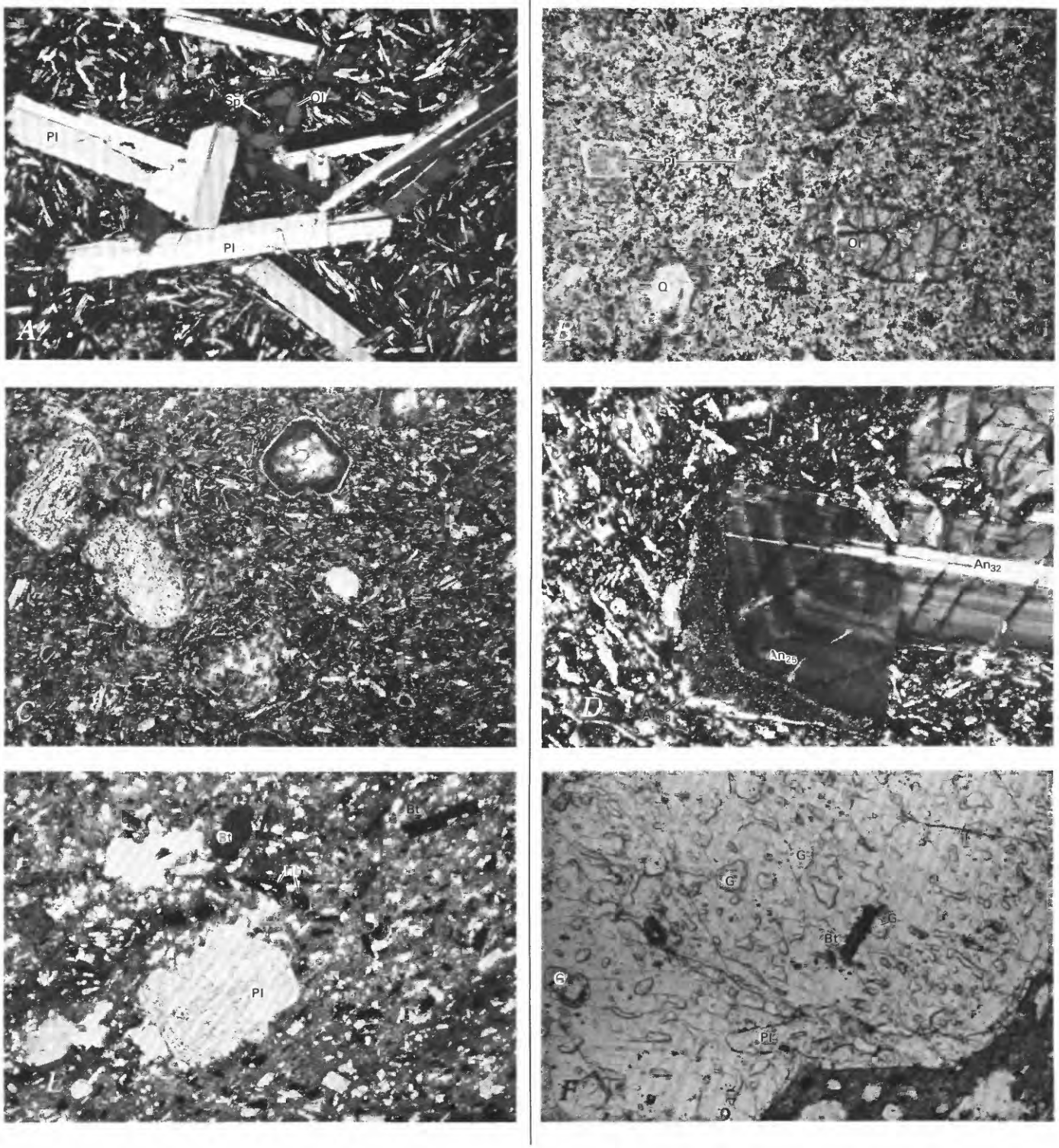

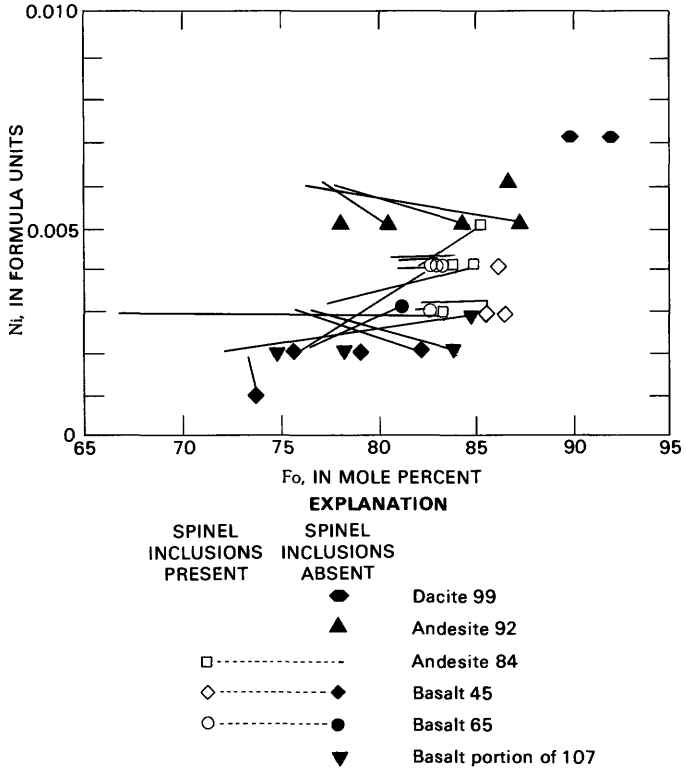

FIGURE 4.—Nickel vs. forsterite content of olivine. Symbols show core composition; lines extend to rim composition.

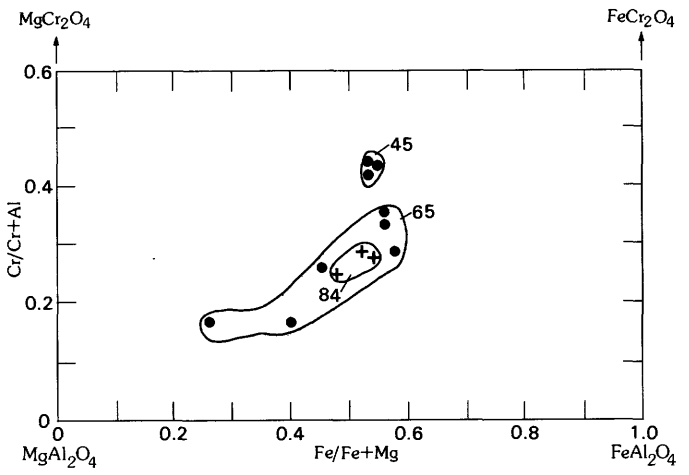

FIGURE 5.—Cr/Cr + Al vs. Fe/Fe + Mg (atomic basis) in chrome spinel. Fields enclosing compositions of crystals from individual samples indicated by sample numbers.

FIGURE 3.—Photomicrographs of representative Pliocene volcanic rocks of the Coso Range. *A*, Basalt (sample 66) showing glomeroporphyritic clot of olivine (Ol) and plagioclase (Pl) phenocrysts. The olivine contains a spinel (Sp) inclusion. Crossed nicols; width of field 18 mm. *B*, Basalt (sample 75) showing phenocrysts of euhedral olivine (Ol) and sieved plagioclase (Pl). Quartz (Q) xenocryst with clinopyroxene rim at lower left. Plane-polarized light; width of field 18 mm. *C*, Andesite (sample 87) showing differing types of sieved plagioclase phenocrysts. Resorbed oval phenocryst on far left (Pl) contains coarse, devitrified melt inclusions. Most inclusions are parallel to or bounded by polysynthetic twin planes. Euhedral grain at upper center (Pz) has a zone of fine interconnected devitrified melt inclusions around a clear core. A thin continuous overgrowth of clear plagioclase surrounds the entire grain. Textures of both these grains are interpreted as resulting from incomplete resorption. Crossed nicols; width of field 9 mm. *D*, Andesite (sample 84) showing a zoned and partially resorbed plagioclase phenocryst. Numbers on figure indicate anorthite content of the grain as determined by microprobe analyses. Crossed nicols; width of view 7 mm. *E*, Rhyodacite (sample 100) showing phenocrysts of hornblende (Hb), biotite (Bt), and coarsely sieved plagioclase (Pl) in glassy groundmass. Plane-polarized light; width of view 18 mm. *F*, Detail of coarsely sieved plagioclase phenocryst in rhyodacite (sample 100). Angular blebs are inclusions of highly silicic glass (G). One inclusion near the center of the figure contains a biotite (Bt) crystal. A small plagioclase (Pl) is also present. This texture apparently resulted from rapid growth of plagioclase. Plane-polarized light; width of view 2.6 mm.

gioclase phenocrysts in the Pliocene basalts of the Coso volcanic field developed sieve texture during partial dissolution and reaction with liquid, rather than by rapid growth. The dissolution origin also is suggested by the composition of plagioclase phenocrysts.

Compositions of plagioclase phenocrysts and microphenocrysts in basalt are plotted in figure 6. Plagioclase phenocrysts in basalt that lacks sieved plagioclase are very calcic (An_{60-70}). Most phenocrysts are zoned to more sodic rims, but the compositional range is not large. Rim compositions match those of groundmass feldspars, suggesting the rims formed during the last stages of crystallization of the basalt. In basalt with sieved plagioclase, cores of phenocrysts are more sodic and show a greater range of anorthite content. The sieved phenocrysts are either normally or reversely zoned; rim compositions match those of microphenocrysts. Plagioclase compositions within sieve zones are highly variable. Sieve zones are clearly more sodic than cores of nonsieved crystals or than phenocryst rims. These findings are consistent with the dissolution hypothesis in which sieve zones form when relatively sodic plagioclase is introduced into basaltic magma during a mixing event, later to be overgrown with clear rims of a composition in equilibrium with the hybrid liquid.

CLINOPYROXENE

Euhedral phenocrysts of clinopyroxene compose up to 3 percent of a few basalt samples, and interstitial clinopyroxene grains are a common groundmass constituent of all the mafic lavas. In a few generally diktytaxitic basalts, clinopyroxene also forms larger ophitic crystals in the groundmass. Clinopyroxene phenocrysts

in some higher silica, contaminated basalts have fine sieve texture similar to that of plagioclase. We consider this to reflect partial dissolution of clinopyroxene phenocrysts, which had grown in more silicic magma, as a result of magma mixing.

Clinopyroxene compositions (fig. 7) have been determined in sample 45, one of a few basalts with euhedral clinopyroxene phenocrysts. The compositions cluster tightly on the pyroxene quadrilateral and appear to be appropriate for equilibrium with basaltic magma. This sample is representative of the basalt of Coso Peak, the only known basaltic unit in the Coso Range that con-

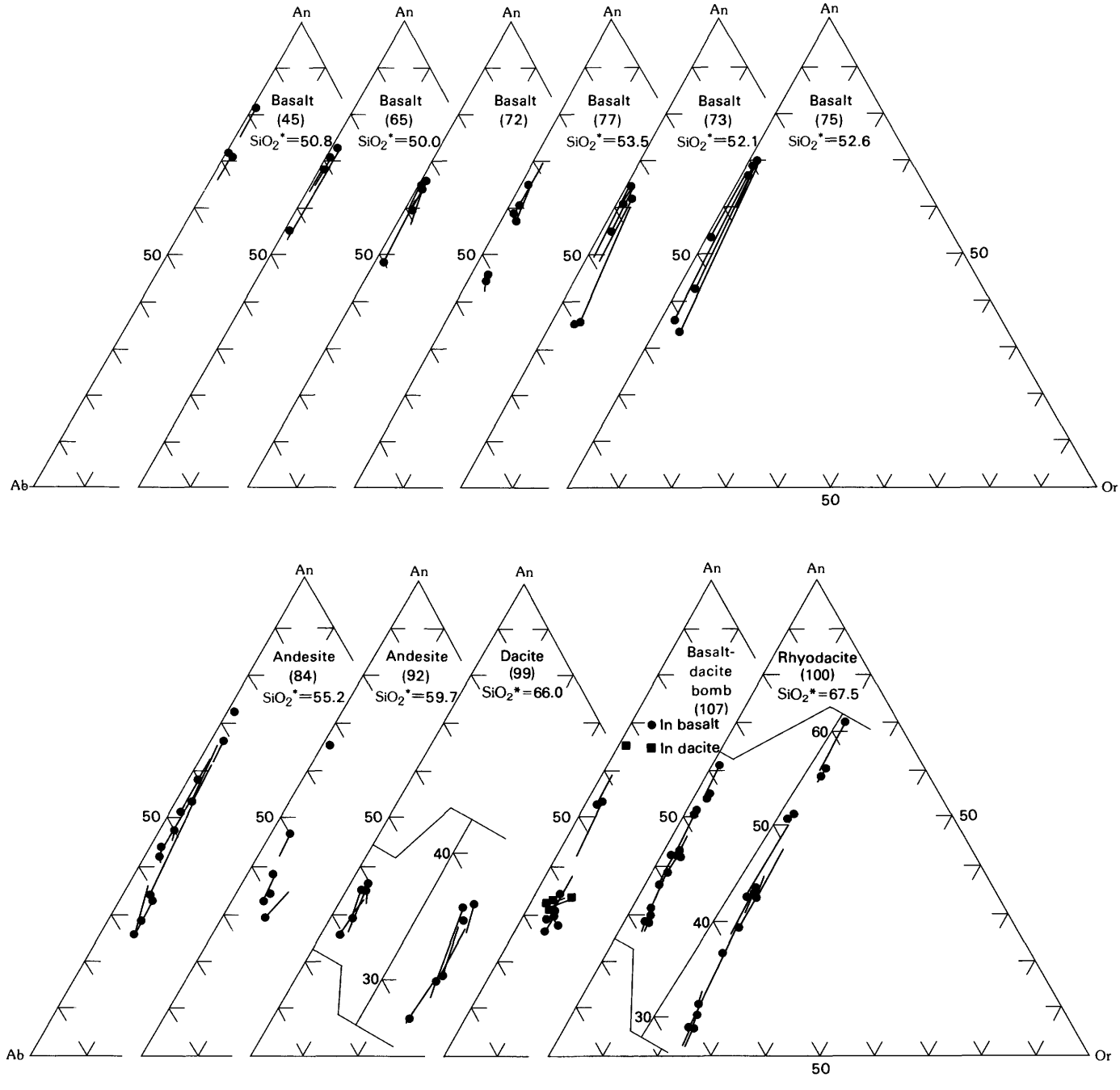

FIGURE 6.—Anorthite, albite, and orthoclase contents (mole percent) of plagioclase (sample number given in parentheses). Each plot shows crystal compositions for a single sample, solid circles are core composition; lines extend to rim composition. Plots for samples 99 and 100 also shown enlarged for clarity.

tains euhedral olivine and clinopyroxene phenocrysts. Most of the Coso Peak flows also lack plagioclase phenocrysts.

XENOCRYSTS

Several of the higher silica basalt samples contain xenocrysts that provide evidence of contamination. Sieved plagioclase and clinopyroxene evidently are xenocrystic, having been derived from admixed more silicic magma. In addition, resorbed quartz rimmed by fine-grained clinopyroxene occurs in three analyzed samples and many other specimens. One sample contains a large aggregate of oxide grains that appears to be a completely reacted amphibole crystal. Another has a small metamorphic xenolith that consists of fine-grained polygonal plagioclase enclosing oval aggregates of green spinel.

The presence of xenocrysts suggests that the more silicic basalt has been contaminated with crustal material or with more silicic magma. Even the most primitive basalt may contain minor quartz xenocrysts. The basalt of Rose Valley is notable among the Pliocene basalts for containing the largest amount of xenocrystic material. This is among the most silicic of all the basaltic lavas, and many samples fall in the andesite compositional range. Large resorbed clinopyroxene crystals and gabbroic and metamorphic microxenoliths are common in some of these rocks, in addition to more familiar xenocrystic plagioclase and quartz. Apatite needles are common in xenocrysts and zircon has been noted. The most silicic (sample 81) of the three analyzed samples from the basalt of Rose Valley (Duffield and Bacon, 1981) contains only euhedral olivine, clinopyroxene, and plagioclase phenocrysts, suggesting that all xenocrysts had been completely dissolved.

INTERMEDIATE-COMPOSITION ROCKS

Andesite and dacite are considered together here because the intermediate-composition volcanic rocks form a continuum ranging from highly contaminated basalt to dacite. Most of these rocks are coarsely porphyritic, but nearly aphyric silicic andesite also is present. Rock compositions within specific map units may be highly variable. For instance, the andesite northwest of Petroglyph Canyon (Duffield and Bacon, 1981) probably varies from highly contaminated basalt at the margins of the flow to low-silica dacite near the vent. Similar compositional variation exists in other units. Some rocks called dacite on the basis of field characteristics may actually fall in the andesite range according to their anhydrous SiO_2 content.

Evidence for mixing or contamination in these rocks is widespread. Phenocryst assemblages are mixed, containing crystals of both basaltic and silicic origins. Plagioclase phenocrysts are euhedral to rounded and almost always sieved or resorbed. Resorbed olivine phenocrysts may be present, although less commonly than in basalt. Both orthopyroxene and clinopyroxene are

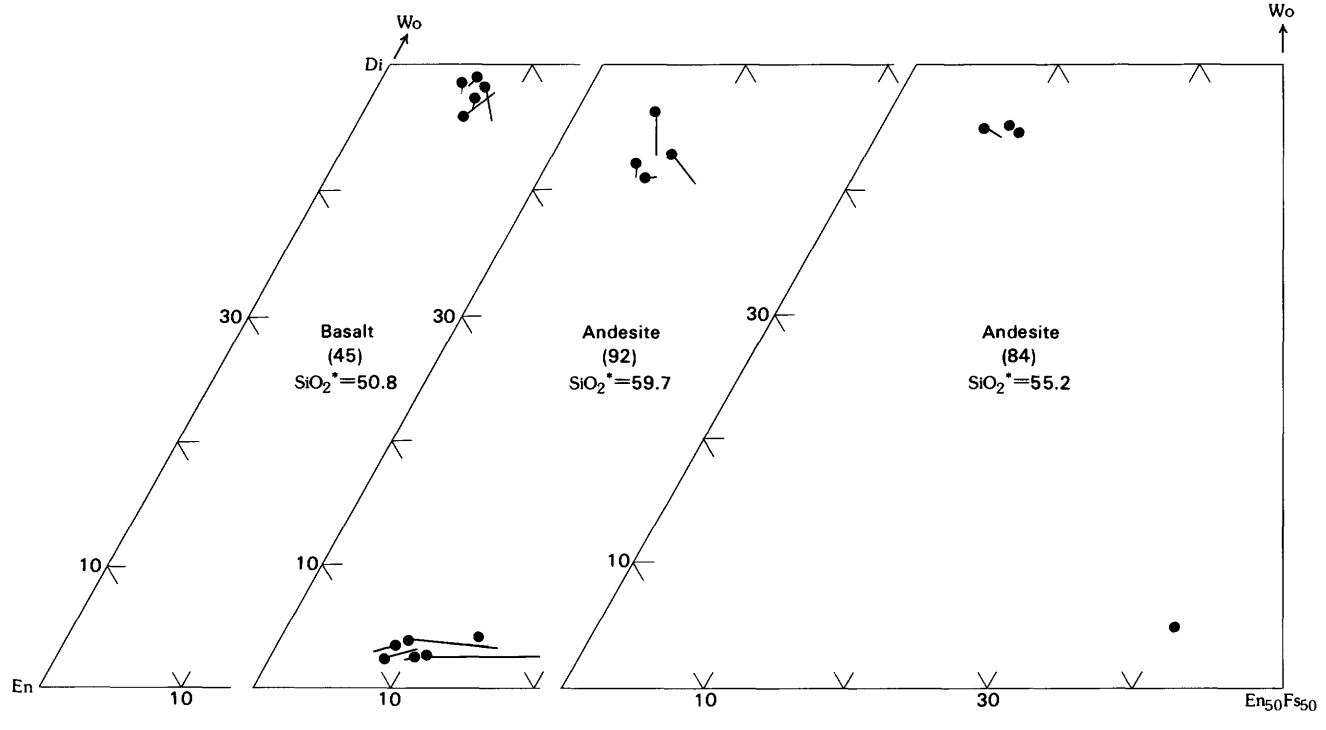

FIGURE 7.—Wollastonite, enstatite, and ferrosilite contents (mole percent) of pyroxene. Sample numbers in parentheses. Solid circles are core composition; lines extend to rim composition.

found in many samples. Resorbed quartz xenocrysts are ubiquitous and commonly are rimmed by fine-grained clinopyroxene. Pseudomorphs after amphibole occur rarely in the andesite, but resorbed amphibole and biotite rimmed or replaced by fine-grained oxides characterize the dacite. The following sections describe the petrographic and compositional characteristics of phenocryst minerals throughout the broad range of rock compositions present.

OLIVINE

Olivine phenocrysts ≤3 mm make up less than 3 percent of the andesite and are common only in rocks with less than 60 percent SiO_2. The phenocrysts typically are slightly resorbed and rimmed by iddingsite, and they may contain chrome spinel inclusions. As in the basalt, olivine cores with spinel inclusions vary little in Fo content (fig. 4). All crystals are zoned to rims richer in Fe and Mn; the Ni content of rims can be higher or lower than the cores (table 2). Resorbed microphenocrysts (<1 mm) of strongly iddingsitized olivine make up about 1 percent of the analyzed dacite (sample 99). These crystals have the highest forsterite content ($Fo_{91.5}$) of any analyzed olivine, yet occur in the most silicic rock that contains olivine. The presence of forsterite-rich olivine, particularly when it is intergrown with anorthite-rich plagioclase, as described below, is further evidence for contamination of silicic magma by basaltic material to form the dacite.

PLAGIOCLASE

Plagioclase phenocrysts dominate the appearance of the andesites. Euhedral blocky 1-5 mm phenocrysts make up 5-20 percent of the rocks and commonly are sieved. The sieve zones are usually much finer textured than those of plagioclase in the basalt. They may occur as oval zones around a clear core and are commonly overgrown by clear euhedral rims (fig. 3*C*). These features, plus the fact that in at least one crystal the sieve zone cuts across compositional zoning in the core, suggest that sieving of plagioclase in intermediate-composition rocks was formed by preferential melting of the outer zones of crystals.

A particularly instructive example of sieved plagioclase in an andesite (sample 84) is illustrated in figure 3*D*. This crystal consists of an oscillatory-zoned clear core surrounded by a finely sieved zone that cuts across the compositional zoning. The sieved zone is in turn overgrown by a euhedral clear rim. Microprobe analyses show that the clear core is normally zoned from An_{32} to An_{25}, compositions that are substantially more sodic than expected equilibrium phenocrysts in this rock. The outer euhedral rim, however, is An_{38} (fig. 6). We infer that the core of this crystal grew in relatively sodic silicic magma and that the sieve zone represents resorption of the most sodic zones of the crystal when it was incorporated into hotter, more mafic magma. A euhedral rim of more calcic plagioclase later grew over the sieved zone. The crystal was apparently broken after the overgrowth formed, and nonsieved sodic plagioclase in the core is now in direct contact with the groundmass along part of the break.

Plagioclase in the dacites commonly is subhedral and has rounded outlines with a finely sieved zone near the rim. A clear rim may occur around the sieved zone as in the andesites. The cores of these crystals are clear or have coarse silicic melt inclusions, and many show oscillatory zoning.

Plagioclase composition can vary widely within a given rock. In the andesite (sample 84) containing the sieved crystal described earlier, core compositions range from An_{29} to An_{58}. Most of these crystals have euhedral rims of An_{60} to An_{67}, and one euhedral microphenocryst has a composition of An_{71} (fig. 6). Euhedral rims have compositions similar to groundmass plagioclase crystals and probably crystallized at the same time. In the other analyzed andesite (sample 92), plagioclase cores vary from An_{30} to An_{65} and show both normal and reverse zoning to rims of An_{35-42}. In this sample, two crystals of An_{35-40} are intergrown with a completely oxidized amphibole pseudomorph, suggesting they originally crystallized in a more silicic and more hydrous melt. Also present in this sample is plagioclase of An_{69} intergrown with olivine. Both andesites thus contain a wide range of plagioclase core compositions, suggesting that some phenocrysts originated from basaltic magma while others originated from rhyodacitic or even rhyolitic magma.

Plagioclase phenocrysts in the analyzed dacite (sample 99) show a much narrower range of composition. This sample is somewhat atypical of the dacite in that it is the most silicic, it contains little basaltic material, and the plagioclase phenocrysts do not exhibit the sieving that is common in the other intermediate rocks. Phenocryst cores range from An_{38} to An_{28} and are both reversely and normally zoned to rims of An_{35} to An_{29} (fig. 6). An An_{55} plagioclase inclusion in forsteritic olivine provides evidence of the basaltic component in this rock.

PYROXENES

Clinopyroxene and orthopyroxene phenocrysts of 2 to 7 mm make up from 1 to 5 percent of many andesite samples (table 1). Relative proportions vary, but

clinopyroxene is usually more common than orthopyroxene. Some clinopyroxene phenocrysts are sieved. Both pyroxenes may occur as euhedral to subhedral crystals in the groundmass. In dacite, orthopyroxene is present as small laths that have V-shaped or swallowtail terminations and skeletal growth forms. In another dacite, clinopyroxene forms rims on resorbed orthopyroxene cores.

Compositions of analyzed pyroxenes are plotted in figure 7 and representative analyses are given in table 4. Clinopyroxene in andesite has lower Ca than that in basalt but is otherwise similar. Most crystals are zoned to more Fe-rich rims, but some orthopyroxene is reversely zoned. The pyroxene projection of Lindsley (1983) shows that many of the Coso Range pyroxene phenocrysts contain more than 10 percent "other" components and thus are not suitable for geothermometry. Tieline orientation shows that the pyroxene in sample 92 represents equilibrium conditions; two pairs yield temperatures near 1,030 °C. The single, comparatively Fe-rich, Cr-poor orthopyroxene in sample 84 definitely was not in equilibrium with Mg- and Cr-rich clinopyroxene in the same rock. This orthopyroxene occurs within a sieved plagioclase phenocryst and apparently was derived from magma more silicic than that from which the clinopyroxene crystallized.

HORNBLENDE

Hornblende crystals as large as 5 mm characterize the dacite and elongate or lathlike aggregates of very fine-grained oxides, which are apparently pseudomorphs after amphibole, are present in some andesite. Amphibole crystals in dacite generally are ovoid and have rims of fine-grained oxides. Sample 99 is an exception and was chosen for microprobe study because its amphibole and biotite phenocrysts are not highly altered. The amphibole is magnesian hastingsite and magnesio-hastingsitic hornblende according to the classification of Leake (1978). All crystals are slightly zoned to rims with higher Fe/Fe + Mg ratios and higher fluorine contents. Representative analyses are presented in table 5; figure 8 compares the composition of Coso amphibole with that of amphibole from some other calc-alkalic volcanic suites.

BIOTITE

Biotite phenocrysts are common constituents of the dacite, forming up to 5 percent of the rock. Biotite occurs as books up to 1 mm thick that commonly contain minute apatite needles. In the single dacite studied with the microprobe (sample 99), the biotite is quite similar to that of the high-silica rhyolitic Bishop Tuff (Hildreth, 1979), although containing slightly more Al and Ti (fig. 9, table 6). Biotite in the dacite is richer in Fe than that in Haiwee Ridge rhyodacite, despite the former's occurrence in a less silicic rock. The Fe/Fe + Mg ratio in biotite is strongly affected by the temperature and oxygen fugacity of the magma from which it crystallized; these biotite compositions suggest either a lower temperature or more reducing conditions for the dacite than for the rhyodacite. Alternatively, the slightly rounded biotite

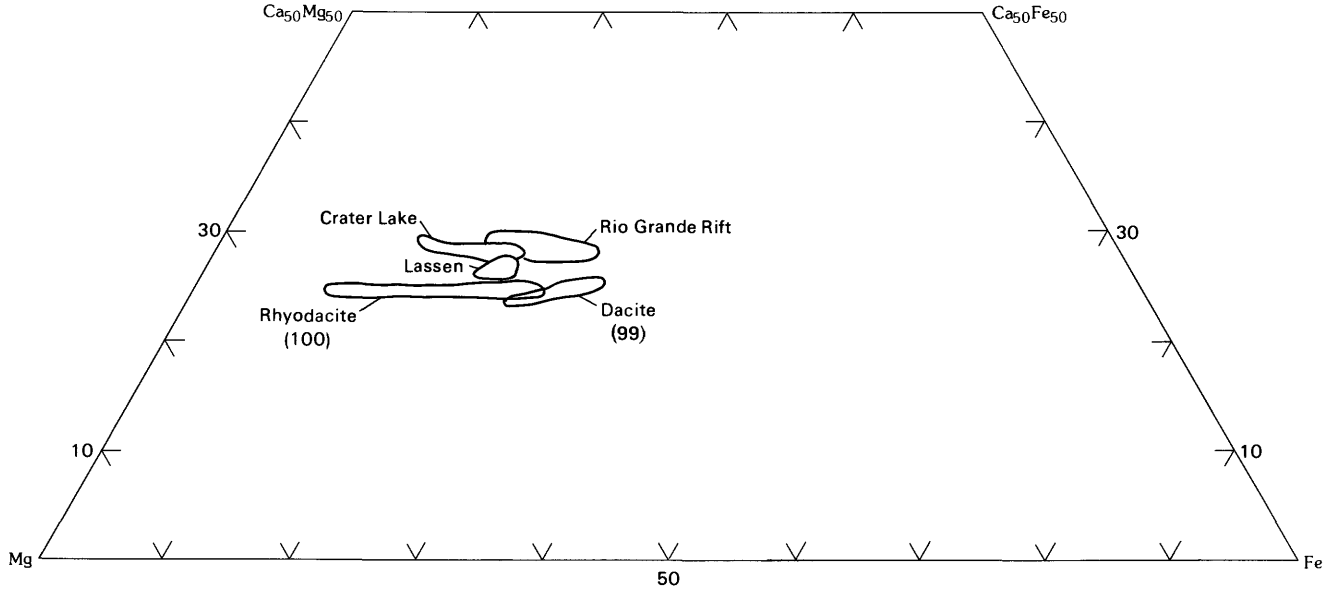

FIGURE 8.—Fields of Ca, Mg, and Fe proportions (atomic basis) of amphibole from samples 99 and 100. Plotted for comparison are compositions of amphibole from Crater Lake rhyodacites (Ritchey, 1979), Lassen dacites (Carmichael, 1967), and Rio Grande Rift andesites (Zimmerman and Kudo, 1979).

phenocrysts may have been derived from a rhyolitic end member of the demonstrably mixed dacite and have been out of equilibrium with the hybrid liquid.

COMMINGLED BASALT-DACITE BOMB

A bomb composed of commingled basalt and dacite (sample 107) is described separately because it contains discrete areas of differing bulk composition and illustrates the process of magma mixing (fig. 10). This specimen is from a polygenetic center located 2 km south of Petroglyph Canyon and 4 km west of Volcano Butte (fig. 1). The 10-cm bomb consists of light-brown dacite and dark olivine basalt interfingered on a scale of centimeters. The groundmass of the basaltic part is composed of randomly oriented plagioclase laths, finely granular pyroxenes and Fe-Ti oxides, and very small patches of brown interstitial glass. Phenocrysts consist of about 5 percent subhedral to euhedral plagioclase, some crystals of which are finely sieved, and about 2 percent microphenocrysts of olivine. Most olivine is in small bipyramidal crystals with square or elongate central voids that represent sections of hopper-shaped crystals. Some larger olivine crystals with dendritic terminations are also present.

The dacitic part of sample 107 consists dominantly of greenish-brown glass containing about 15 percent plagioclase phenocrysts. Plagioclase phenocrysts are both larger and more abundant in the dacite than in the basalt. A few crystals have finely sieved zones around their margins, but most are clear. Approximately 5 percent of the dacite consists of aggregates of fine-grained oxides in lathlike or oval patches set in plagioclase(?). The oxides are arranged in linear arrays parallel to the long axes of the patches. These aggregates are probably pseudomorphs after amphibole, although no relict amphibole remains in them. Vesicles in the glass are associated with the pseudomorphs, but are rare elsewhere in the rock. Fine-grained granular clinopyroxene forms less than 1 percent of the dacite, and a single resorbed quartz crystal was observed.

The contact between the two rock types is sharp but crenulate, the basalt convex toward the dacite. This form of contact is typical of mafic inclusions in silicic volcanic rocks (see Bacon and Metz, 1984), including many Pliocene dacites of the Coso volcanic field, and probably results from differences in surface tension and viscosity of the two magmas. The basalt of the bomb could be an erupted mafic inclusion. Mafic inclusions are believed usually to crystallize at depth after incorporation into cooler silicic magma, and their groundmass textures generally reflect crystallization at substantial undercooling. Because such textures are lacking in the bomb, we believe it represents concurrent venting of basaltic and dacitic magmas.

Between the two rock types in the bomb is a zone about 0.25 cm wide that appears to be a zone of reaction or diffusive mixing. This zone consists of an interlocking mass of minute plagioclase laths with scattered clinopyroxene crystals and rare olivine. It appears tex-

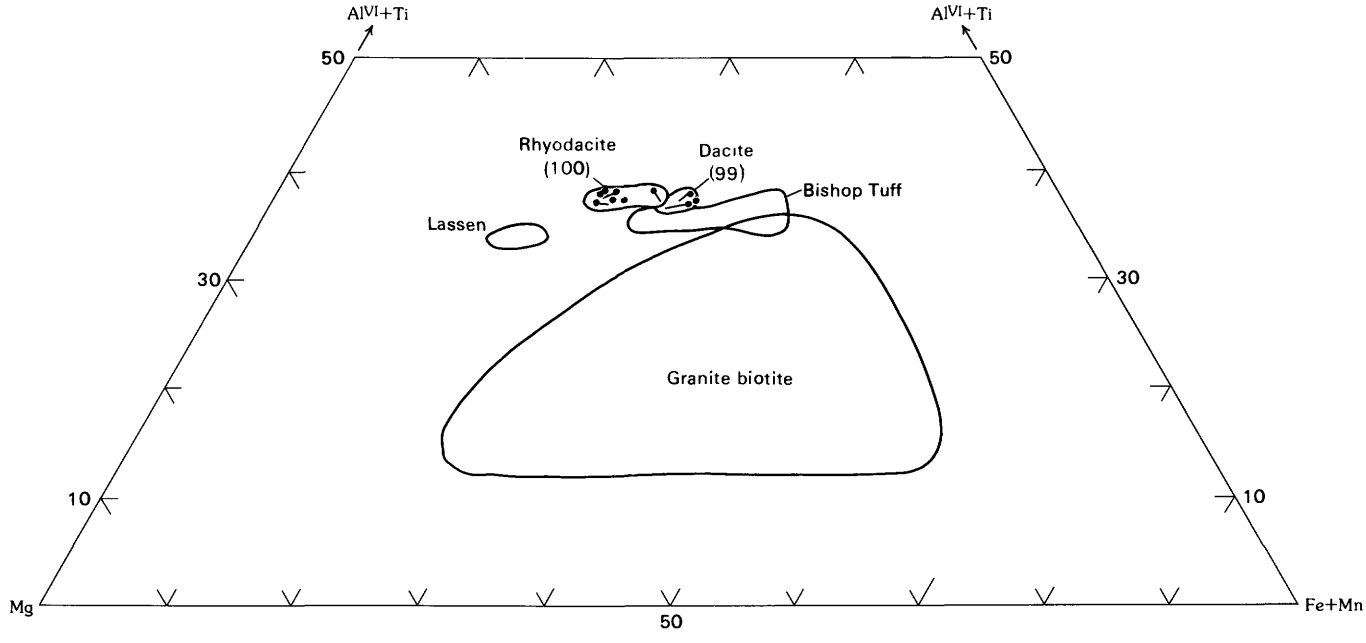

FIGURE 9.—Mg, Al^{VI} + Ti, and Fe + Mn proportions (atomic basis) in biotite of dacite (sample 99) and rhyodacite (sample 100). Solid points are core composition; lines extend to rim composition. Plotted for comparison are compositions of biotite in Lassen dacites (Carmichael, 1967), the Bishop Tuff (Hildreth, 1977), and granitic biotite (Foster, 1960).

turally similar to the basalt groundmass, but is lighter colored and lacks fine-grained oxides.

Rounded phenocrysts from the dacite occur in the basalt singly or in clusters or trains linked with dacitic glass. One elongate group of quartz and plagioclase phenocrysts is surrounded by a lighter colored aureole similar to the reaction or mixing zone separating the rock types; small patches of clear dacitic glass remain between the crystals. Rounded and embayed quartz phenocrysts with fine-grained clinopyroxene rims are common in the basalt.

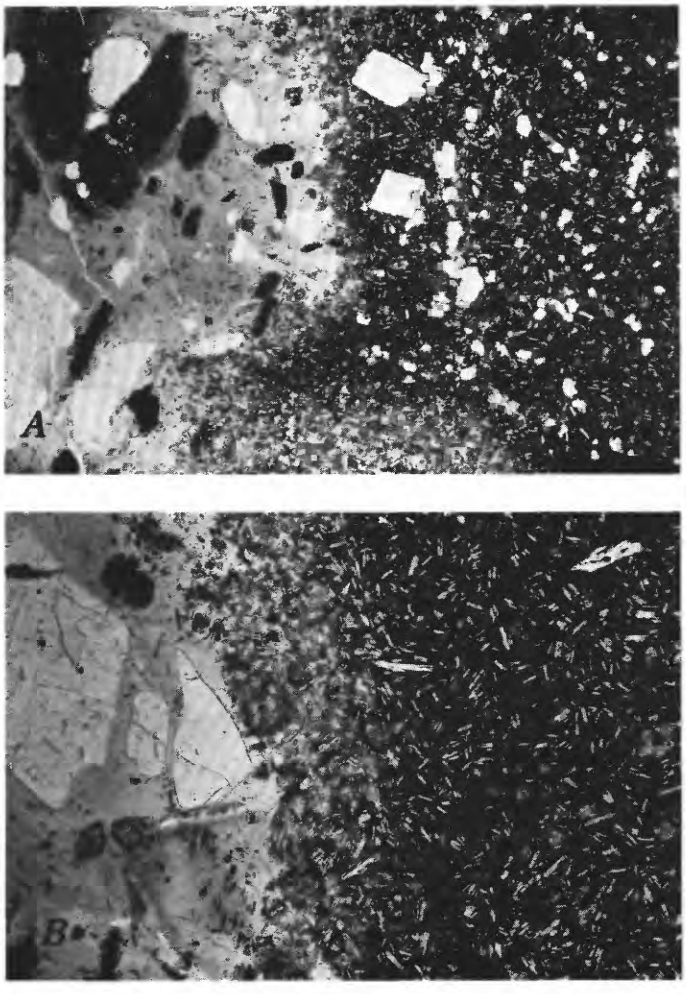

FIGURE 10.—Photomicrographs of commingled basalt-dacite bomb. *A*, Commingled sample 107 showing two rock types in contact. Light area on left is dacite containing phenocrysts of plagioclase and opaque aggregates, which probably are pseudomorphs after amphibole. Note vesicle (clear) between two largest aggregates. Dark area on right is basalt containing phenocrysts of plagioclase. Olivine and clinopyroxene phenocrysts also are present in basalt, but are not visible here. Plane-polarized light; width of view 7 mm. *B*, Detail of reaction zone between two rock types in figure 10A. Dacite on left, basalt on right. Phenocrysts in dacite are plagioclase and small granular olivine. Phenocrysts in basalt are olivine and plagioclase. Note central void in bipyramidal olivine at extreme right. Plane-polarized light; width of view 2.6 mm.

A few crystals in the dacite have been derived from the basalt. The dacite contains a plagioclase phenocryst that has inclusions of deep-red-brown glass similar to that of the basalt. In addition, this crystal has patches of dark glass on its margin that appear to be basaltic groundmass trapped in embayments of the crystal rim. Near this crystal several small olivine grains with clinopyroxene rims form a trail back to the basaltic part of the sample.

Interchange of phenocrysts is also shown by mineral compositions (figs. 4 and 6). Cores of plagioclase crystals within the sample range from An_{65} to An_{28}. The many crystals near An_{30} are mainly in the dacite, but some are in the basalt. The most calcic plagioclase analyzed is a microphenocryst intergrown with olivine that occurs in the dacite. Most of the sodic plagioclase phenocrysts incorporated in the basalt are not sieved.

This bomb speciman documents the textures formed by commingling of differing magmas erupted at the same time. It shows that crystals from different magmas may be intermixed without complete homogenization of the two liquids. The texture of the bomb probably illustrates syneruptive magma mixing, but similar processes may have operated within magma reservoirs and conduits during the formation of many of the intermediate-composition magmas erupted in the Coso volcanic field.

RHYODACITE

Rocks classified as rhyodacite occur in a large complex of flows and domes near Haiwee Ridge and as scattered deposits of air-fall pumice throughout the Coso area (Duffield and others, 1980). The lavas are highly porphyritic, some containing more than 20 percent phenocrysts (figure 3*E* and table 1). Unlike the less silicic rocks, the rhyodacite consistently has a glassy groundmass. Plagioclase phenocrysts are very abundant and generally coarsely sieved, the sieve pockets containing silicic glass. Rounded quartz phenocrysts are present in the more silicic samples of rhyodacite. Mafic phenocrysts consist of euhedral hornblende and biotite, which may contain oxide, zircon, or apatite inclusions. The glassy groundmass is generally crowded with microlites of most of the above minerals.

PLAGIOCLASE

Plagioclase phenocrysts of 1 to 5 mm make up 10 to 20 percent of the rhyodacites. Most plagioclase phenocrysts are euhedral and coarsely sieved. A few relatively small phenocrysts lack sieve texture and are rounded.

The composition of plagioclase phenocrysts in the rhyodacite studied with the microprobe (sample 100)

varies widely, cores ranging from An_{28} to An_{62} (fig. 6). Both normally and reversely zoned crystals are present. The most calcic and the most sodic crystals are normally zoned, but zoning of intermediate-composition phenocrysts can be either normal or reverse. Some of the phenocrysts show oscillatory zoning. Many of the intermediate-composition crystals have rim compositions from An_{39} to An_{42}, while others, along with the most calcic crystals, have rim compositions from An_{51} to An_{56}. A sharply euhedral microphenocryst is An_{39}. The intermediate-composition phenocrysts are generally euhedral and sieved. Sodic phenocrysts with rims near An_{30} and crystals with cores more calcic than about An_{52} are nonsieved and tend to be rounded as though partially resorbed. Hornblende is intergrown with or included in crystals spanning the entire compositional range, and more magnesian hornblende is associated with more calcic plagioclase.

The texture of the coarsely sieved plagioclase phenocrysts is unique to the rhyodacite. Most of the sieve pockets, which can be as large as 0.5 mm, are filled with glass, commonly appearing similar to the light brownish glass of the groundmass (fig. 3*F*). Some of the larger plagioclase phenocrysts have biotite, hornblende, Fe-Ti oxide, apatite, or zircon microphenocrysts trapped within large glass inclusions. Boundaries of the inclusions may be straight and show sides that parallel faces of the host crystal. A few biotite inclusions have step like outlines that mimic the shape of nearby glass inclusions; some groups of such biotite inclusions are in optical continuity, indicating they form part of a single crystal intimately intergrown with the surrounding plagioclase. Some coarsely sieved phenocrysts are composed of a few adhering skeletal plagioclase crystals with an overall euhedral shape. These may enclose euhedral earlier-formed plagioclase or glass inclusions containing ferromagnesian phases. Some of these plagioclase phenocrysts have a crude hopper shape, and appropriate sections show a core of glass surrounded by inward-projecting euhedrally terminated tablets within a rectangular euhedral ring of plagioclase. These textural features suggest that the glass inclusions in coarsely sieved plagioclase are primary and thus represent a growth feature (Hibbard, 1981; Kuo and Kirkpatrick, 1982) rather than resorption. Similar textures in granitic rocks Hibbard (1981) attributed to skeletal growth following mixing of magmas.

Partial microprobe analyses indicate that glass inclusions within large coarsely sieved plagioclase phenocrysts have compositions that are nearly identical to those of groundmass glass immediately adjacent to the phenocrysts. They are severely depleted in CaO and are richer in K_2O and SiO_2 than would be expected of glass produced by partial melting of the plagioclase or influx of reacting liquid. The highly silicic glass in the sieve pockets probably formed, in the same manner as that in the groundmass, from local domains of residual liquid that was depleted in plagioclase components, particularly anorthite, owing to comparatively slow diffusion of Al in the melt during rapid phenocryst growth.

The wide range of plagioclase phenocryst core compositions in the rhyodacite argues for contamination or mixing of different magmas. Crystals that were in equilibrium with a given melt should be zoned to a similar rim composition, and the large number of rims of An_{51} to An_{55} suggests that these rims crystallized at the same time from the same melt (fig. 6). Note that both normally and reversely zoned crystals are included. A number of crystals also have compositions that converge to a more sodic rim composition near An_{40}. There may have been two (or more) mixing episodes causing rims to crystallize toward different compositions at different times. The absence of relict plutonic microxenoliths and lack of evidence for deformation in crystals argues against a wallrock xenocrystic origin for any of the plagioclase. Most likely the more calcic plagioclase phenocrysts originated in relatively mafic (dacitic?) magma that underlay the more silicic magma. Convective mixing could have introduced these comparatively refractory crystals into the silicic melt, causing them to partially dissolve and resulting in the observed rounded forms.

ALKALI FELDSPAR

A single large crystal of alkali feldspar was found in sample 102. Resorbed and optically slightly zoned, the crystal shows exsolution lamellae that might suggest a wallrock xenocrystic origin. We infer that this xenocryst was derived from rhyolitic magma that mixed with the rhyodacitic magma.

AMPHIBOLE

Large green-brown pleochroic, euhedral 1 to 3 mm phenocrysts of amphibole form up to 3 percent of the rhyodacite. Smaller crystals are present throughout the glassy groundmass and commonly are included in plagioclase phenocrysts. Representative amphibole analyses are given in table 5. Amphiboles in the Coso rhyodacite is classified as magnesian hastingsite in the scheme of Leake (1978). Figure 8 compares the Coso amphibole to those of Lassen dacites (Carmichael, 1967) and of andesites of Mount Mazama (Ritchey, 1979) and the Rio Grande Rift (Zimmerman and Kudo, 1979). Coso amphibole is notably lower in Ca than those from the other localities. The Fe/Fe + Mg ratio for amphibole in the rhyodacite (sample 100) is highly variable but generally lower than amphibole in the dacite (sample 99). This is opposite to the Fe/Fe + Mg relations of the rocks

and is consistent with the inference that the amphibole in the dacite originated in more silicic magma.

A relationship exists between the compositions of amphibole and coexisting plagioclase in the dacite and rhyodacite studied. Figure 11 shows compositions of pairs of crystals in contact with each other. The plot indicates that Mg-rich amphibole coexists with calcic plagioclase and Fe-rich amphibole with sodic plagioclase. Note that crystals in the rhyodacite (sample 100) span a wide compositional range. This suggests a protracted crystallization history for this phenocryst-rich lava, with the various mineral pairs forming at different times as the magma evolved to a more silicic composition. Alternatively, the different mineral pairs could have formed in different parts of a compositionally zoned magma reservoir and subsequently been brought together by convective mixing. The relationship between amphibole and plagioclase compositions also suggests that the spread in phenocryst composition is not due to contamination by wallrock materials. The fact that plagioclase phenocrysts of different compositions are separate entities, not joined together or overgrown in compositional sequence, argues against their origin in a protracted crystallization history and favors the convective mixing hypothesis.

BIOTITE

Biotite phenocrysts occur as euhedral brown books up to 1 mm thick that make up 1 to 5 percent of the rock. Most are strongly pleochroic from chocolate brown to a lighter reddish brown, and some are sieved, showing a texture similar to the clinopyroxene in the intermediate rocks. Many biotite phenocrysts contain minute crystals of zircon and apatite. Biotite commonly is present also as small inclusions in plagioclase and as microlites scattered throughout the glassy groundmass of the rhyodacite. Compositions of biotite from the rhyodacite are given in table 6 and plotted in figure 7, where they are compared to those of the Coso dacites and to biotite in some other volcanic suites. Biotite in the rhyodacite is quite similar to that in the dacite, having only slightly higher TiO_2 and Na_2O contents. The crystals are slightly zoned to rims that are lower in total Fe and higher in F. The Coso biotite is lower in F and Cl than biotite from the Bishop Tuff (Hildreth, 1977) and has a more restricted compositional range.

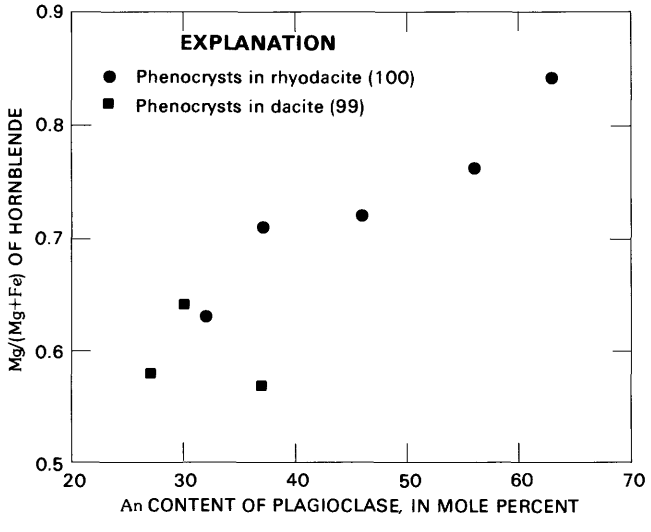

FIGURE 11.—Mg/Mg + Fe in amphibole (atomic basis) vs. anorthite content of coexisting plagioclase in dacite and rhyodacite.

Fe-Ti OXIDES

Both ilmenite and magnetite are present in the rhyodacite but make up less than 1 percent of the rock. They occur as minute (less than 0.01 mm) euhedral titanomagnetite and subhedral ilmenite microphenocrysts scattered throughout the groundmass and as inclusions in other phenocryst phases. Microprobe analyses of these crystals yielded low oxide totals and are not presented here. The low totals may be due to submicroscopic hematite intergrowths, formed during oxidation of the oxide grains, although the rock is unaltered apart from hydration of the glass. Oxide composition is much less varied than in the dacite, suggesting that the crystals may have been in equilibrium at one time and variations are now mainly due to differences in alteration. Minor elements vary somewhat both in ilmenite and in titanomagnetite.

ACCESSORY PHASES

The rhyodacite contains tiny needles of apatite as inclusions in most, if not all, phenocryst phases. Zircon is a less abundant companion that also can be found in the groundmass. Very rare allanite has been identified intergrown with hornblende in sample 106, the most differentiated rhyodacite.

RHYOLITE

Rocks classified as rhyolite occur locally as ash-flow and air-fall tuffs on Haiwee Ridge (Duffield and others, 1980). White cellular pumice in these rocks contains about 5 percent euhedral phenocrysts of quartz, plagioclase, and sanidine and less than 1 percent each of biotite, titanomagnetite, and ilmenite. Compositions of plagioclase ($An_{18.5}$ $Ab_{79.4}$ $Or_{2.1}$) and sanidine ($An_{0.6}$ $Ab_{26.5}$ $Or_{72.9}$) have been determined by Bacon and others (1982). Microprobe analyses of ilmenite and titanomagnetite crystals in a mineral concentrate from the pumice yielded low oxide totals similar to those of Fe-Ti oxides in the previously described rhyodacite samples. The sole analyzed ilmenite crystal has much more

MnO and less MgO and Al_2O_3 than ilmenites in the rhyodacite. Titanomagnetite also has relatively high MnO and low MgO, Al_2O_3, and TiO_2 contents. These compositional differences are consistent with the oxide minerals in the rhyolite having crystallized in a relatively low-temperature, differentiated rhyolitic melt.

COMPOSITIONAL VARIATION

A broad spectrum of magmas ranging from basaltic to rhyolitic was erupted during the Pliocene volcanic episode in the Coso Range. In the following sections we describe the compositional variations of the Coso suite as a whole, but it should be kept in mind that these rocks represent magmas erupted over a long time interval and across a broad area. Major- and trace-element analyses are given in table 7 (see fig. 2 and table 10 for sample localities). Compositionally similar volcanic rocks have been described from several other areas in the western United States. Analyses of some of those rocks are presented in table 8 for comparison. Particularly pertinent to the present discussion is the study of Doe and others (1969) on basalt of the southern Rocky Mountains. These authors document contamination of basalt by crustal material and show that this type of contamination can produce quartz-bearing intermediate-composition lavas quite similar to those of the Coso volcanic field. Chemical analyses of volcanic rocks from areas near the Coso Range appear in papers by Ross (1970) and Moore and Dodge (1980).

MAJOR ELEMENTS

A plot of total alkalis and CaO against SiO_2 (fig. 12) shows that the Pliocene Coso volcanic suite is calc-alkalic, with an alkali-lime index (Peacock, 1931) of 60. This plot also demonstrates that according to the alkalic-subalkalic division of Miyashiro (1978), the Coso basalts are alkalic to transitional. Most of the basalt is hypersthene normative, but some of the most mafic samples contain small amounts of normative nepheline (<2 percent). All Coso rocks with more than 54 percent SiO_2 are quartz normative. Small amounts of corundum (<2 percent) appear in the rhyodacite and rhyolite norms, probably because alkalis were selectively depleted during hydration of these glassy rocks, leaving excess Al_2O_3.

Oxide variation diagrams for the Coso suite (fig. 13) show roughly linear trends with much scatter in basalt and andesite. This is partially due to the fact that SiO_2 makes up an increasing percentage of the silicic rocks, allowing less scatter in the other oxides. However, we suggest that much of the scatter is due to mixing of variably fractionated basaltic magma with silicic magma. Several diagrams (CaO, Na_2O, P_2O_5) have slight inflections below about 53 percent SiO_2, suggesting that crystal fractionation produced chemical variation in the basalt. Both MgO and Al_2O_3 are extremely variable in the basalt and andesite; variation in MgO, particularly in andesite may be attributed to the combined effects of olivine fractionation in a basaltic end member and addition of an MgO-poor silicic contaminant. Na_2O varies about a subhorizontal line but decreases, probably because of Na loss during hydration of glass, in rhyodacite and rhyolite.

Crystal fractionation from a single parent composition should produce well-defined curved paths on variation diagrams because the oxides are removed at different rates at different stages depending on which phases are crystallizing. On the other hand, mixing of two different magma compositions should produce linear trends, the position of a point depending on the proportions of the end members. The well-defined linear trends on most of the plots of Coso data (for example, K_2O, CaO) strongly suggest mixing was important in producing compositional variations. Curvature and scatter in other diagrams (for example, MgO, Al_2O_3) suggest that multiple end members, variable amounts of contamination by crustal melts, and some degree of crystal fractionation all contributed to the overall variations in the Coso suite.

The plot of P_2O_5 against MgO (fig. 14) is useful for demonstrating mixing versus fractionation processes. Varying degrees of partial melting or fractional crystallization should produce a systematic increase of P_2O_5 with decreasing MgO, followed by decreasing P_2O_5 in fractionated magmas once melts become saturated with apatite; mixing of silicic and basaltic magmas would tend to produce a covariance. The wide range of P_2O_5 contents in Coso rocks with more than 5 percent MgO argues that neither crystal fractionation nor varying degrees of partial melting was the only process responsible for variation in the basalt and mafic andesite. The low-P_2O_5, intermediate-MgO rocks probably formed by addition of silicic material, and the high-P_2O_5 basalts can be explained by partial melting or crystal fractionation. The very high-P_2O_5, intermediate-MgO rocks (basalt of Rose Valley (Duffield and Bacon, 1981) = andesites with >1.2 percent P_2O_5) probably cannot be explained by extreme fractionation, but may call for either unusual parent magmas or contamination with unusual materials. The decrease in P_2O_5 with decreasing MgO in rhyodacite reflects crystal fractionation of apatite, which is common as inclusions in phenocryst phases (table 1).

An important feature of the variation diagrams (figs. 13 and 14) is the compositional gap between the

TABLE 7.—*Chemical analyses of Coso Range Pliocene volcanic rocks*

[Major elements determined at Reston Rapid Rock Analysis Laboratory of the U.S. Geological Survey by methods described under "single solution" by Shapiro (1975); analysts: K.Coates, Z.A. Hamlin, N. Skinner, and H. Smith. Trace elements determined by instrumental neutron activation analysis at the U.S. Geological Survey, Reston, Virginia; analyst: P.A. Baedecker. SiO_2^* = SiO_2 recalculated with analysis normalized to total 100 percent volatile free and with atomic $Fe^{+2}/Fe^{+2}+Fe^{+3}$ = 0.86]

Sample No.----	64	65	66	67	68	45	69	56	70	71	72	63	73	74	75	76
SiO_2*----------	49.5	50.0	50.1	50.3	50.4	50.8	50.8	51.0	51.0	51.5	51.7	51.8	52.1	52.5	52.6	52.7
Major elements, in weight percent																
SiO_2---------	48.6	49.1	50.2	49.5	50.0	50.6	50.0	50.5	49.8	50.5	50.9	51.6	51.6	52.0	52.4	52.7
Al_2O_3--------	17.0	16.8	16.8	16.9	18.1	16.5	15.5	17.0	18.2	16.5	16.5	17.2	18.5	16.0	16.2	18.3
Fe_2O_3--------	4.6	3.6	1.5	2.5	2.6	3.5	6.9	3.2	5.6	4.9	2.5	2.0	3.0	3.3	3.4	3.1
FeO---------	4.8	6.1	7.5	6.2	5.3	5.0	3.9	5.2	2.8	3.7	6.0	6.0	5.0	4.0	5.0	4.8
MgO---------	7.0	7.5	8.9	7.4	5.9	7.8	5.4	6.9	5.2	5.9	6.8	6.7	5.3	7.5	7.6	5.5
CaO---------	9.3	9.6	9.5	10.2	10.5	9.9	10.2	9.8	8.8	10.2	9.3	9.5	8.1	9.9	8.5	8.1
Na_2O--------	3.5	3.2	3.3	3.5	3.5	3.3	3.8	3.7	4.1	3.8	3.6	3.8	4.3	3.3	3.4	4.3
K_2O---------	1.3	.62	.71	.67	1.5	1.4	.82	1.2	1.3	.91	1.0	.88	1.4	1.5	1.4	1.4
H_2O^+--------	.40	.33	.28	.25	.23	.36	.46	.21	.93	.33	.34	.28	.28	.47	.45	.26
H_2O^---------	.21	.17	.23	.21	.17	.08	.27	.23	.55	.32	.18	.12	.38	.34	.47	.16
TiO_2--------	1.8	1.4	1.3	1.3	1.4	1.3	1.9	1.2	1.8	1.4	1.4	1.5	1.6	1.2	1.4	1.5
P_2O_5--------	.47	.29	.29	.30	.41	.43	.38	.33	.47	.44	.35	.39	.36	.50	.42	.38
MnO---------	.12	.12	.12	.12	.11	.12	.16	.13	.11	.13	.13	.11	.11	.11	.11	.11
CO_2---------	.09	.23	.07	.04	.04	.02	.03	.02	.09	.09	.02	.02	.05	.06	.06	.04
Total-----	99.19	99.06	100.70	99.05	99.76	100.31	99.72	99.62	99.75	99.12	99.02	100.10	99.98	100.18	100.81	100.65
Trace elements, in parts per million																
Sc----------	-	30.5	30.5	-	27.0	28.8	-	26.3	21.0	-	-	25.0	-	25.5	-	21.8
Cr----------	-	207.1	300.2	-	50.4	222.4	-	138.2	58.4	-	-	153.6	-	264.2	-	94.1
Co----------	-	40.5	42.4	-	29.3	35.5	-	32.3	28.6	-	-	30.2	-	30.4	-	29.8
Zn----------	-	114	118	-	110	111	-	110	102	-	-	115	-	112	-	103
Rb----------	-	60	50	-	50	70	-	50	26	-	-	40	-	50	-	24
Zr----------	-	600	500	-	160	500	-	500	190	-	-	290	-	500	-	270
Cs----------	-	3	3	-	2	3	-	2	2	-	-	2	-	2	-	2
Ba----------	-	284	495	-	952	1020	-	724	685	-	-	539	-	968	-	533
La----------	-	12	14	-	26	25	-	20	30	-	-	20	-	32	-	20
Ce----------	-	26	32	-	54	52	-	39	62	-	-	41	-	62	-	44
Nd----------	-	14	16	-	29	29	-	25	32	-	-	25	-	30	-	23
Sm----------	-	4.1	4.4	-	5.7	5.6	-	1.7	6.3	-	-	5.0	-	5.9	-	4.9
Eu----------	-	1.23	1.26	-	1.52	1.47	-	1.23	1.81	-	-	1.44	-	1.33	-	1.50
Gd----------	-	3.6	3.7	-	4.8	3.8	-	3.5	5.2	-	-	4.2	-	3.1	-	4.8
Tm----------	-	.34	.33	-	.33	.24	-	.33	4.2	-	-	.33	-	.25	-	.51
Yb----------	-	2.9	2.7	-	2.1	2.1	-	2.4	2.2	-	-	2.2	-	1.9	-	2.5
Lu----------	-	.38	.39	-	.33	.29	-	.34	.32	-	-	.31	-	.27	-	.35
Hf----------	-	3.0	2.8	-	4.1	3.9	-	3.5	4.5	-	-	3.5	-	3.3	-	4.5
Ta----------	-	.48	2	-	.51	.38	-	.64								
Th----------	-	.6	1.3	-	2.3	2.4	-	2.2	2.4	-	-	1.2	-	2.7	-	2.0
U----------	-	.9	.9	-	7	-	-	.9	2	-	-	2	-	1.1	-	.8

TABLE 7.—*Chemical analyses of Pliocene volcanic rocks of the Coso Range*—Continued

Sample No.	77	78	79	80	81	82	83	84	85	40	86	87	88	89	62	90
SiO_2*	53.5	53.5	53.6	54.5	54.5	54.5	55.1	55.2	55.3	56.5	56.7	56.7	56.9	57.2	57.5	57.8
Major elements, in weight percent																
SiO_2	52.6	53.3	52.9	53.4	53.6	54.1	54.0	55.1	55.1	56.9	57.0	56.7	56.8	56.3	58.0	57.2
Al_2O_3	18.9	19.5	16.3	16.7	17.3	18.7	17.6	16.4	16.7	17.4	16.8	16.7	16.3	16.6	16.8	16.6
Fe_2O_3	2.7	2.8	5.4	2.0	2.6	3.3	3.5	3.2	3.6	1.9	1.8	1.7	1.4	2.4	2.1	2.0
FeO	3.8	4.1	4.0	5.6	5.0	3.2	3.3	4.6	3.2	4.3	4.5	4.6	4.2	4.0	4.4	4.2
MgO	5.0	4.9	4.8	3.6	3.5	5.0	5.2	6.2	5.6	5.5	5.4	5.3	7.3	5.1	5.3	4.6
CaO	8.2	7.8	7.4	6.8	6.8	7.4	7.3	7.1	8.7	7.6	8.2	7.7	7.0	7.1	6.4	6.9
Na_2O	4.0	4.2	3.7	4.2	4.1	4.2	4.3	3.6	3.6	3.9	3.6	3.9	3.7	3.8	4.2	4.2
K_2O	1.7	1.6	1.9	2.5	2.5	2.0	1.6	1.9	1.9	1.8	1.9	1.9	2.0	1.9	2.2	1.8
H_2O^+	.40	.42	.40	.39	.73	.66	.71	.38	.60	.26	.42	.48	.14	.78	.10	.41
H_2O^-	.19	.30	.42	.52	.51	.34	.74	.44	.33	.32	.24	.23	.22	.23	.16	.24
TiO_2	1.2	1.2	2.0	1.7	1.6	1.3	1.1	1.4	1.0	1.1	.98	1.2	.89	.99	1.2	1.1
P_2O_5	.32	.27	.58	1.5	1.3	.28	.27	.50	.36	.26	.34	.29	.20	.26	.34	.31
MnO	.09	.09	.15	.12	.12	.11	.09	.11	.09	.08	.08	.08	.07	.09	.09	.09
CO_2	.10	.01	.03	1.7	-	.03	.06	.08	.02	.02	-	.09	.02	.07	.03	.01
Total	99.20	100.49	99.98	100.73	99.66	100.62	99.77	101.01	100.80	101.34	101.26	100.87	100.24	99.62	101.32	99.66
Trace elements, in parts per million																
Sc	-	17.6	-	-	14.1	18.3	19.3	19.0	-	-	20.8	-	-	-	16.5	16.3
Cr	-	24.9	-	-	33.4	40.6	43.1	197.1	-	-	81.5	-	-	-	16.5	16.3
Co	-	27.0	-	-	21.3	26.0	27.4	29.2	-	-	22.8	-	-	-	176.9	113.7
Zn	-	95	-	-	105	92	97	103	-	-	97	-	-	-	84	87
Rb	-	23	-	-	80	24	50	21	-	-	25	-	-	-	22	80
Zr	-	190	-	-	250	210	500	270	-	-	180	-	-	-	320	400
Cs	-	.5	-	-	3	2.0	2.0	2.0	-	-	0.6	-	-	-	2	3.0
Ba	-	863	-	-	711	846	849	995	-	-	1130	-	-	-	874	1030
La	-	16	-	-	36	18	17	32	-	-	31	-	-	-	25	33
Ce	-	32	-	-	67	34	37	63	-	-	60	-	-	-	45	55
Nd	-	18	-	-	34	19	50	29	-	-	32	-	-	-	19	27
Sm	-	4.0	-	-	6.3	3.9	4.1	6.5	-	-	5.6	-	-	-	4.9	5.0
Eu	-	1.15	-	-	1.48	1.12	1.22	1.55	-	-	1.43	-	-	-	1.15	1.38
Gd	-	4.1	-	-	4.5	3.1	3.0	4.0	-	-	4.6	-	-	-	3.2	3.5
Tm	-	.30	-	-	.32	.29	.26	.32	-	-	.28	-	-	-	.31	.29
Yb	-	1.8	-	-	2.6	1.7	1.6	2.0	-	-	1.7	-	-	-	2.3	1.9
Lu	-	.25	-	-	.34	.24	.24	.31	-	-	.23	-	-	-	.32	.26
Hf	-	3.0	-	-	4.6	3.5	3.4	4.0	-	-	3.3	-	-	-	4.5	4.1
Ta	-	.47	-	-	1.63	.51	.56	1.07	-	-	.46	-	-	-	1.12	.68
Th	-	1.3	-	-	4.4	1.8	1.7	2.9	-	-	3.3	-	-	-	3.8	2.8
U	-	2.0	-	-	1.8	0.6	-	1.1	-	-	0.9	-	-	-	1.2	.8

TABLE 7.—*Chemical analyses of Pliocene volcanic rocks of the Coso Range*—Continued

Sample No.----	91	92	93	94	95	96	97	98	99	100	101	102	103	104	105	106	44
SiO_2*----------	58.8	59.7	61.3	61.4	62.1	63.4	63.7	64.0	66.0	67.5	68.3	68.7	68.9	68.9	69.4	70.4	76.2
Major elements, in weight percent																	
SiO_2--------	57.0	59.0	60.5	60.9	61.6	63.0	63.0	63.6	62.6	66.4	65.7	67.3	66.1	67.0	66.9	68.5	74.0
Al_2O_3-------	16.2	15.3	16.8	16.8	16.5	16.2	16.3	16.5	15.0	15.9	15.5	15.8	15.5	15.8	14.9	15.5	13.1
Fe_2O_3-------	1.6	2.1	1.3	1.5	1.1	1.6	1.4	1.2	2.9	1.3	1.5	1.4	1.2	1.0	1.4	1.2	.45
FeO---------	4.0	3.0	3.4	3.2	3.1	2.6	2.6	2.6	.12	1.8	1.6	1.4	1.6	1.5	1.2	.92	.20
MgO---------	3.2	6.5	3.6	3.5	4.3	3.5	3.2	3.2	2.4	1.5	1.3	1.3	1.2	1.1	1.1	.81	.10
CaO---------	8.0	6.0	5.2	6.1	5.0	4.8	4.5	4.3	4.5	3.4	3.5	3.0	3.0	2.9	2.7	2.4	.84
Na_2O--------	3.7	3.7	4.0	3.7	4.0	4.1	3.7	4.1	3.6	3.9	3.4	3.8	3.3	3.9	3.0	3.8	3.1
K_2O---------	1.9	2.3	2.8	2.6	2.6	2.7	3.3	3.0	3.2	3.4	3.1	3.4	3.4	3.5	4.6	3.8	5.2
H_2O^+--------	1.1	.53	.91	1.1	.63	.72	1.1	1.4	2.0	1.8	3.7	2.0	3.2	2.2	2.6	2.1	3.4
H_2O^---------	.48	.50	.33	.25	.12	.52	.35	-	1.1	.15	.53	.24	.47	.21	.28	.35	.44
TiO_2---------	1.0	.79	.87	.72	.74	.73	.68	.68	.50	.58	.54	.46	.50	.44	.48	.34	.09
P_2O_5--------	.31	.21	.21	.25	.22	20	.20	.19	.18	.20	.15	.03	.16	.15	.15	.13	.04
MnO---------	.08	.07	.06	.06	.05	.05	.05	.04	.03	.06	.04	.04	.04	.03	.04	.02	.04
CO_2--------	.90	.02	.03	.01	.06	-	.11	.01	.80	.03	.01	.05	.02	-	.04	.06	.03
Total-----	99.47	100.02	100.01	100.69	100.02	100.72	100.49	100.82	98.93	98.47	100.04	98.08	99.2	97.32	96.51	97.48	100.6
Trace elements, in parts per million																	
Sc----------	-	14.1	11.8	13.2	10.4	9.9	-	9.03	5.12	5.18	5.00	-	4.52	4.16	-	3.65	2.19
Cr----------	-	262.2	50.5	56.4	132.6	95.7	-	65.7	15.5	13.1	10.1	-	9.5	10.0	-	8.7	5
Co----------	-	26.8	17.2	14.7	17.8	16.3	-	14.1	6.4	6.2	5.7	-	5.1	4.9	-	4.5	.5
Zn----------	-	81	70	82	69	74	-	72	42	58	56	-	5.1	4.9	-	4.5	.3
Rb----------	-	44	53	24	52	63	-	64	64	71	74	-	76	80	-	87	207
Zr----------	-	120	600	400	170	230	-	400	200	190	300	-	240	200	-	220	120
Cs----------	-	0.7	2	1.0	1.1	1.0	-	1.4	1.3	1.8	1.8	-	2.0	1.9	-	3.2	11.5
Ba----------	-	1400	1230	1270	1180	1330	-	1220	1260	1190	1310	-	1150	1260	-	843	300
La----------	-	21	24	26	21	21	-	24	28	25	23	-	23	25	-	21	8
Ce----------	-	38	45	49	38	41	-	49	50	48	44	-	41	47	-	39	18
Nd----------	-	19	17	21	17	16	-	50	21	20	19	-	19	19	-	16	6
Sm----------	-	3.7	4.0	4.2	3.2	3.6	-	3.6	3.4	3.8	3.5	-	3.1	3.0	-	2.8	1.2
Eu----------	-	.96	1.01	1.01	.88	.90	-	.94	.79	.87	.74	-	.69	.76	-	.68	.13
Gd----------	-	3.4	2.6	2.6	2.8	2.4	-	2.4	2.7	2.6	2.5	-	2.0	2.6	-	2.0	2.0
Tm----------	-	.24	.22	.18	.23	.15	-	.22	.21	.2	.20	-	.14	.20	-	.13	.20
Yb----------	-	1.6	1.3	1.3	1.3	1.1	-	1.3	1.2	1.3	1.1	-	1.0	1.0	-	1.2	1.3
Lu----------	-	.23	.19	.19	.17	.17	-	.19	.18	.18	.15	-	.16	.16	-	.21	.26
Hf----------	-	3.1	3.8	3.4	3.5	3.5	-	4.5	3.5	3.5	3.6	-	3.7	3.8	-	4.1	3.0
Ta----------	-	.43?	.81	.57	.66	.67	-	.78	.81	.93	.84	-	.74	.77	-	1.12	1.9
Th----------	-	2.5	3.6	3.3	3.3	3.6	-	4.5	5.6	5.4	5.4	-	5.6	5.2	-	7.5	14.9
U----------	-	.7	1.4	1.0	1.1	1.4	-	-	1.7	2.2	-	-	2.2	1.8	-	2.8	8.2

rhyodacite and most of the dacite. The single dacite pumice (sample 99) plots at the mafic end of the rhyodacite trend, presumably because it is unique among the analyzed dacite samples in containing a very small basaltic component. The compositional gap may indicate that hybrid magmas with less than some minimum component of basaltic material are unlikely to form in zoned systems for mechanical reasons. Compositional gaps in the dacite range are very common in volcanic systems that produce relatively silicic rocks (Smith, 1979; Hildreth, 1981).

An AFM plot (fig. 15) shows a broad band not unlike trends of other calc-alkaline suites, although the Coso rocks are somewhat lower in Fe than continental margin suites (Gill, 1981). Rhyodacite and rhyolite form a linear array, dacite a tight cluster (excepting the pumiceous sample 99, which has suffered oxidation and Na loss), and basalt and andesite overlapping fields. The scatter in andesite is notable and is mainly due to variation of the Fe/Fe + Mg ratio at constant alkali content. The marked dispersion of the andesite data on figure 15 is probably due to competing effects of crystal fractionation and mixing, superimposed on original variation in basaltic end-member composition. If the dacite was derived in part by mixing, the silicic end member apparently had a lower Fe/Fe + Mg ratio than the erupted rhyodacite.

The $FeO^*/FeO^* + MgO$ ratio plotted against SiO_2 for the Coso Pliocene volcanic rocks shows a broad diffuse pattern that trends subhorizontally from basalt to dacite, but the rhyolite and rhyodacite cluster at comparatively high levels (fig. 12). The lowest $FeO^*/FeO^* + MgO$ ratios occur in andesite and dacite. Such low values are hard to reconcile with fractionation of observed phenocrysts in reasonable proportions but can be explained by addition of a silicic component to relatively primitive basaltic magma. Conversely, andesite and silicic basalt with high $FeO^*/FeO^* + MgO$ ratios might be derived by crystal fractionation. Most of the andesitic rocks, however, would be most readily formed by mixing of moderately differentiated basalt and a silicic component.

TRACE ELEMENTS

Trace-element abundances have been determined by instrumental neutron activation analysis (INAA) for selected samples (table 7).

TRANSITION METALS (Sc, Cr, Co, Zn)

The transition metals Sc, Cr, Co, and Zn tend to be partitioned into early formed crystals during the crys-

TABLE 8.—*Chemical analyses of basalts and andesites from the western United States*
[Oxides in weight percent]

Sample ------	1	2	3	4	5	6	7	8
SiO_2--------	48.4	56.3	50.54	54.25	51.3	56.8	49.2	53.6
Al_2O_3-------	17.4	17.0	15.97	16.40	17.1	14.3	15.7	15.4
Fe_2O_3--------	3.4	5.1	2.81	2.63	2.9	3.0	-	-
FeO----------	5.9	1.8	5.02	4.24	6.1	4.9	[1]10.5	[1]8.5
MgO----------	2.5	4.1	8.96	6.24	6.6	5.6	7.6	6.6
CaO----------	9.1	6.8	9.20	8.04	7.6	6.6	8.7	7.6
Na_2O--------	5.1	4.0	3.50	3.72	4.2	3.5	3.6	3.8
K_2O----------	1.6	2.7	1.51	1.50	1.7	2.4	1.4	1.8
H_2O^+--------	2.7	.66	.13	.68	.25	.43	-	-
H_2O^---------	.17	.12	.14	.28	.10	.47	-	-
TiO_2--------	1.9	1.1	1.36	1.09	1.6	1.3	1.7	1.6
P_2O_5--------	.80	.41	.44	.38	.45	.39	-	-
MnO----------	.12	.12	.14	.12	.14	.12	-	-
CO_2----------	.14	.26	.38	.25	.05	.21	-	-
Total-----	99.23	100.47	100.10	99.82	100.04	100.02	98.4	98.9

1. Trachyandesite caprock, Saline Range, CA (Ross, 1970).
2. Trachyandesite caprock, Saline Range, CA (Ross, 1970).
3. Alkali olivine basalt, Kern volcanic field, CA (Moore and Dodge, 1980).
4. Andesite, Kern volcanic field, CA (Moore and Dodge, 1980).
5. "Primitive" basalt of the Hinsdale Formation, CO (Doe and others, 1969).
6. Very contaminated basalt of the Hinsdale Formation, CO (Doe and others, 1969).
7. Hawaiite, AZ (Best and Brimhall, 1974).
8. Quartz-bearing basaltic andesite, AZ (Best and Brimhall, 1974).

[1] - Total Fe expressed as FeO.

tallization of magmas; consequently, abundances of these elements tend to correlate with one another and to decrease with increasing SiO_2. This trend is generally shown by the Coso rocks (fig. 16). Chromium varies considerably in the basalt because of widely differing proportions of chrome spinel inclusions in olivine phenocrysts (table 1); the most magnesian basalt has Cr contents several times that of less magnesian basalt of the same silica content. The Cr-rich primitive basalt (for example samples 65, 66) also has the lowest abundance of incompatible elements such as K, Ba, and Th.

Rhyodacite has monotonically lower contents of Sc, Cr, Co, and Zn with increasing differentiation. The rhyolite has the lowest abundance of these compatible elements, which are greatly depleted relative to even the most differentiated rhyodacite. The single dacite pumice (sample 99) extends the rhyodacite trend to slightly higher values (fig. 16). Andesite and less differentiated dacite have highly variable compatible-element abundances, and this is reflected particularly well by Cr. Because crystal fractionation should result in rather similar Cr contents for a given degree of differentiation, the only conceivable mechanism for producing this great variation is mixing of silicic magma and relatively primitive Cr-rich basaltic magma.

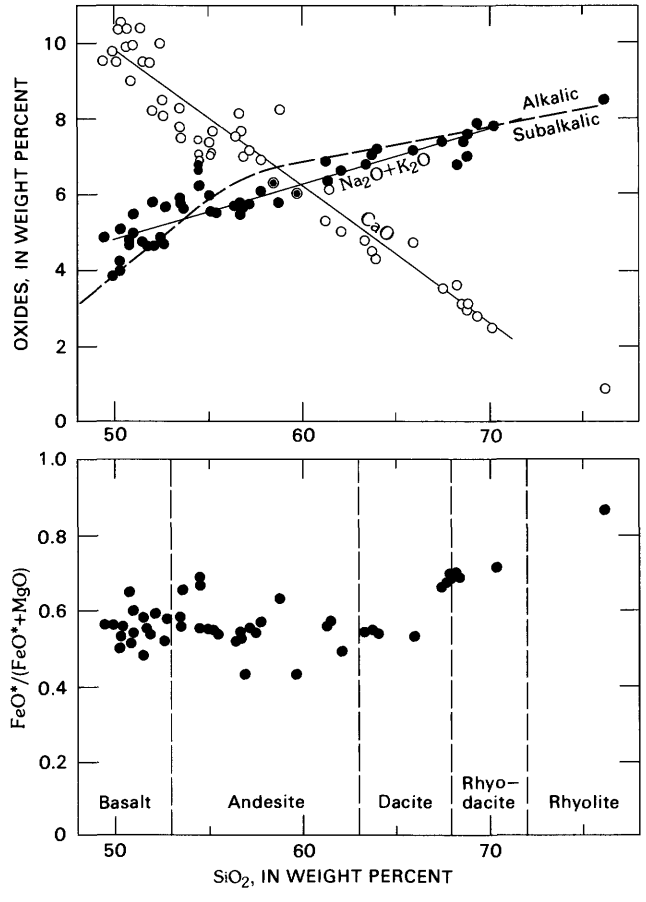

FIGURE 12.—CaO (circles), Na_2O+K_2O (dots), and FeO*/FeO* + MgO (dots) vs. SiO_2 for Pliocene Coso Range volcanic rocks. Alkalic-subalkalic fields (separated by dashed line) from Miyashiro (1978). Crossing point of CaO and Na_2O+K_2O trend lines gives alkali-lime index of 60, indicating that the Coso suite is calc-alkalic (Peacock, 1931).

ALKALI METALS AND ALKALINE EARTHS (Rb, Cs, Ba)

Concentrations of the alkali metals Rb and Cs are high enough to be detected by neutron activation (INAA) only in silicic andesite and more differentiated rocks. Both these elements are present at nearly uniform levels in the rhyodacite and are highly enriched in the rhyolite. Dacite and silicic andesite have lower and variable Rb contents. The same appears to be true of Cs, but the abundance of Cs commonly is below the detection limit.

Barium is the only alkaline-earth trace element determined by INAA. Of the common phenocryst species, only alkali feldspar and biotite have a strong affinity for Ba. Thus Ba would be expected to rise rapidly with differentiation of basaltic magma and drop in silicic melts from which biotite or alkali feldspar was being removed. The plot of Ba versus SiO_2 (fig. 16) confirms this general model, but several complications are worth noting. Some of the most Ba-rich basalt samples also have very high Cr and other compatible-element contents, characteristic of primitive basalt; these lavas also have unusual rare-earth-element patterns. Mixing with silicic magma will not readily explain these chemical characteristics. Barium contents of silicic andesite, dacite, and the less-differentiated rhyodacite are similar, possibly reflecting the opposing effects on silicic magma of separation of biotite and addition of basaltic magma. Like most trace elements in the andesite, Ba shows wide variation at a given SiO_2 content. This is readily explained by the effects of crystal fractionation and of mixing with variably differentiated or contaminated basaltic magma, as will be discussed later with reference to all of the analytical data. Barium content decreases with increasing SiO_2 in the rhyolite and the more differentiated rhyodacite.

RARE EARTHS

The rare-earth elements (REE) La, Ce, Nd, Sm, Eu, Yb, and Lu were determined with acceptable precision in all samples; Gd and Tm also were determined, but results are believed to be less accurate because of inconsistency with those for other REE. In this discussion, light rare earth elements (LREE) are those with atomic numbers less than Eu, and heavy rare earth elements (HREE) are those with atomic numbers greater than Sm. Chondrite-normalized REE abundances are plotted

for different rock types in figure 17. The two most primitive basalt samples (65 and 66) have moderately fractionated REE patterns. They are similar to Pleistocene basalt erupted in the Coso Range (Bacon and Metz, 1984), but have slightly lower LREE and higher HREE contents. Other Pliocene basalt samples that are unfractionated based on high compatible-element contents have higher LREE contents than samples 65 and 66. These LREE-enriched rocks also have higher K_2O, P_2O_5, and Ba contents than the most primitive basalt (for example, samples 68, 74). More extreme enrichments of these elements occur in the ultrapotassic basaltic lavas of the Sierra Nevada studied by Van Kooten (1980).

Dacite and rhyodacite have rather similar REE abundance patterns. Relative to the primitive basalt, they are enriched in LREE and strongly depleted in HREE. The patterns are similar in overall shape to those of many Sierra Nevada granitoids (Dodge and others, 1982), but abundances of all REE are notably lower in the volcanic

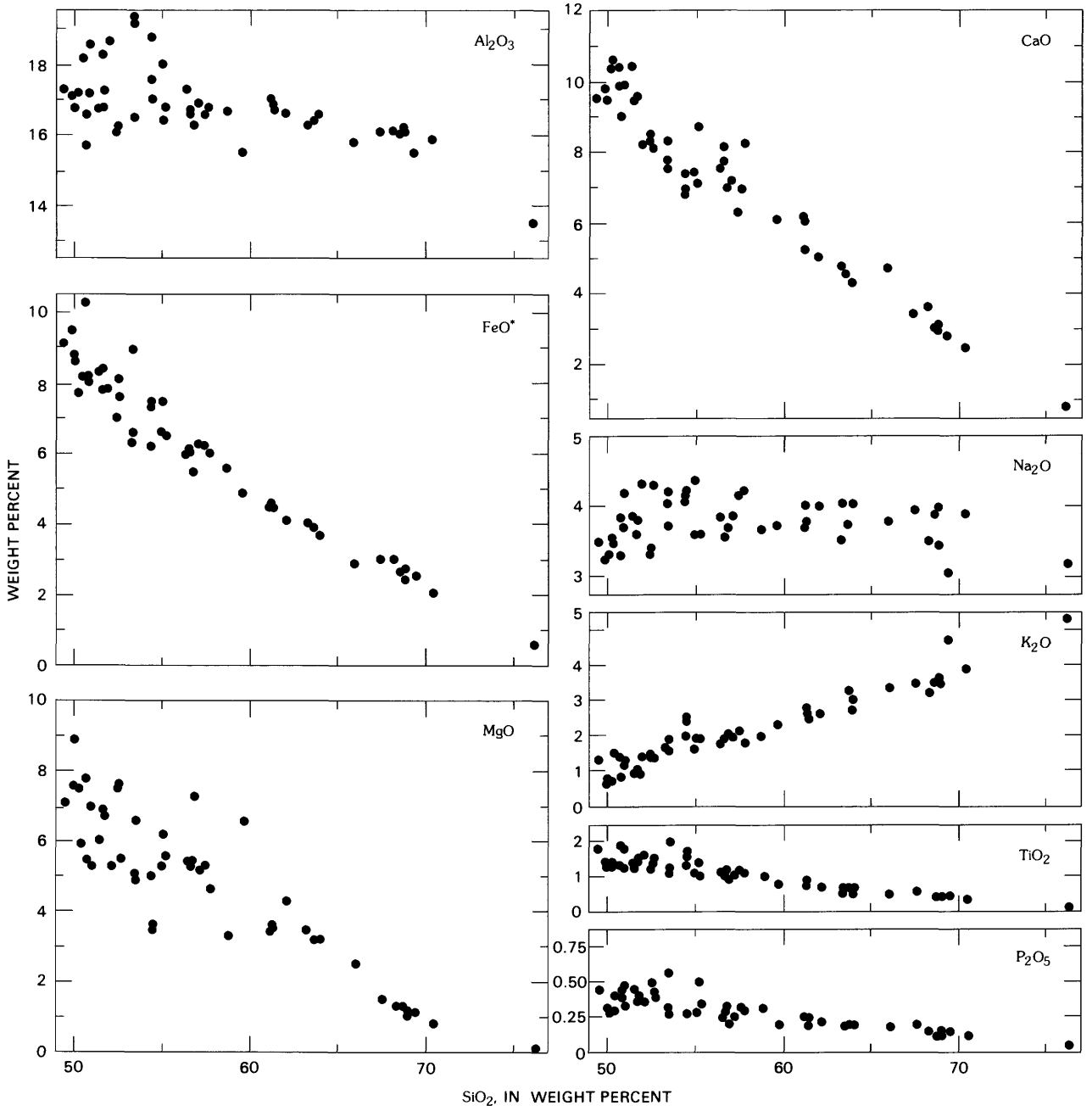

FIGURE 13.—Major-element oxide variation diagrams for Pliocene Coso Range volcanic rocks. Prior to plotting, analyses were recalculated to 100 percent as described in text.

rocks. Patterns for andesite generally are displaced from those of primitive basalt in the same sense as for the silicic rocks, rotating clockwise about a point between Nd and Sm, a feature consistent with an origin involving magma mixing. Absence of a Eu anomaly in all of the lavas except the rhyolite argues against significant plagioclase fractionation.

One mafic andesite (sample 81) is unusual in that it has the highest REE (except Eu) concentrations of any of the analyzed rocks. Its REE pattern is similar in shape to those of some LREE-rich basalt samples, but is displaced upward. The lava flow from which this sample was obtained issued from a vent near the western margin of the volcanic field, in the vicinity of the Sierra Nevada fault zone. Another sample from the same unit (basalt of Rose Valley; Duffield and Bacon, 1981) shows petrographic evidence of contamination (table 1; sample 80), and both these samples have very high K_2O and, especially, P_2O_5 contents. Bacon and Metz (1984) suggested that Pleistocene lavas erupted in this same area which have unusual trace-element contents were contaminated by crustal material. Alternatively, an enriched mantle source could be postulated, but this appears inconsistent with the petrographic data.

The high-silica rhyolite (sample 44) is depleted in all REE relative to basalt and it is the only analyzed rock with a significant Eu anomaly. Although the abundances are low, the LREE show a steep fractionated pattern and the HREE have a positive slope. Note that although mixing of basaltic and silicic magma is proposed to explain variations in REE patterns of intermediate-composition rocks, the silicic end member is not represented by the analyzed high-silica rhyolite. None of the Pleistocene high-silica rhyolites of the Coso Range have REE patterns similar to that of the Pliocene rhyolite (Bacon and others, 1981). A small Pleistocene high-silica rhyolite dome in the southern Sierra Nevada has an REE pattern somewhat similar to that of the Coso Pliocene rhyolite, but with higher abundances, especially of HREE (Bacon and Duffield, 1981).

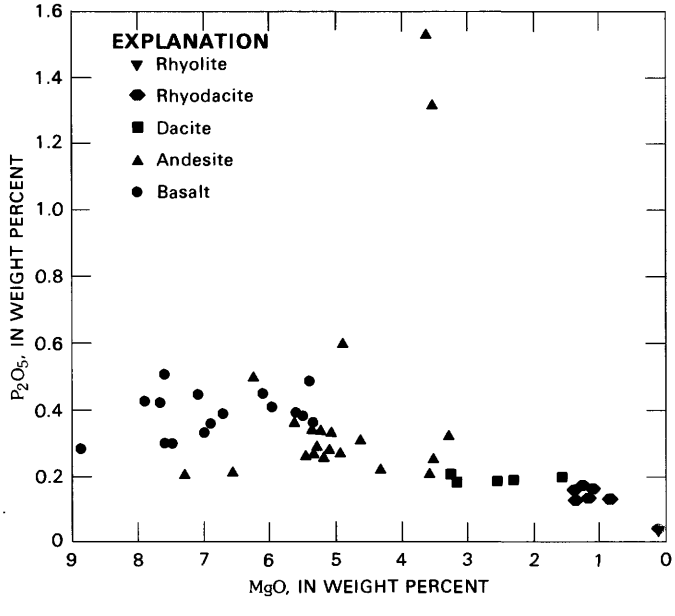

FIGURE 14.—MgO vs. P_2O_5 for Pliocene Coso Range volcanic rocks. Andesites with very high P_2O_5 contents (two samples) are from the basalt of Rose Valley (Duffield and Bacon, 1981).

HIGHLY CHARGED CATIONS (Zr, Hf, Ta, Th, U)

Concentrations of Hf, Ta, and Th are believed to be accurately determined in virtually all samples. The contents of U and Zr are less well known, particularly Zr in basalt and andesite, and they will not be described in detail. The behavior of Hf is similar to that of many incompatible elements—levels are relatively constant in rhyodacite and dacite and variable in basalt and andesite. Rhyodacite and rhyolite do not have the highest Hf contents. The may be because zircon, which is a common accessory in these rocks, preferentially incorporates Hf and was probably a fractionating phase during their generation.

Tantalum abundance is erratic. The rhyolite has the highest concentration of Ta, but basalt and andesite show the widest range among the other rocks. Dacite and rhyodacite have moderate Ta content, and the combined effects of mixing and fractionation may explain the variable concentration of this strongly incompatible element in the basalt and andesite.

Thorium behaves in a manner similar to many other incompatible elements in that abundances generally increase with SiO_2, but scatter in a manner that is consistent with combined crystallization differentiation and magma mixing. Concentrations are high and relatively constant in the most silicic dacite and all but the most differentiated rhyodacite, which has an elevated Th content (fig. 16). The rhyolite contains nearly three times the Th of most of the rhyodacite. Primitive basalt has the lowest Th levels. The mafic andesite of sample 81 is an exception to this pattern, possessing unusually high Th, as well as high U and Ta. Uranium levels in all rocks are roughly one-third those of Th, except in the rhyolite, where U is approximately one-half Th. A low Th/U ratio is characteristic of high-silica rhyolite.

A plot of Th versus Cr (fig. 18) is instructive in showing possible effects of mixing and crystal fractionation. Cr is a highly compatible trace element that is depleted by fractionation of early-formed spinel and pyroxene. Therefore, its concentration drops rapidly to low levels in early stages of crystallization. Th is a highly incompatible element, so its concentration remains relatively

low until a significant amount of crystallization has taken place. Crystal fractionation will therefore produce curved paths on the Th versus Cr plot; two calculated possible paths are shown in figure 18. Mixing, on the other hand, will produce compositions that plot along straight lines within the concavity of the fractionation curves. Such possible mixing trends are schematically shown by dashed lines on figure 18. The Coso data scatter widely on the diagram, basalt varying in both Cr and Th content and most rhyodacite and differentiated dacite forming a tight cluster. Intermediate-composition rocks commonly have Th concentration in excess of what might be expected for a given Cr content. We suggest that the variation in Cr content of the basalt is due to varying amounts of crystal fractionation and that most of the spread in the andesite values is due to mixing of basaltic magma with silicic melts much like the rhyodacite. Note that some low-Cr andesite also has quite low Th content, however, and may have been derived from relatively Th-rich basalt mainly by crystal fractionation.

DISCUSSION

In this section we discuss models for petrogenesis of the Pliocene volcanic rocks, based on the data presented earlier. These models include specific fractionation and mixing schemes, which are quantitatively evaluated, and inferred processes that operated to form the compositional spectrum of volcanic rocks. We also attempt to relate the dominant processes to changes in the tectonic regime of the Coso Range.

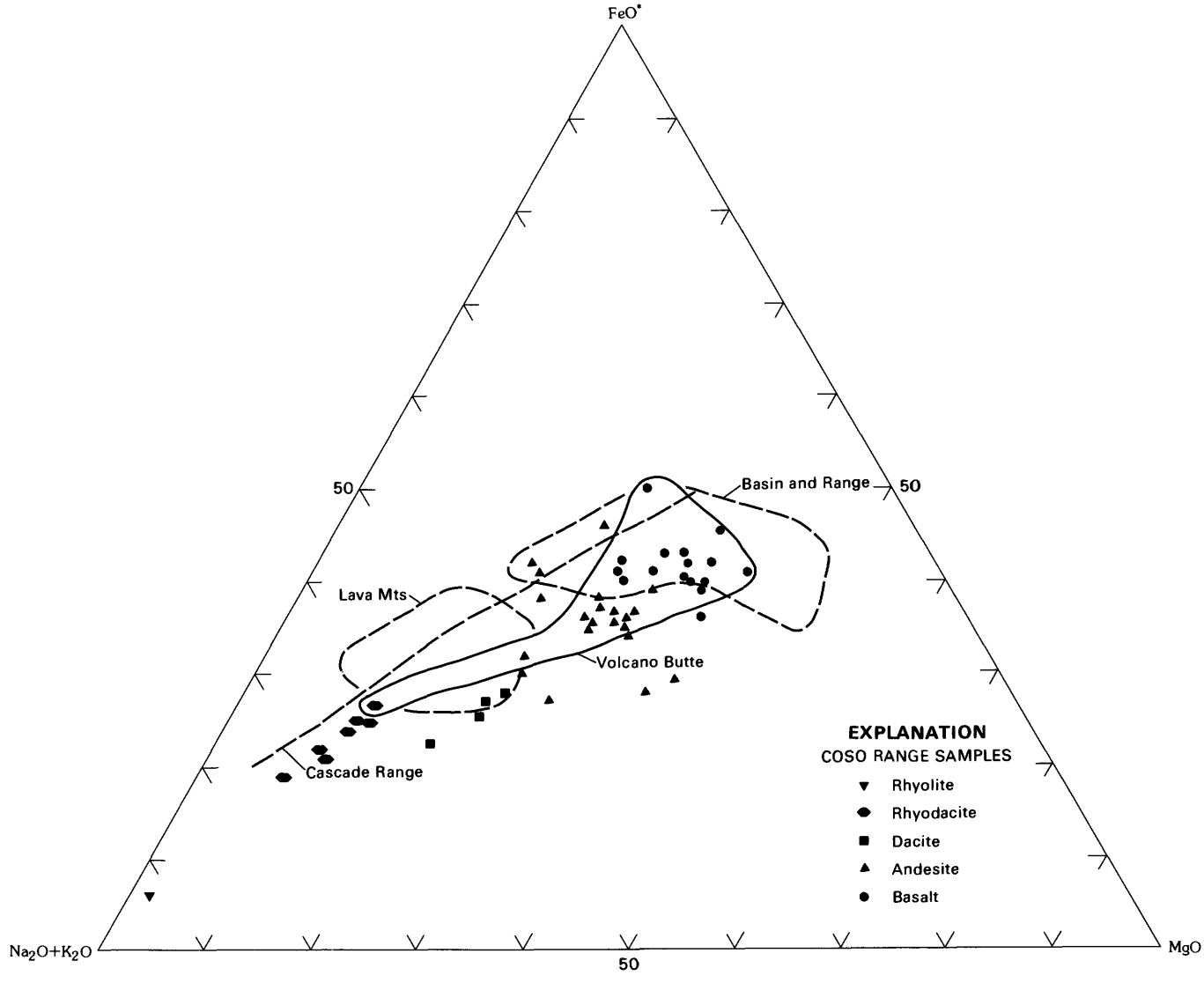

FIGURE 15.—Ternary AFM diagram for Pliocene volcanic rocks. The field labeled Volcano Butte shows variation within a single polygenetic Coso Range volcano. Field for Basin and Range basalts from Leeman and Rogers (1970); field for Pliocene andesite of the Lava Mountains, Calif., from Smith (1964); Cascade Range trend from Smith and Carmichael (1968).

Quantitative mass-balance calculations referred to in this section (table 9) were performed using the program of Stormer and Nicholls (1978). Input for the calculations consisted of major-element analyses of the lavas and microprobe analyses of phenocrysts. In an attempt to provide additional constraints, most of the modelling was done on lavas erupted from the Volcano Butte center (fig. 1), all of which appear to be nearly contemporaneous.

PETROGENESIS

BASALT

Few basaltic lavas of the Coso volcanic field have chemical characteristics that would be considered primitive (for example, high MgO and Cr, low incompatible-element contents). Those that do generally form extensive, thin diktytaxitic flows that erupted from monogenetic vents. These rocks are the closest to unmodified partial melts of the mantle, but even they may have undergone some fractionation prior to eruption. The samples of primitive basalt have gently sloping LREE-enriched chondrite-normalized REE patterns that suggest derivation from a garnet-bearing mantle source. Compositional variation among these samples may be ascribed to small heterogeneities in source composition and to differing degrees of partial melting, with superimposed fractionation of olivine+chrome spinel. All other basaltic lavas are believed to have been significantly affected by fractional crystallization, commonly accompanied by assimilation of crustal material.

Some basalt samples (45 and 74) have high MgO and Cr contents and also high contents of K_2O, P_2O_5, Ba, and LREE. The primitive characteristics of these rocks contrast with their high contents of many elements that are believed to behave as incompatible elements in

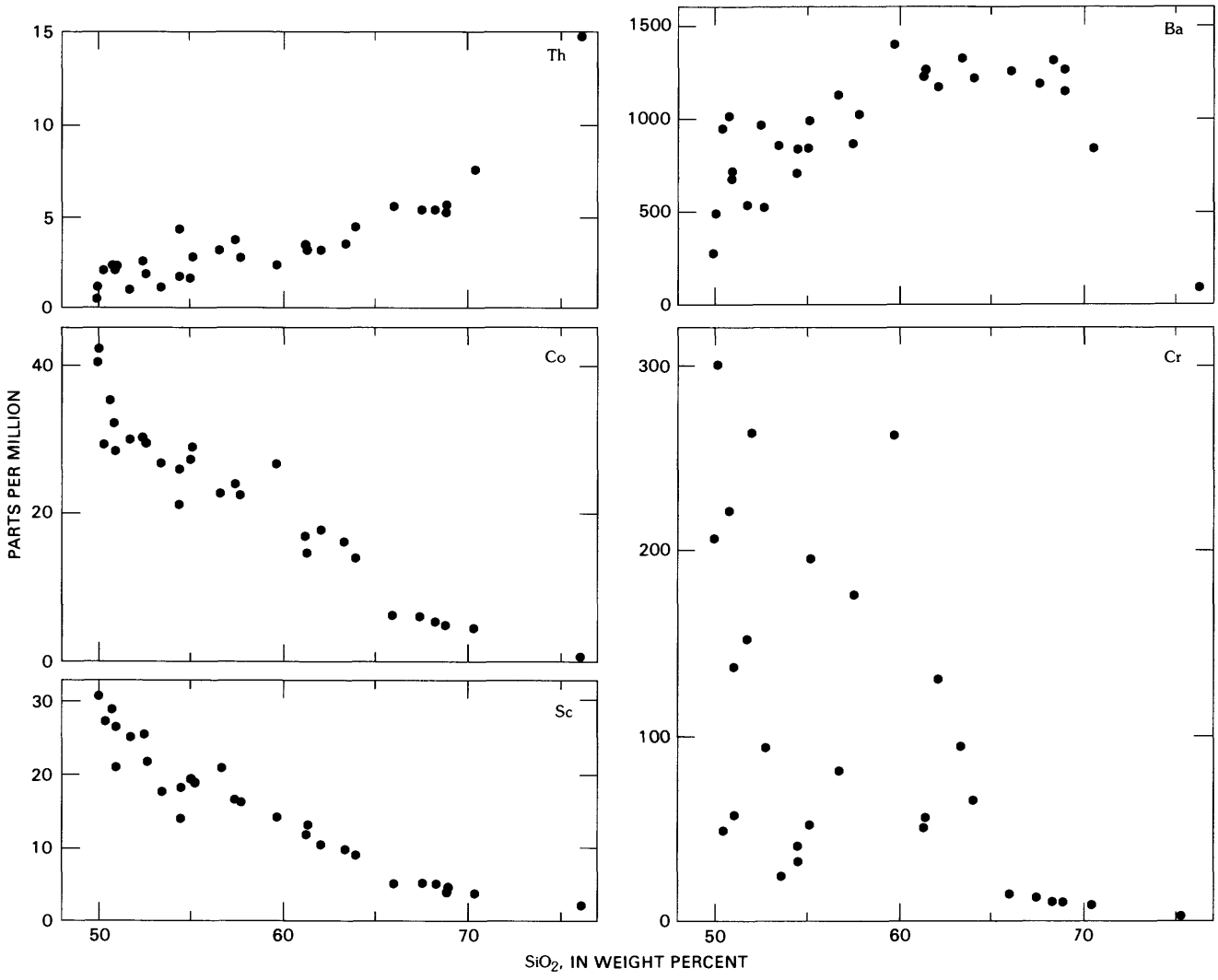

FIGURE 16.—Th, Co, Sc, Ba, and Cr vs. SiO_2 content for Pliocene Coso Range volcanic rocks.

basaltic magmas. They have SiO_2 contents 1 to 2 percent higher than other "primitive" lavas erupted at approximately the same time (Duffield and Bacon, 1981). Van Kooten (1980) described ultrapotassic mafic lavas from the Sierra Nevada which show extreme development of many of these chemical characteristics. The Sierran lavas, however, have relatively low SiO_2 contents and much higher trace-element abundances. Van Kooten

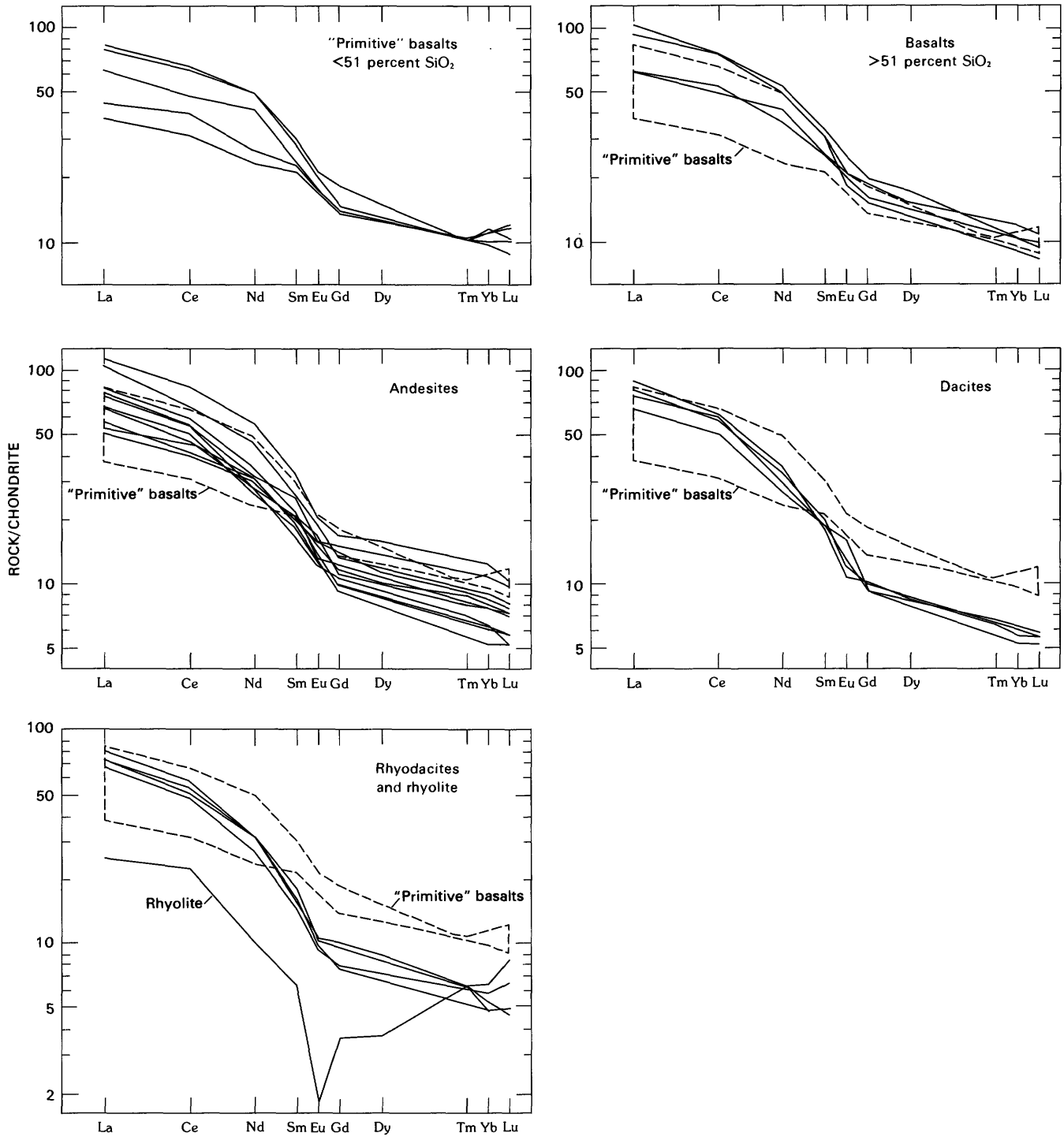

FIGURE 17.—Chondrite-normalized rare earth element plots for Pliocene Coso Range volcanic rocks. Analyses are normalized to values for the Leedey Chondrite (Masuda and others, 1973) divided by 1.2 and plotted as a function of ionic radius (Whittaker and Muntus, 1970).

(1980) appealed to a phlogopite-bearing mantle source to explain the composition of the Sierran lavas, whereas Dodge and Moore (1981) called upon a source containing amphibole. Some Pleistocene lavas of the Coso volcanic field are comparable to the LREE-rich Pliocene rocks, and Bacon and Metz (1984) suggested that contamination with deep crustal material caused at least some trace-element enrichment in those Pleistocene rocks. Watson (1982) showed experimentally that certain elements, notably K, are preferentially incorporated into basaltic magma interacting with partially melted crustal rocks. Selective contamination provides an attractive mechanism for increasing some incompatible-element concentrations in basaltic magma erupted through continental crust. Some crystallization would be expected to accompany assimilation of crustal material because of the loss of heat necessary to partially fuse country rocks. MgO and Cr contents of the LREE-rich Coso basalts are high, however, implying that extensive crystal fractionation could not have occurred. Heterogeneity of the mantle source remains a possible explanation for the chemical characteristics of these basalt samples.

Basalts with MgO contents below 7 percent are believed to have undergone some fractional crystallization and will be referred to as differentiated. Mass-balance calculations employing microprobe analyses of representative phenocrysts suggest that separation of reasonable amounts of olivine + plagioclase ± clinopyroxene will account for most of the major-element variation in differentiated basalt (table 9, model 1). Residuals for K_2O typically are greater than for other oxides and suggest that additional processes, such as selective contamination (Watson, 1982), must have been operative. The assimilation of some crustal material seems inevitable for mantle-derived magmas intruded into, and perhaps stored in, the deeper part of the crust. The most sensitive indicator of crustal interaction would be expected to be K. Indeed, Doe and others (1969) cited elevated K content as one of the criteria for recognizing contamination in basaltic lavas from the Rocky Mountain region which showed isotopic evidence of a crustal component. Pleistocene differentiated and contaminated basaltic lavas of the Coso volcanic field have relatively radiogenic Pb and Sr isotopic compositions consistent with the addition of crustal material (Bacon and others, 1984). Simple two-component mixing of primitive basaltic magma and small amounts of silicic magma would have recognizable effects on the major-element composition, and perhaps phenocryst mineralogy, of the basalt and cannot readily produce the composition of the differentiated basalt. Least-squares fractionation calculations, however, show that separation of olivine + plagioclase ± clinopyroxene combined with assimilation of small amounts of crustal material (table 9, model 4) can account for that composition.

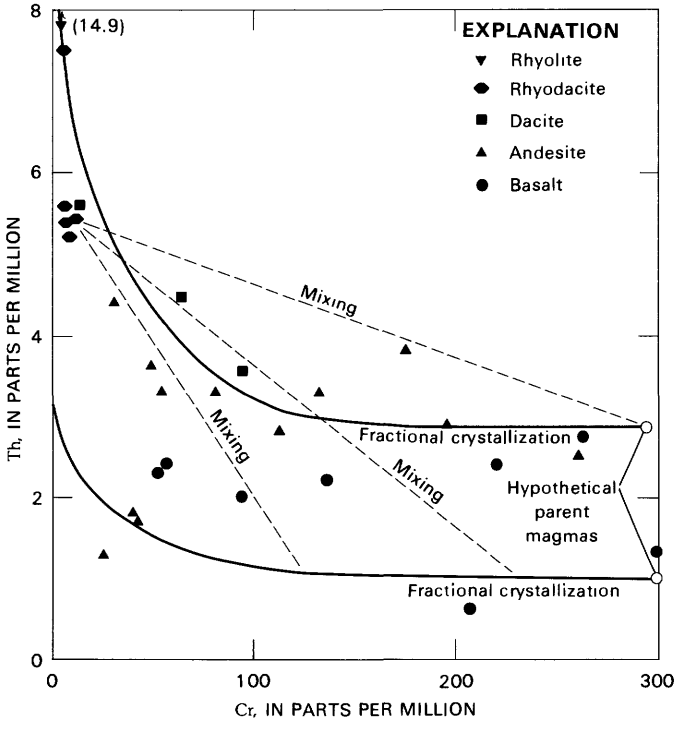

FIGURE 18.—Th vs. Cr content for Pliocene Coso Range volcanic rocks. Open circles represent hypothetical parent magmas for the calculated fractionation curves shown. Dashed lines show possible compositions formed by mixing variably fractionated basaltic magma with rhyodacitic magma. Arrow indicates that rhyolite sample is off scale at a Th content of 14.9 ppm.

A significant difference between Pliocene and Pleistocene basalt of the Coso volcanic field is the commonly high TiO_2 content of the younger rocks (Bacon and Metz, 1984). None of the Pleistocene lavas has such low K_2O, P_2O_5, or TiO_2 content as some of the Pliocene basalt. This may be because prolonged igneous activity affects the extent to which basaltic magma differentiates and interacts with crustal rocks. In the later history of the volcanic field, cumulative advection of heat to the deep crust may have promoted partial melting and caused increased modification of basaltic magma on its trip from the mantle to the surface.

INTERMEDIATE-COMPOSITION ROCKS

Andesite and most dacite samples contain mixed populations of phenocrysts and have textures that reflect sudden thermal disturbances brought about by mixing of magmas of contrasting composition and temperature (see Hibbard, 1981; Lofgren and Norris, 1981). Many previously noted geochemical features also suggest the derivation of intermediate-composition rocks by mixing of magmas. Mass-balance calculations indicate that the

Coso andesites cannot be derived from primitive basalt by crystal fractionation unless unrealistic amounts of hornblende are removed (table 9, model 2). Because hornblende is not present as a stable phase in rocks less silicic than dacite, its participation in the genesis of andesite is considered unlikely. Acceptable mass-balance solutions were obtained on the assumption that the andesite was generated from basalt by crystal fractionation combined with assimilation of silicic material (table 9, model 5; DePaolo, 1981). Because the calculations indicate a very large fraction of silicic material must be added, mixing with silicic magma is favored over assimilation of crustal rocks to avoid excessive cooling. Since the very common xenocrysts in the intermediate rocks neither appear deformed nor show subsolidus reequilibration effects, it is more likely that they originated as phenocrysts in silicic magma than as disaggregated plutonic or metamorphic rocks.

Fractional crystallization may have produced some variation within the intermediate rocks, for example from andesite to dacite, if small amounts of hornblende were present in the fractionating assemblage (table 9, model 3). In addition, the more silicic intermediate magmas could be derived from less silicic magmas by separation of plagioclase + clinopyroxene combined with assimilation of silicic magma (table 9, model 6). As in the previous assimilation-fractionation model, the amount of assimilated material is much greater than the amount of crystals removed.

Trace-element plots and ratio-ratio plots also can be used to quantify mixing relationships (Langmuir and others, 1978). The Th versus Cr plot (fig. 18) already has been discussed in this connection. A number of ratio-ratio plots were constructed in an attempt to further quantify the amount of mixing needed to derive the Coso intermediate-composition rocks. Some plots show regular relationships, but none meet the criteria for rigorously demonstrating two-end member mixing. This probably is a result of our inadequate knowledge of specific end members, since the Coso suite represents rocks of many ages erupted from widely distributed centers.

Trace-element contents of intermediate-composition rocks are most readily explained by mixing of variably differentiated and (or) contaminated basaltic magma with silicic magma. Chondrite-normalized REE patterns for most andesite samples fall between those of basalt and silicic rocks. Absence of marked Eu anomalies virtually rules out significant plagioclase fractionation. The rotation of patterns about a point between Nd and Sm, such that LREE become enriched and HREE depleted, is inconsistent with fractionation of observed

TABLE 9.—*Least squares solutions to magmatic differentiation models*

[Each model used pairs of analyzed Coso Range Pliocene rocks and the listed phenocrysts or rock compositions. Granodiorite BP-2 is from Bateman and others (1984). SiO_2^* = SiO_2 in weight percent recalculated with analysis normalized to total 100 percent volatile free and with atomic $Fe^{+2}/Fe^{+2}+Fe^{+3}$ = 0.86]

Model	1	2	3	4	5	6
Parent: (sample)	66	66	92	66	66	88
SiO_2*	50.1	50.1	59.7	50.1	50.1	56.9
Derivative: (sample)	56	83	95	56	89	92
SiO_2*	51.0	55.1	62.1	51.0	57.2	59.7
Mineral Phases: (wt. percent)						
Dacite (99)						
Olivine	[1]-6.1	[1]-8.1	[1]-4.4	[1]-5.2	[2]-3.9	-
Plagioclase	[3]-4.2	[3]-18.9	[4]-4.8	[4]-2.0	[3]-1.9	[5]-10.5
Clinopyroxene	-	[6]-3.7	[6]-5.1	-	[6]-4.5	[6]-1.6
Hornblende	-	[7]-20.8	[7]-2.9	-	-	-
Ilmenite	[8]-.6	[8]-.7	[8]-.21	-	-	-
Whole Rock analyses: (wt. percent)						
Dacite (99)	-	-	-	-	+68.4	+39.0
Granodiorite (BP-2)	-	-	-	+3.1	-	-
$\Sigma resid^2$	.34	.17	.02	.38	.11	.33

Compositions of mineral phases used in fractionation calculations are given in tables 2-5. Mineral phases used in the calculations are phenocrysts that occur in the parent or derivative, or are in compositionally similar rocks.

[1] olivine in sample 65
[2] olivine in sample 45
[3] plagioclase in sample 65
[4] plagioclase in sample 99
[5] plagioclase in sample 92
[6] clinopyroxene in sample 45
[7] hornblende in sample 99
[8] ilmenite in sample 65

phenocryst minerals, a process which should not deplete differentiates in HREE. Mafic andesite (sample 81), which has elevated REE but rather low compatible-element abundances, could have been derived by fractionation of LREE-rich basaltic magma, although its high Al_2O_3 content and lack of a Eu anomaly suggests plagioclase was not involved. Abundant mineralogic evidence for contamination in this lava is not consistent with simple crystallization differentiation.

Continental interior andesite compositionally similar to andesite of the Coso Range has been described from the San Juan volcanic field in southwestern Colorado. The San Juan andesite has REE patterns nearly identical to those of the Coso rocks (Zielinski and Lipman, 1976; Lipman, unpub. data 1982). Zielinski and Lipman (1976) surmised that the REE patterns of the San Juan rocks suggest they were ultimately formed as mafic melts from a garnet-bearing source; however, isotopic evidence indicates extensive contamination with lower crustal material (Lipman, unpub. data, 1982). Such an origin is consistent with that inferred for the Coso andesites, in which the lower crustal component is thought to have been silicic magma derived by partial fusion of garnet-bearing rocks.

The first intermediate-composition magmas were erupted several hundred thousand years after the inception of basaltic volcanism in the Coso Range. Most of the andesite and dacite was erupted about 3.6 to 3.3 m.y. ago from polygenetic centers where volcanism was focused for relatively long periods; intermediate-composition lavas from monogenetic vents were only erupted later in the history of the field. Clear evidence for the coexistence of more than one magma composition in specific centers is present in the form of commingled bombs and of lava flows with magmatic inclusions. Separation of liquids from crystals, by whatever process, was accompanied by episodes of mixing. Magma mixing is easily imagined to take place in igneous systems, particularly those of comparatively small volume, which are zoned from relatively differentiated magma downward into basaltic roots. Such a model will be more fully developed later, after the silicic rocks have been treated.

RHYODACITE

Major-element compositions of rhyodacite and silicic dacite may be consistent with derivation of these lavas by fractional crystallization of less-differentiated intermediate-composition magmas. Mass-balance calculations suggest that this is a feasible origin for the less evolved silicic rocks if hornblende is a fractionating phase (table 9, model 3). Trace-element abundances in the rhyodacite, however, do not appear to be consistent with such an origin. Rather, partial melting of deep crustal rocks is suggested. The LREE-enriched, HREE-depleted patterns imply the presence of garnet in the residual assemblage. Fractionation of hornblende may indeed have played a role in the genesis of the rhyodacite, but this probably took place after generation of a silicic melt. In any fractionation or partial melting scheme, the abundance of plagioclase in both Coso lavas and prospective lower crustal rocks suggests that it would have to be an important participant. This is inconsistent with REE data which do not show the expected negative Eu anomalies. Partition coefficients for Eu between many crystalline phases, especially apatite, and silicic melts are very small relative to those for other REE (Arth, 1976; Watson and Green, 1981; Mahood and Hildreth, 1983). Perhaps absence of Eu anomalies in the silicic rocks was brought about by a tendency for the effects of other phases to balance those of feldspar in a fractionating or residual assemblage.

Although trends in elemental abundances indicate that the silicic rocks have experienced some fractional crystallization, the high Ba content of the rhyodacite and silicic dacite is best explained by the parental silicic liquids originating through partial melting of deep crustal rocks, during which all K-feldspar and biotite are consumed. Wyllie (1979) summarized a large amount of experimental data on fusion of typical crustal rocks, including several from the Sierra Nevada. These studies show that quartz and alkali feldspar are the first phases to melt during partial fusion of granodioritic to tonalitic rocks under H_2O-saturated conditions. Because the majority of the Ba in such rocks resides in alkali feldspar, liquids created by small to moderate degrees of melting, in which alkali feldspar is consumed, will be enriched in Ba. More extensive melting increasingly involves other phases and would be expected to cause the Ba content of liquids to decrease toward that of the parent material. A similar process may contribute to Ba enrichment of basaltic magmas during interaction with crustal material.

Mafic inclusions in dacite, commingled bombs, and basaltic xenocrysts in andesite and dacite indicate that the dacite of the 3.6- to 3.0-m.y.-old part of the volcanic field evolved in compositionally zoned igneous systems. The most silicic magmas in these relatively small reservoirs may have been derived in part by fractionation of more mafic intermediate-composition magmas and in part by partial melting of country rocks, probably deep in the system. Signatures of these processes are blurred by the effects of magma mixing. The most differentiated erupted dacite (sample 99) itself contains forsteritic olivine xenocrysts derived from mixing, so the true silicic end member has not been sampled. This end member very likely would be similar in composition to the rhyodacite of Haiwee Ridge.

The Haiwee Ridge silicic center, which produced rhyodacite 3.0 to 2.5 m.y. ago, has no associated basaltic or intermediate-composition lavas (Duffield and Bacon, 1981). The rhyodacite is nearly uniform in composition and crystal content, is relatively volumious, and was erupted from vents spread over a comparatively large area. This magma probably came from a reservoir substantially larger than those of the earlier, polygenetic centers to the east. The wide range of plagioclase composition in individual samples and resorption and rapid-growth textures of the phenocrysts in the rhyodacite suggest that the fairly uniform composition of this rock may be related to convection and mixing of silicic magma that previously had been zoned. Explosive eruption of highly differentiated rhyolite at 3.1 m.y., followed at 3.0 m.y. by explosive eruption of rhyodacite, and final emplacement of thick lava flows as late as 2.5 m.y. ago (Duffield and others, 1980) suggests degassing and gradual death of a compositionally zoned system. High-silica rhyolitic magma erupted from the upper part of the system, which subsequently extruded less-differentiated, higher-temperature magmas; the earliest rhyodacite originally may have underlain this rhyolitic cap. The longevity of the Haiwee Ridge center necessitates a basaltic heat source, unless the uniform rhyodacites represent independent igneous events. A magma reservoir of several cubic kilometers or more is indicated by the erupted volume and the 0.6-m.y.-long eruptive history. The greater extent of differentiation and far larger volume of silicic eruptives than found at earlier Coso volcanoes is consistent with this hypothesis.

Depletion of Ba in the most differentiated rhyodacite suggests fractionation of either biotite or alkali feldspar. Gradual increase in Rb and Cs throughout the rhyodacite series suggests that biotite was not a major fractionating phase because it has partition coefficients for these elements of the same order as that for Ba, whereas alkali feldspar concentrates Ba relative to Rb and Cs. Alkali feldspar has not been recognized in the rhyodacite, but K-rich sanidine is present in the rhyolite. If the rhyodacite contains a component derived from high-silica (Ba-poor) rhyolitic liquid that was mixed with less-silicic differentiated magma, the decreased Ba in the most evolved rhyodacite (sample 106) might be reconciled with the lack of evidence for saturation with alkali feldspar. In fact, textural evidence for mixing supports this suggestion.

RHYOLITE

The rhyolite is a special case because of its highly differentiated composition. Extreme depletion and enrichment of trace elements in high-silica rhyolite have been attributed to various processes, notably fractionation of accessory minerals (for example, Miller and Mittlefehldt, 1982) and liquid-state differentiation (Hildreth, 1979, 1981). Because rhyolite is spatially and temporally associated with the rhyodacite and because many trace-element abundances seem to fall on projections of trends defined by the rhyodacite, the two rock types are probably genetically related. Mahood and Hildreth (1983) showed that partition coefficients for most trace elements between phenocrysts and high-silica rhyolitic liquids are substantially larger than for less silicic magmas because it is difficult for highly polymerized melts to accept trace constituents. For this reason, we believe that the trace-element abundances in the rhyolite largely reflect extreme fractional crystallization of silicic magma.

Fractionation of feldspars and quartz tends to enrich differentiates in most trace elements and deplete them in Ba, Sr, and Eu. Conversely, fractionation of mafic silicates, Fe-Ti oxides, and accessory minerals depletes high-silica liquids in most trace elements except alkaline earths (apart from micas) and alkali metals. Accessory phases, such as sphene, allanite, zircon, and apatite have characteristic patterns of partition coefficients, as shown well by the REE. The concave REE pattern for the rhyolite may be attributed to combined fractionation of apatite, which has an affinity for the middle REE (Watson and Green, 1981), and of allanite, which has very large partition coefficients for LREE (Mahood and Hildreth, 1983). Apatite inclusions are ubiquituous in phenocrysts of the rhyodacite and a single crystal of allanite intergrown with hornblende has been found in the most differentiated rhyodacite (sample 106). Alternatively, sphene might be the phase responsible for depleting the differentiated rhyolite liquid in the middle REE because of high partition coefficents for these relative to other REE (Simmons and Hedge, 1978). The Eu anomaly is presumably caused by feldspar fractionation. The REE pattern is not similar to that of high-silica rhyolite postulated to have been affected by thermogravitational diffusion (Hildreth, 1981), although diffusion-controlled processes may have been important. Recent experimental studies (Harrison and Watson, 1983) suggest that the common occurrence of apatite inclusions in phenocrysts in silicic volcanic rocks (see Bacon and Duffield, 1981) is brought about by very slow diffusion of P in the liquid, causing local saturation in apatite near growing crystals of other phases. Apatite, and possibly other accessory minerals, included in unexpectedly great amounts in larger phenocrysts by such a process could produce enhanced fractionation effects. In addition the Soret effect, in which species migrate under the influence of a thermal gradient, may produce enhanced mobility of many ele-

ments toward cooling surfaces (Lesher and Walker, 1983). Equilibrium fractionation thus may not be such a common process as fractionation enhanced by diffusion and thermal gradient effects.

Various studies, particularly the exhaustive analysis of the Bishop Tuff by Hildreth (1979), have shown that crystal settling is not a viable mechanism for differentiation of silicic magmas. More likely, crystallization causes bouyant rise of low-density differentiated liquid near the margins of a magma reservoir (McBirney, 1980); this liquid may be mixed into a convecting chamber or lodge near its roof. Steep thermal gradients and liquid-state diffusion processes may enhance the ability of such boundary-layer differentiation to strongly deplete liquids in some components and enrich them in others. The magmatic system is kept active by repeated intrusion of basaltic magma below the silicic volume, and thermal gradients are maintained by conduction of heat into country rocks, generally greatly aided by hydrothermal convection. The Haiwee Ridge volcanic center must have been fed by such a system, whose highly differentiated portion was eventually mixed into the main volume. Silicic magmas at other Pliocene centers in the Coso volcanic field may have experienced the same processes, but the igneous systems beneath these centers were smaller in volume and shorter-lived. As a result, magma erupted from them was universally contaminated with more mafic magma from deeper in the systems.

AGE AND DURATION OF VOLCANISM

Volcanism in the Coso Range was episodic, consisting of discrete eruptive episodes separated by relatively lengthy periods of inactivity. The earliest episode, which produced basalt, high-silica rhyolite, and minor amounts of intermediate-composition lava occurred between about 6.0 and 5.3 m.y. ago in the northeastern Coso Range (Bacon and others, 1982). These late Miocene rocks are not discussed in this paper because they are geographically separated from the main Pliocene volcanic field. Extensive K-Ar dating (Duffield and others, 1980) has shown that a second volcanic episode took place in the eastern part of the Coso Range around 4.0 to 3.0 m.y. ago. Basalt was erupted from monogenetic vents throughout this period, a time when basaltic volcanism was commonplace near the present western margin of the Basin and Range province and within the adjacent Sierra Nevada. Most of the polygenetic centers that produced dacitic lava in the eastern part of the Coso Range were active approximately 3.5 to 3.3 m.y. ago; local dacitic flows were erupted as late as about 3.0 m.y. The volume of volcanic products increased to a maximum during the period of activity at polygenetic centers; at the same time, the proportion of intermediate-composition products was greatest (Duffield and others, 1980). This pattern probably reflects about one million years of continuity in the flux of mantle-derived basaltic magma intruded into and, in many cases, flowing through the crust beneath this region. Approximately 0.5 m.y. after the onset of basaltic volcanism, the local crust had become sufficiently heated and tectonic conditions (discussed in the next section) were appropriate to allow differentiation and assimilation processes to generate evolved magmas. These silicic magmas mixed to varying degrees with basaltic magma beneath them to form the intermediate-composition volcanics erupted from the comparatively long-lived polygenetic centers.

Before the main stage of volcanism in the eastern Coso Range had ended, silicic eruptions began approximately 10 km to the west, near Haiwee Ridge. High-silica rhyolitic explosive eruptions took place at 3.1 m.y., followed about 0.1 m.y. later by more voluminous explosive eruption of rhyodacite (Duffield and others, 1980). Rhyodacitic lava was erupted from several widespread vents at least as late as 2.5 m.y. ago. More than 9 km^3 of silicic magma erupted from the Haiwee Ridge center, a volume at least twice as great as that of dacite from the eastern center. Moreover, no basaltic or intermediate-composition rocks have been recognized that could have erupted from within the area of silicic vents. The closest intermediate to mafic eruption was that of the andesite of Cactus Flat (Duffield and Bacon, 1981) from a small polygenetic center about 5 km northeast of the nearest rhyodacite vent, probably before the end of rhyodacitic volcanism at Haiwee Ridge. These observations, coupled with the compositional homogeneity of the rhyodacite and other petrologic information presented earlier, argue for a relatively large crustal magma reservoir that may have been active for at least 0.6 m.y. This reservoir presumably was created and sustained by intrusion of subjacent basaltic magma. Tectonic conditions in this part of the volcanic field evidently allowed this chamber to develop such that it prevented any basaltic or intermediate magma from reaching the surface.

Other than the rhyodacite of Haiwee Ridge, no volcanic rocks are known in the Coso Range that have ages between about 3.0 and 2.1 m.y. A few basaltic to andesitic monogenetic vents were active in Rose Valley 2.1 m.y. ago, and several were active east of Volcano Butte, one of which has been dated at 1.8 m.y. (Duffield and others, 1980). Both sets of vents are considered as one eruptive episode here because they are separated by 0.7 m.y. of inactivity from the next younger volcanic episode (Duffield and others, 1980; Bacon and Metz, 1984). The duration of activity at these clusters of monogenetic cones is unknown, but is thought to have been

comparatively brief. The highly porphyritic basalt of Rose Valley (samples 79, 80, and 81) (Duffield and Bacon, 1981) is compositionally unusual in having elevated K_2O, P_2O_5, Rb, and Th contents (table 7). It is similar in this respect to younger lavas erupted nearby along the Sierra Nevada fault zone (for example, the basalt of Red Hill and basalt southeast of Little Lake; Duffield and Bacon, 1981; Bacon and Metz, 1984). Less is known about the composition of rocks east of Volcano Butte, but they appear to be typical basaltic (sample 70) and andesitic lavas, compositionally and texturally similar to those of the main Pliocene volcanic field nearby.

RELATION OF VOLCANISM TO TECTONIC PROCESSES

Neogene extension of the western Basin and Range province, including the Coso area, is well established (see Stewart, 1978). Volcanism has been associated with this tectonic activity in many places, some of which have developed into volcanic fields with longevities of several million years (Smith and Luedke, 1984). The Coso volcanic field is no exception: Evidence abounds for faulting during the lifetime of the field. Results of our petrologic study suggest that the variation in composition of erupted products is tied to the extent of interaction of mantle-derived magma and crustal rocks, or, in other words, to the crustal residence time of magma. In the Coso Range there is sufficient control on the timing of volcanism and tectonism to formulate some general relations between residence time and long-term measures of deformation.

There are intriguing correlations between times and styles of volcanism in entire provinces that suggest that these qualities are functions of regional tectonic processes. In the Sierra Nevada 40 km northwest of the Coso volcanic field, three rhyolite domes were emplaced 2.4 m.y. ago, and a high-silica rhyolite dome 0.2 m.y. ago (Bacon and Duffield, 1981). Monogenetic basaltic vents 3.6 m.y. old (Dalrymple, 1963) and a small field of Quaternary basaltic vents, one of which is approximately 0.2 m.y. old, (Moore and Lanphere, 1983) are present about 20 km southwest and 10 km northwest, respectively, of the rhyolite domes. Approximate synchroneity, for both basaltic and silicic lavas, of volcanism in the Sierra Nevada and the Coso Range thus suggests tectonic influence on the timing and nature of igneous activity (Bacon and Duffield, 1981).

Because the tectonic-magmatic pattern alluded to above is regional, some tectonic factor that affects large areas and that ultimately can be quantified is needed to relate activity in one area to that in another and to relate tectonic processes to igneous products. A useful concept is that of the regional stress regime, defined in terms of magnitude and orientation of principal compressive stresses; these stresses are believed to be virtually constant within large provinces (Zoback and Zoback, 1980) which have narrow transistion zones between them (McGarr, 1982). At present, there are few areas in which magnitudes of stresses are known, but it is possible to express tectonic styles in terms of the orientations and relative magnitudes of the principal stresses (see Nakamura and Uyeda, 1980). We have deduced qualitatively the principal stresses that existed within the Coso Range at various times during the last 4 m.y. The results allows us to speculate on the relation between the stress field and the composition and eruptive style of igneous products. We confine our analysis to the area south of 36°15'N.; this is the approximate northern limit of Pliocene volcanic rocks, and the transition to the tectonically different Owens Valley deformational province lies north of this latitude.

Some assumptions and principles upon which our analysis is based are: (1) orientations of principal stress axes (S_1,S_2, and S_3) and relative magnitudes of tectonic stresses can be inferred from geologic observations; (2) magma typically migrates in tabular conduits oriented perpendicular to the least principal stress, S_3; (3) driving pressure of magma is proportional to $P_{magma} - S_3$ such that a decrease in S_3 may cause intrusion by extensional failure; (4) for large crustal domains, the magnitude of S_3 is inversely related to the externally induced extension rate; and (5) the residence time of magma in the crust at any particular depth depends upon the magnitude of S_3 at that depth. From these it follows that the volume ratio of eruption to intrusion depends upon the magnitude of S_3. Decreasing S_3, which might be brought about by an increase in extension rate, would lead to increasing residence time and decreasing eruption/intrusion ratio, allowing greater differentiation and interaction with crustal rocks.

Application of this model to the Pliocene history of the Coso Range involves some speculation. Although the volcanic history is well documented, long-term rates of extension can only be inferred from limited information on the timing of basin formation and normal faulting. Thus, the relative magnitudes of principal stresses can only be estimated; orientations of stress axes, however, can be specified with some confidence. For example, Bacon and others (1980) synthesized data on azimuths of faults and alignments of volcanic vents with earthquake focal mechanisms (Weaver and Hill, 1978/79; Walter and Weaver, 1980) to define the orientation of stress axes for the Coso Range during the Quaternary: S_3 is west-northwest, S_1 is vertical, and S_2 is north-northeast; because both strike-slip and normal faulting take place from time to time, S_1 and S_2 are thought to be similar in magnitude such that locally, during periods of strike-slip faulting, S_1 may be oriented north-northeast

and S_2 vertically. Pliocene vent alignments and fault traces are consistent with these orientations of stresses, but the geologic history suggests their magnitudes were slightly different as the region underwent the change from relative stability to extension.

Prior to about 4 m.y. ago the Coso Range evidently did not exist and the landscape was one of subdued topography developed on intrusive rocks of the Sierra Nevada batholith. Remnants of this erosion surface are visible where volcanic cover is sparse. To the north, clastic sediments were accumulating and volcanoes were active at least as early as 6 m.y. ago in the basin that became Owens Valley (Bacon and others, 1982). Accumulation of basalt flows in a shallow basin was the first indication of tectonism within the present Coso Range (south of 37°15'N.) (fig. 19A). These flows erupted from monogenetic vents, begining around 4 m.y. ago, and flowed southwest or west-southwest into a generally north-trending elongate depression. Normal faults with detectable offset of this age are unknown, yet the presence of a shallow basin suggests that extensional deformation had begun. This activity continued for 0.5 m.y., during which time at least 5 km^3 of fluid basalt were erupted. The abundance of K-Ar ages of about 3.6 m.y. for these diktytaxitic basalt flows (Duffield and others, 1980) implies that this was a time of particularly intense tectonic activity. In any case, the long-term eruption rate was high, and the composition reflects rapid transport of mantle-derived magma to the surface. This would have been a period of high eruption/intrusion ratio, one in which the magnitude of S_3 perhaps was the largest for any time during evolution of the volcanic field.

By about 3.5 m.y. ago intermediate-composition magmas had begun to be erupted in substantial volumes from polygenetic centers within the basalt field (fig. 19*B*). This type of activity reached a maximum between 3.5 and 3.3 m.y. ago, and declined thereafter until only local, monogenetic centers erupted dacite as late as 3.0 m.y. ago. At the close of this period, lavas were still flowing toward the center of the same shallow elongate, north-south basin, as evidenced by intermediate-composition flows erupted near both east and west margins of the field (Duffield and Bacon, 1981). Basalt continued to be erupted from monogenetic vents throughout this interval. The overall eruption rate was probably comparable to the earlier rate but the eruption/intrusion ratio was smaller (mean residence time was greater). If the inferred high extension rate of the late Quaternary was achieved by an approximately monotonic increase, then the rate was somewhat higher 3.5-3.0 m.y. ago than it was 4.0-3.5 m.y. ago. We can assume that S_1 remained constant, since it reflected the weight of overburden, and S_2 would have had no particular reason to change, being perpendicular to the direction of extension. By inference, therefore, S_3 had decreased below its value in the previous 0.5 m.y.

The calc-alkaline trend shown by the Pliocene Coso lavas may reflect the same kind of tectonic environment in which arc volcanism occurs. In arcs, the volcanic front probably forms in the zone where S_3 changes from vertical to horizontal as one moves onland from the trench. The magnitude of S_3 would be relatively large there, allowing only short to medium residence time for magma in the crust and opportunity for mixing. Early in the history of extension in the Coso Range, the relative magnitudes of principal stresses may have been similar to those in the typical arc case. Only when extension was well underway would S_3 have decreased to a level such that magmas could have long crustal residence times and large volumes of silicic magma could form as a result.

Eruption of high-silica rhyolitic pumice from the Haiwee Ridge silicic center took place 3.1 m.y. ago, before the last intermediate-composition lava had erupted in the eastern part of the volcanic field. Voluminous explosive eruptions of rhyodacitic pumice occurred approximately 0.1 m.y. later from the same general part of the field. Air-fall deposits of the rhyodacitic pumice are interbedded with coarse alluvial fan deposits that overlie the intermediate-composition lavas to the east (fig. 19*C*). The fans developed as normal faulting began and granitic debris was shed into a north-south-trending left-stepping series of echelon grabens that bisects the Coso Range. We surmise from this that extension was then proceeding at an increased rate in comparison to the previous 1 m.y. and that S_3 had decreased further. The surface manifestation of this extension was normal faulting along the western margin of the earlier basin. The absence of volcanic products less silicic than rhyodacite in the Haiwee Ridge area and the moderate long-term eruption rate of silicic magma indicate a decreased eruption/intrusion ratio. This episode evidently lasted until at least 2.5 m.y. ago, by which time several thick rhyodacitic lava flows had been emplaced, some of which flowed down canyons cut into earlier pyroclastic and lacustrine deposits (Duffield and others, 1980).

Extension continued from 2.5 to 0.6 m.y. ago, as evidenced by larger offsets on normal faults that cut older rocks than those which cut younger rocks, and was punctuated by brief local eruptions of monogenetic basaltic cones (fig. 19*D*). A single high-silica rhyolite dome was extruded 1.04 m.y. ago, a few tens of thousands of years after several basaltic lava flows. Most of this period of nearly 2 m.y., however, left little record of volcanism. We have no evidence of how the extension rate may have varied during this period between the

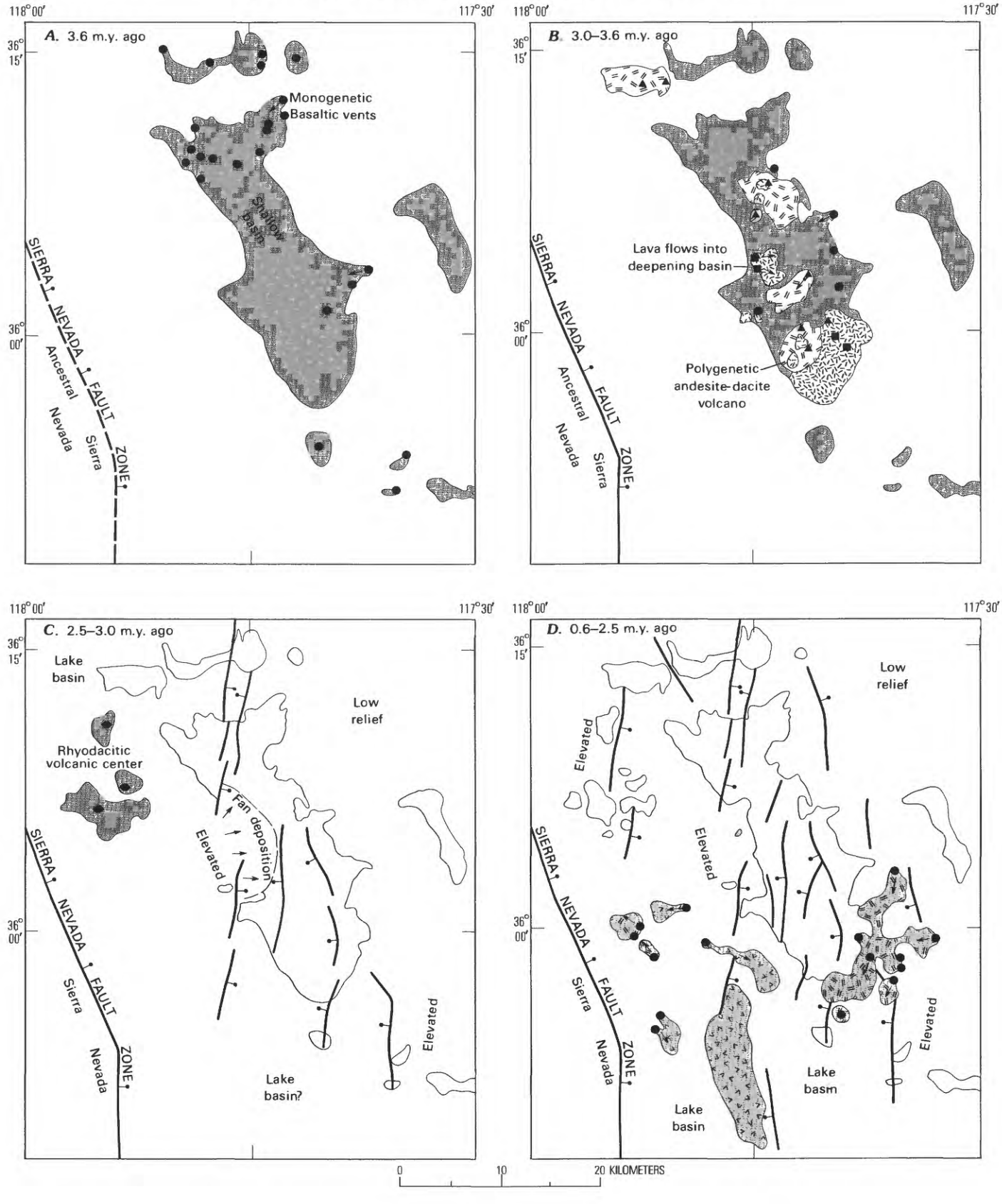
118°00′
117°30′
36°15′
36°00′
A. 3.6 m.y. ago
Monogenetic
Basaltic vents
Shallow basin
SIERRA NEVADA FAULT ZONE
Ancestral Nevada Sierra
B. 3.0–3.6 m.y. ago
Lava flows into deepening basin
Polygenetic andesite-dacite volcano
C. 2.5–3.0 m.y. ago
Lake basin
Low relief
Rhyodacitic volcanic center
Fan deposition
Elevated
Lake basin?
D. 0.6–2.5 m.y. ago
Low relief
Elevated
Lake basin
0
10
20 KILOMETERS

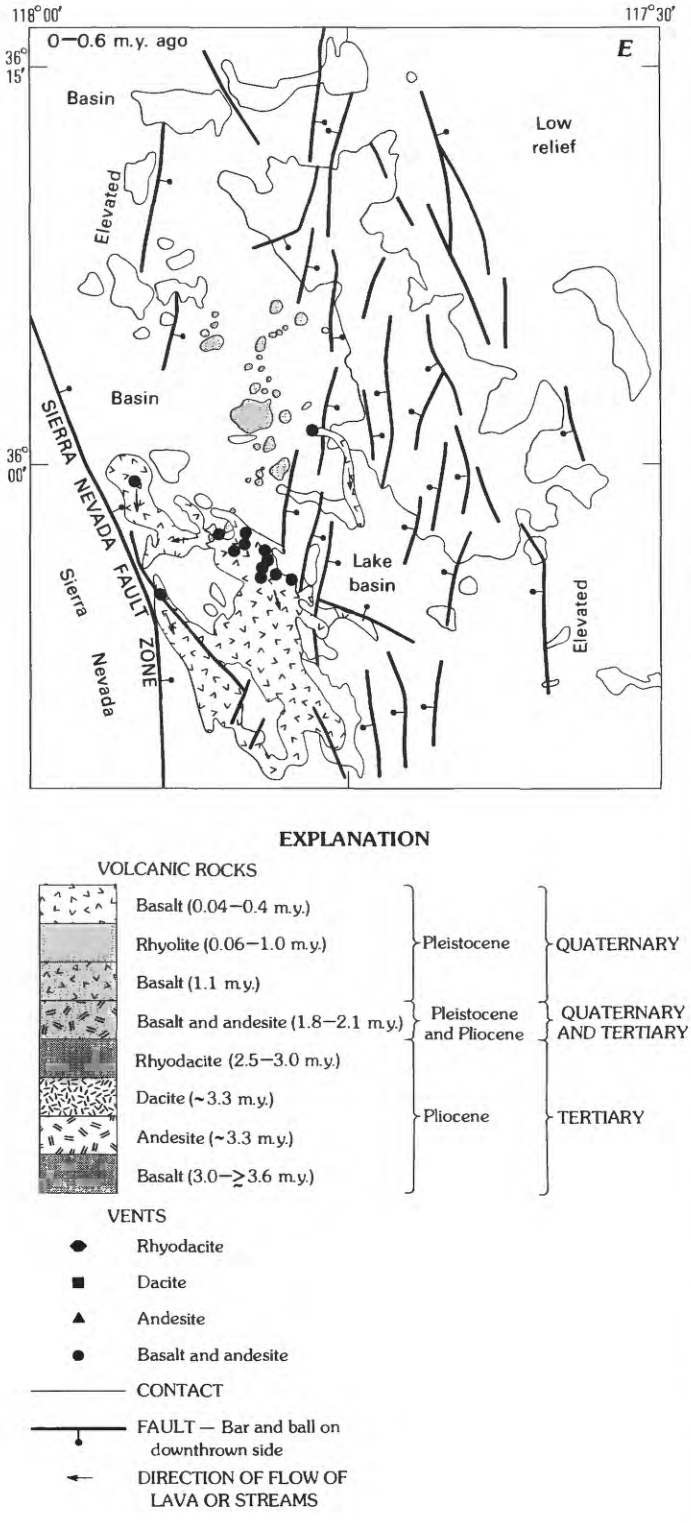

Pliocene tectonic regime, which was characterized by the inception and gradual increase of extension and the onset of normal faulting, and the Quaternary, in which extension may have reached a steady state and both normal and strike-slip faulting acted concurrently.

Extrusion of numerous high-silica rhyolite domes and eruption of peripheral basaltic lava flows in the southwest part of the Coso volcanic field appear to have taken place at approximately constant long-term rates (Bacon, 1982) for about the past 0.3 m.y. (fig. 19*E*). These rates are low compared to those of the Pliocene volcanic episode. One high-silica rhyolite dome was emplaced 0.6 m.y. ago in the center of the area of later rhyolitic extrusions. The highly differentiated composition of the rhyolite implies a very low eruption/intrusion ratio, and anomalously high heat flow in the central part of the rhyolite field (Combs, 1980) is consistent with the continuance of the underlying magmatic system. Holocene fault scarps immediately east of the rhyolite field and historical seismicity show that extension is continuing. Focal mechanisms demonstrate that strike-slip faulting alternates with normal faulting, indicating that S_1 and S_2 are similar in magnitude. We suggest that during the last 0.3, or even 0.6 m.y. S_3 has been less than at any other time in the history of the volcanic field and that it may have reached a steady-state minimum value.

FIGURE 19.—Maps showing development of Coso volcanic field (modified from Duffield and Bacon, 1981). Areas of rock units not restored to pre-extension configuration. Most faults dominantly normal but some, particularly those that trend northwest, have a strike-slip component of motion. Vents indicated only where location is certain. *A*, Approximate minimum area of volcanic rocks 3.6 m.y. ago. Basement surface beneath volcanic rocks was characterized by low relief. Inferred north-northwest-trending shallow basin may have resulted from incipient west-northwest–east-southeast extension. Age of two patches of basaltic rocks near east margin of map inferred. *B*, Approximate minimum area of volcanic rocks 3.6-3.0 m.y. ago. Flow of lava towards axis of shallow basin suggests continuing basin subsidence. Differentiated magma evolved at polygenetic volcanoes within the area of earlier basaltic volcanism. *C*, Approximate minimum area of volcanic rocks 3.0-2.5 m.y. ago. Rhyodacitic volcanic center, from which minor rhyolite was first erupted, developed at northwest corner of volcanic field. Onset of faulting and deposition of coarse alluvial fan deposits from western source about 3.0 m.y. ago. *D*, Approximate minimum area of volcanic rocks 2.5-0.6 m.y. ago. Basalt and andesite (contaminated basalt) erupted in southern part of volcanic field; high-silica rhyolite dome emplaced 1.04 m.y. ago near center of field. Faulting continued. *E*, Minimum area of volcanic rocks 0.6 m.y. ago to present. Continued basaltic volcanism near southwestern corner of volcanic field. High-silica rhyolite formed extensive field of domes and short thick flows near west-central part of field (vents not shown). Faulting continued.

CONCLUSIONS

Pliocene volcanism in the Coso Range progressed through a sequence of compositions and eruptive patterns at the same time as the area was making the tectonic transition from stability to extension. Early lavas were of comparatively primitive basalt, erupted from monogenetic vents during a period of shallow basin formation 4.0 to 3.5 m.y. ago. Subsequent eruptions in this area consisted of concurrent intermediate-composition magmas from polygenetic centers and basaltic magmas from outlying monogenetic vents. Together with the onset of normal faulting and alluvial fan formation about 3 m.y. ago, major silicic eruptions began in the northwest part of the field near Haiwee Ridge. The silicic activity ceased about 2.5 m.y. ago. The rest of the Pliocene and the early Pleistocene were characterized by local eruptions from short-lived monogenetic, generally basaltic centers.

The compositional variety of eruption products can be related to the upward movement of basaltic magma, ultimately derived from the mantle, into and through the crust. Differentiation of basaltic magma took place by separation of phenocrysts, a process commonly accompanied by assimilation of crustal material. With time, crystallization of basalt in the deep crust locally produced sufficient heating to cause partial melting of the crust and formation of relatively silicic magma. Small-volume zoned magmatic systems developed, in which silicic magma derived from the crust overlay basaltic magma. Eruptions from these systems formed polygenetic volcanic centers. Because of the relatively small volume of silicic magma in these short-lived reservoirs, there was abundant opportunity for the basaltic and silicic material to mix and hybridize, producing the nearly continuous spectrum of intermediate rocks found in the Coso Range. Toward the end of the Pliocene magmatic episode, when volcanism had shifted to the Haiwee Ridge center, the volume of silicic magma was sufficient that intermediate magma never erupted. Mixing in the Haiwee Ridge chamber probably took place between a dominant volume of rhyodacitic magma and more differentiated high-silica rhyolitic magma.

Sparse data on fault displacements and on the deformational history of the Coso Range suggest a gradual change during the late Cenozoic from stability to tectonic extension. Extension may have reached a steady state by the late Pleistocene. The development of the volcanic field seems to reflect this change in tectonic environment. We have attempted to relate this change to decrease in the least principal compressive stress, S_3. By encouraging longer residence of magma in the crust, decrease in S_3 may lead to increased differentiation and the tendency to form large volumes of silicic magma. We conclude that in the evolution of the calc-alkaline Coso volcanic field, magma mixing was an important petrogenetic process that occurred during a time when S_3 was intermediate between a value characteristic of tectonic stability and one typical of rapid extension.

REFERENCES CITED

Arth, J. G., 1976, Behavior of trace elements during magmatic processes — a summary of theoretical models and their applications: U.S. Geological Survey Journal of Research, v. 4, p. 41-47.

Bacon, C. R., 1982, Time-predictable bimodal volcanism in the Coso Range, California: Geology, v. 10, p. 65-69.

Bacon, C. R., and Duffield, W. A., 1981, Late Cenozoic rhyolites from the Kern plateau, southern Sierra Nevada, California: American Journal of Science, v. 281, p. 1-34.

Bacon, C. R., Duffield, W. A., and Nakamura, K., 1980, Distribution of Quaternary rhyolite domes of the Coso Range, California: Implications for extent of the geothermal anomaly: Journal of Geophysical Research, v. 85, p. 2425-2433.

Bacon, C. R., Giovanneti, D. M., Duffield, W. A., Dalrymple, G. B., and Drake, R. E., 1982, Age of the Coso Formation, Inyo County, California: U.S. Geological Survey Bulletin 1527, 18 p.

Bacon, C. R., Kurasawa, H., Delevaux, M. H., Kistler, R. W., and Doe, B. R., 1984, Lead and strontium isotopic evidence for crustal interaction and compositional zonation in the source regions of Pleistocene basaltic and rhyolitic magmas of the Coso volcanic field, California: Contributions to Mineralogy and Petrology, v. 85, p. 366-375.

Bacon, C. R., Macdonald, R., Smith, R. L., and Baedecker, P. A., 1981, Pleistocene high-silica rhyolites of the Coso volcanic field, Inyo County, California: Journal of Geophysical Research, v. 86, p. 10223-10241.

Bacon, C. R., and Metz, J., 1984, Magmatic inclusions in rhyolites, contaminated basalts, and compositional zonation beneath the Coso volcanic field, California: Contributions to Mineralogy and Petrology, v. 85, p. 346-365.

Bateman, P. C., F. C. W. Dodge, and P. E. Bruggman, 1984, Major oxide analyses, CPW norms, modes and bulk specific gravities of plutonic rocks from the Mariposa 1 × 2° sheet, central Sierra Nevada, California. U.S. Geol. Survey Open-File Report 84-162, 50 p.

Best, M. G., and Brimhall, W. H., 1974, Late Cenozoic alkalic basaltic magmas in the western Colorado Plateaus and the Basin and Range transition zone, USA., and their bearing on mantle dynamics: Geological Society of America Bulletin, v. 85, p. 1677-1690.

Combs, J., 1980, Heat flow in the Coso geothermal area, Inyo County, California: Journal of Geophysical Research, v. 85, p. 2411-2424.

Carmichael, I. S. E., 1967, The iron-titanium oxides of salic volcanic rocks and their associated ferromagnesian silicates: Contributions to Mineralogy and Petrology, v. 14, p. 36-64.

Dalrymple, G. B., 1963, Potassium-argon dates of some Cenozoic volcanic rocks in the Sierra Nevada, California: Geological Society of America Bulletin, v. 74, p. 379-390.

DePaolo, D. J., 1981, Trace element and isotopic effects of combined wallrock assimilation and fractional crystallization: Earth and Planetary Science Letters, v. 53, p. 189-202.

Dodge, F. C. W., Millard, H. T., and Elsheimer, N. H, 1982, Compositional variations and abundances of selected elements in granitoid rocks and constituent minerals, central Sierra Nevada batholith, California: U.S. Geological Survey Professional Paper 1248, 24 p.

Dodge, F. C. W., and Moore, J. G., 1981, Late Cenozoic volcanic rocks of

the southern Sierra Nevada, California: II. Geochemistry: Geological Society of America Bulletin, part II, v. 92, p. 1670-1761.

Doe, B. R., Lipman, P. W., Hedge, C. E., and Kurasawa, Hajime, 1969, Primitive and contaminated basalts from the southern Rocky Mountains, USA.: Contributions to Mineralogy and Petrology, v. 21, p. 142-156.

Duffield, W. A., and Bacon, C. R., 1981, Geologic map of the Coso volcanic field and adjacent areas, Inyo County, California: U.S. Geological Survey Map I-1200.

Duffield, W. A., Bacon, C. R., and Dalrymple, G. B., 1980, Late Cenozoic volcanism, geochronology, and structure of the Coso Range, Inyo County, California: Journal of Geophysical Research, v. 85, no. B5, p. 2381-2404.

Dungan, M. A., and Rhodes, J. M., 1978, Residual glasses and melt inclusions in basalts from DSDP Legs 45 and 46: Evidence for magma mixing: Contributions to Mineralogy and Petrology, v. 67, p. 417-431.

Foster, M. D., 1960, Interpretation of the composition of trioctahedral micas: U.S. Geological Survey Professional Paper 354-B, p. 11-49.

Gerlach, D. C., and Grove, T. L., 1982, Petrology of Medicine Lake Highland volcanics: Characterization of endmembers of magma mixing: Contributions to Mineralogy and Petrology, v. 80, p. 147-159.

Gill, J. B., 1981, Orogenic andesites and plate tectonics: Springer-Verlag, New York, 385 p.

Harrison, T. M., and Watson, E. B., 1983, The behavior of apatite during crustal anatexis: American Geophysical Union Transactions, v. 64, no. 45, p. 878.

Hibbard, M. J., 1981, The magma mixing origin of mantled feldspars: Contributions to Mineralogy and Petrology, v. 76, p. 158-170.

Hildreth, E. W., 1977, The magma chamber of the Bishop Tuff: Gradients in temperature, pressure, and composition: Berkeley, University of California, Ph.D. thesis, 328 p.

Hildreth, W., 1979, The Bishop Tuff: Evidence for the origin of compositional zonation in silicic magma chambers: Geological Society of America Special Paper 180, p. 43-75.

Hildreth, W., 1981, Gradients in silicic magma chambers: Implications for lithospheric magmatism: Journal of Geophysical Research, v. 86, p. 10153-10192.

Kuo, L., and Kirkpatrick, R. J., 1982, Pre-eruption history of phyric basalts from DSDP Legs 45 and 46: Evidence from morphology and zoning patterns in plagioclase: Contributions to Mineralogy and Petrology, v. 79, p. 13-27.

Langmuir, C. H., Vocke, R. O., Hanson, G. N., and Hart, S. R., 1978, A general mixing equation with applications to Icelandic basalts: Earth and Planetary Science Letters, v. 37, p. 380-392.

Leake, B. E., 1978, Nomenclature of amphiboles: American Mineralogist, v. 63, p. 1023-1052.

Leeman, W. P., and Rogers, J. J. W., 1970, Late Cenozoic alkali-olivine basalts of the Basin-Range province, U.S.A.: Contributions to Mineralogy and Petrology, v. 25, p. 1-24.

Lesher, C. E., and Walker, D., 1983, Soret fractionation of high silica rhyolite magma: American Geophysical Union Transactions, v. 64, no. 45, p. 883.

Lindsley, D. H., 1983, Pyroxene thermometry: American Mineralogist, v. 68, p. 477-493.

Lipman, P. W., 1982, Rare-earth-element compositions of Cenozoic volcanic rocks in the southern Rocky Mountains and adjacent areas: regional variations and implications for fractionation of silicic magmas: M.S.

Lofgren, G., 1974, An experimental study of plagioclase crystal morphology: isothermal crystallization: American Journal of Science, v. 274, p. 243-273.

Lofgren, G. E., and Norris, P. N., 1981, Experimental duplication of plagioclase sieve and overgrowth textures: Geological Society of America Abstracts with Programs, v. 13, no. 7, p. 498.

Mahood, G., and Hildreth, W., 1983, Large partition coefficients for trace elements in high-silica rhyolites: Geochimica et Cosmochimica Acta, v. 47, p. 11-30.

Masuda, A., Nakamura, N., and Tanaka, T., 1973, Fine structures of mutually normalized rare-earth patterns of chondrites: Geochimica et Cosmochimica Acta, v. 37, p. 239-248.

McBirney, A. R., 1980, Mixing and unmixing of magmas: Journal of Volcanology and Geothermal Research, v. 7, p. 357-371.

McGarr, A., 1982, Analysis of states of stress between provinces of constant stress: Journal of Geophysical Research, v. 87, p. 9279-9288.

Miller, C. F., and Mittlefehldt, D. W., 1982, Depletion of light rare-earth elements in felsic magmas: Geology, v. 10, p. 129-133.

Miyashiro, A., 1978, Nature of alkalic volcanic rock series: Contributions to Mineralogy and Petrology, v. 66, p. 91-104.

Moore, J. G., and Dodge, F. C. W., 1980, Late Cenozoic volcanic rocks of the southern Sierra Nevada, California: I. Geology and petrology: Summary: Geological Society of America Bulletin, Part I, v. 91, p. 515-518.

Moore, J. G., and Lanphere, M. A., 1983, Age of the Golden Trout Creek volcanic field, Sierra Nevada, California: American Geophysical Union Transactions, v. 64, no. 45, p. 895.

Nakamura, K., and Uyeda, S., 1980, Stress gradient in arc-back arc regions and plate subduction: Journal of Geophysical Research, v. 85, p. 6419-6428.

Peacock, M. A., 1931, Classification of igneous rock series: Journal of Geology, v. 39, p. 54-67.

Ritchey, J. L., 1979, Origin of divergent magmas at Crater Lake, Oregon: Eugene, University of Oregon, Ph.D. thesis, 209 p.

Ross, D. C., 1970, Pegmatitic trachyandesite plugs and associated volcanic rocks in the Saline Range-Inyo Mountains region, California: U.S. Geological Survey Professional Paper 614-D, p. D1-D28.

Shapiro, L., 1975, Rapid analysis of silicate, carbonate, and phosphate rocks—revised edition: U.S. Geological Survey Bulletin 1401, 76 p.

Simmons, E. C., and Hedge, C. E., 1978, Minor-element and Sr-isotope geochemistry of Tertiary stocks, Colorado Mineral Belt: Contributions to Mineralogy and Petrology, v. 67, p. 379-396.

Sigurdsson, H., 1971, Feldspar relations in a composite magma: Lithos, v. 4, p. 231-238.

Smith, A. L., and Carmichael, I. S. E., 1968, Quaternary lavas from the southern Cascades, western U.S.A.: Contributions to Mineralogy and Petrology, v. 19, p 212-238.

Smith, G. I., 1964, Geology and volcanic petrology of the Lava Mountains, San Bernardino County, California: U.S. Geological Survey Professional Paper 457, 97 p.

Smith, R. L., 1979, Ash-flow magmatism: Geological Society of America Special Paper 180, p. 5-27.

Smith, R. L., and Luedke, R. G., 1984, Potentially active volcanic lineaments and loci in western conterminous United States, *in* Explosive volcanism: Inception, evolution, and hazards: Washington, National Academy Press, p. 47-66.

Stewart, J. H., 1978, Basin-range structure in western North America: A review, *in* Smith, R. B., and Eaton, G. P.,eds., Cenozoic tectonics and regional geophysics of the western Cordillera: Geological Society of America Memoir 152, p. 1-31.

Stormer, J. C., and Nicholls, J., 1978, XLFRAC: A program for the interactive testing of magmatic differentiation models: Computers and Geosciences, v. 4, p. 143-159.

Tsuchiyama, A., and Takahashi, E., 1984, Melting kinetics of a plagioclase feldspar: Contributions to Mineralogy and Petrology, v. 84, p. 345-354.

Van Kooten, G. K., 1980, Mineralogy, petrology, and geochemistry of an ultrapotassic basaltic suite, central Sierra Nevada, California, U.S.A.: Journal of Petrology, v. 21, p. 651-684.

Walter, A. W., and Weaver, C. S., 1980, Seismicity of the Coso Range, California: Journal of Geophysical Research, v. 85, p. 2441-2458.

Watson, E. B., 1982, Basalt contamination by continental crust: Some experiments and models: Contributions to Mineralogy and Petrology, v. 80, p. 73-87.

Watson, E. B., and Green, T. H., 1981, Apatite/liquid partition coefficients for the rare earth elements and strontium: Earth and Planetary Science Letters, v. 56, p. 405-421.

Weaver, C. S., and Hill, D. P., 1978/79, Earthquake swarms and local crustal spreading along major strike-slip faults in California: Pure and Applied Geophysics, v. 117, p. 51-64.

Whittaker, E. J. W., and Muntus, R., 1970, Ionic radii for use in geochemistry: Geochimica et Cosmochimica Acta, v. 34, p. 945-956.

Wyllie, P. J., 1979, Magmas and volatile components: American Mineralogist, v. 64, p. 469-500.

Zielinski, R. A., and Lipman, P. W., 1976, Trace-element variations at Summer Coon volcano, San Juan Mountains, Colorado, and the origin of continental-interior andesite: Geological Society of America Bulletin, v. 87, p. 1477-1485.

Zimmerman, C., and Kudo, A. M., 1979, Geochemistry of andesites and related rocks, Rio Grande Rift, New Mexico, *in* Rieker, R. E., ed., Rio Grande Rift: Tectonics and magmatism: Washington, American Geophysical Union, p. 355-381.

Zoback, M. L., and Zoback, M. D., 1980, State of stress in the conterminous United States: Journal of Geophysical Research, v. 85, p. 6113-6156.

TABLE 10

TABLE 10.—*Sample localities for Coso Range Pliocene volcanic rocks*

Locality	Field No.	Latitude N.	Longitude W.
40-------	8-195-2	36°07.85'	117°45.61'
44-------	9-85-2	36°59.29'	117°41.78'
45-------	13-108-1	36°11.88'	117°44.30'
56-------	I-103-3	35°59.80'	117°42.52'
62-------	I-88-2	35°56.63'	117°36.00'
63-------	8-191-1	36°14.01'	117°45.20'
64-------	9-12-3	36°13.54'	117°48.65'
65-------	13-114-2	36°01.71'	117°40.46'
66-------	I-103-1	36°00.03'	117°42.44'
67-------	8-128-4	36°02.47'	117°39.97'
68-------	8-194-8	36°09.41'	117°44.75'
69-------	8-128-5	36°02.47'	117°39.97'
70-------	I-87-3	35°56.11'	117°39.62'
71-------	9-7-2	36°02.18'	117°46.91'
72-------	8-193-1	36°10.61'	117°45.86'
73-------	8-195-1	36°08.60'	117°44.68'
74-------	8-194-6	35°09.35'	117°47.26'
75-------	9-10-3	36°09.89'	117°49.18'
76-------	8-196-5	36°05.86'	117°45.06'
77-------	I-89-1	35°53.02'	117°35.30'
78-------	8-128-3	36°03.40'	117°38.24'
79-------	I-106-6	35°59.74'	117°53.01'
80-------	I-106-7	36°00.04'	117°52.74'
81-------	I-106-3	36°00.26'	117°54.23'
82-------	I-103-2	36°00.37'	117°41.74'
83-------	13-114-3	36°00.42'	117°41.24'
84-------	8-194-4	36°09.33'	117°47.16'
85-------	13-111-2	36°06.93'	117°42.91'
86-------	13-111-7	36°07.87'	117°43.02'
87-------	13-113-21	36°02-73'	117°42/42'
88-------	I-101-12	36°00.19'	117°38.75'
89-------	I-103-4	36°00.09'	117°42.08'
90-------	13-47-3	36°12.63'	117°50.95'
91-------	9-87-2	36°13.92'	117°54.82'
92-------	I-101-1	35°57.94'	117°38.58'
93-------	I-101-13	36°00.24'	117°38.69'
94-------	13.111-4	36°07.89'	117°43.29'
95-------	I-101-10	35°59.19	117°38.47'
96-------	I-101-4	35°59.03'	117°38.84'
97-------	13-113-8	36°03.85'	117°44.66'
98-------	13-113-19	36°03.12'	117°43.94'
99-------	I-103-7	35°58.93'	117°41.52'
100-------	13-45-1	36°08.17'	117°52.37'
101-------	13-42-4	36°03.93'	117°50.33'
102-------	13-43-4	36°06.75'	117°53.14'
103-------	13-42-5	36°03.93'	117°50.33'
104-------	13-43-13	36°06.48'	117°53.53'
105-------	13-45-5	36°07.73'	117°53.36'
106-------	9-86-4	36°11.14'	117°53.63'
107-------	I-103-5	35°59.29'	117°41.78'